POLITECNICO DI MILANO

School of Civil, Environmental and Territorial Engineering

Master's Degree Program in Environmental and Territorial Engineering

POLITECNICO
MILANO 1863

Microplastics removal from textile wastewater by filtration technologies

Thesis Supervisor: Prof. Francesca Malpei

Master's Thesis by:

Realini Alessandro

Matricola: 251343

2025/2026

SOMMARIO

Questa tesi analizza le prestazioni delle tecnologie di filtrazione superficiale per la rimozione delle microplastiche dai reflui di origine tessile, con particolare attenzione sul confronto tra applicazioni a scala di laboratorio e a scala dimostrativa. Le prove a scala di laboratorio sono state condotte su tre reflui tessili (Boselli, Comofil, Lipomo) utilizzando tre mezzi filtranti differenti realizzati in acciaio inossidabile (AISI 304), poliestere e poliammide (PA). In parallelo, due unità di filtrazione superficiale a scala dimostrativa, un filtro a nastro e un filtro a disco, sono state valutate in funzionamento continuo presso l'impianto di depurazione centralizzato di Lariana (Fino Mornasco, CO). A scala di laboratorio, le efficienze di rimozione dei solidi sospesi totali (TSS) sono risultate altamente variabili e fortemente dipendenti dalle caratteristiche del refluo, con valori compresi approssimativamente tra 0% e 60%. La rimozione della domanda chimica di ossigeno (COD) è risultata generalmente inferiore, tipicamente compresa tra 10% e 40%, con picchi occasionali fino a circa il 60% per reflui caratterizzati da rapporti COD/TSS più bassi. Questi risultati indicano che la filtrazione superficiale a scala di laboratorio agisce principalmente sulla frazione particolata, mentre la materia organica disciolta rimane in larga parte non influenzata. I risultati relativi alla rimozione delle microplastiche a scala di laboratorio risultano inconcludenti, in quanto i dati relativi ai reflui Boselli e Comofil non sono disponibili, mentre quelli ottenuti per il refluo di Lipomo mostrano rimozioni negative, verosimilmente attribuibili a incertezze ed errori analitici. A scala dimostrativa, il filtro a disco ha evidenziato un funzionamento idraulicamente più stabile del filtro a nastro ma con efficienze di rimozione relativamente basse e variabili, con rimozioni di TSS tipicamente comprese tra 10% e 25% e rimozioni di COD tra 5% e 15%. Al contrario, il filtro a nastro ha raggiunto prestazioni più elevate, con efficienze di rimozione dei TSS generalmente comprese tra 10% e 30% e rimozioni di COD tra 5% e 20%, beneficiando dello sviluppo di un cake filtrante stabile che ha migliorato la ritenzione delle particelle oltre la dimensione nominale del mesh. La rimozione delle microplastiche a scala dimostrativa, dominate per 80-90% da frammenti, è risultata altamente variabile per entrambi i sistemi di filtrazione con efficienze di rimozione estremamente variabili comprese da valori inferiori al 10%, fino a circa il 50-60%. Non è stata osservata alcuna correlazione diretta tra l'efficienza di rimozione dei TSS e l'efficienza di rimozione delle microplastiche, indicando che la ritenzione delle microplastiche è governata da meccanismi aggiuntivi rispetto alla sola rimozione dei solidi sospesi. I risultati ottenuti a scala dimostrativa sono stati confrontati con precedenti prove di filtrazione a scala di laboratorio condotte sul refluo di Lariana, al fine di valutare gli effetti di scala e la trasferibilità dei risultati.

Nonostante la stessa origine del refluo, le concentrazioni di microplastiche differiscono tra le due scale, passando dall'ordine di grandezza di 10^3–10^4 MP/l a scala di laboratorio fino a valori prossimi a 4×10^4 MP/l a scala dimostrativa, a causa di condizioni idrauliche e operative. In entrambe le configurazioni, il mesh AISI 150 µm ha mostrato le migliori prestazioni complessive, suggerendo un compromesso ottimale tra ritenzione e stabilità idraulica. Le prove di laboratorio tendono a sovrastimare le efficienze di rimozione per i mesh più fini, mentre i mesh più grossolani mostrano prestazioni relativamente migliori a scala dimostrativa.

Parole chiave: Filtrazione superficiale; Microplastiche; Reflui tessili; Filtro a nastro; Filtro a disco.

ABSTRACT

This thesis analyses the performance of surface filtration technologies for the removal of microplastics from textile wastewater, with particular focus on the comparison between laboratory-scale and demonstration-scale applications. Laboratory-scale tests were carried out on three textile wastewaters (Boselli, Comofil, and Lipomo) using three different filter media made of stainless steel (AISI 304), polyester, and polyamide (PA). In parallel, two demonstration-scale surface filtration units, a belt filter and a disc filter, were evaluated under continuous operation at the Lariana centralized wastewater treatment plant. At laboratory scale, total suspended solids (TSS) removal efficiencies were highly variable and strongly dependent on wastewater characteristics, with values approximately ranging between 0% and 60%. Chemical oxygen demand (COD) removal was generally lower, typically between 10% and 40%, with occasional peaks of up to about 60% for wastewaters characterized by lower COD/TSS ratios. These results indicate that laboratory-scale surface filtration mainly acts on the particulate fraction, while dissolved organic matter remains largely unaffected. Laboratory-scale microplastics removal results are inconclusive, as data for the Boselli and Comofil wastewaters are not available, while those obtained for the Lipomo wastewater show negative removal efficiencies, likely attributable to analytical uncertainty and errors. At demonstration scale, the disc filter exhibited more stable hydraulic operation than the belt filter, but with relatively low and variable removal efficiencies, with TSS removals typically ranging between 10% and 25% and COD removals between 5% and 15%. In contrast, the belt filter achieved higher performance, with TSS removal efficiencies generally between 10% and 30% and COD removals between 5% and 20%, benefiting from the development of a stable filter cake that enhanced particle retention beyond the nominal mesh size. Demonstration-scale microplastics removal, dominated for 80–90% by fragments, was highly variable for both filtration systems, with removal efficiencies ranging from values below 10% up to approximately 50–60%. No direct correlation was observed between TSS removal efficiency and microplastics removal efficiency, indicating that microplastics retention is governed by additional mechanisms beyond simple suspended solids removal. Demonstration-scale results were compared with previous laboratory-scale filtration tests conducted on Lariana wastewater in order to assess scale effects and result transferability. Despite the same wastewater origin, microplastics concentrations differed between the two scales, increasing from the order of magnitude of 10^3–10^4 MP/l at laboratory scale to values close to 4×10^4 MP/l at demonstration scale, due to hydraulic and operational conditions.

In both configurations, the AISI 150 μm mesh showed the best overall performance, suggesting an optimal compromise between retention and hydraulic stability. Laboratory tests tend to overestimate removal efficiencies for finer meshes, whereas coarser meshes show relatively better performance at demonstration scale.

Keywords: Surface filtration; Microplastics; Textile wastewater; Belt filter; Disc filter

TABLE OF CONTENTS

1 INTRODUCTION

In recent years, the presence of microplastics (MP) in aquatic environments has earned increasing scientific and institutional interest, leading to an intensification of research activities aimed at understanding their sources, environmental behavior, and removal possibilities. In general, microplastics are defined as plastic particles insoluble in water with dimensions between 1 μm and 5 mm and can be classified as primary microplastics, intentionally produced in these size ranges, and secondary microplastics, originating from the fragmentation of larger plastic materials. Among the different forms identified in the environment—fragments, films, pellets, and fibers—microfibers represent the most abundant type in wastewater and aquatic ecosystems, especially in relation to activities of the textile sector. The textile industry is recognized as one of the main sources of fibrous microplastics, particularly during wet processing stages such as dyeing, printing, and finishing. In these processes, textiles are subjected to high mechanical, thermal, and chemical stresses that favor the detachment of synthetic fibers, which are subsequently conveyed into industrial wastewater. Numerous recent studies highlight that microplastic concentrations in textile wastewater can reach extremely high values, with particularly significant loads associated with dyeing and printing processes, making these effluents particularly critical. In this context, wastewater treatment plants play a central role, both as systems for the containment and removal of microplastics and as potential points of residual release into the environment when the adopted technologies are not sufficiently effective. Once introduced into treatment systems, microplastics are partially removed through preliminary, primary, and secondary treatments; however, a non-negligible fraction can pass through the entire treatment line and reach the receiving water body, mainly due to the high treated flow rates. In this scenario, research attention is progressively shifting toward advanced and tertiary treatment technologies, with the aim of understanding whether they can contribute to increasing the overall efficiency of microplastic removal. Among these, surface filtration represents a potentially relevant technology, generally used for the removal of suspended solids, but whose specific effectiveness toward microplastics, particularly in textile wastewater, is not yet clear. The evidence available in the literature is in fact limited and often refers to heterogeneous experimental contexts.

1.1 Motivation for the Thesis

The present thesis aims to reduce the knowledge gaps that still exist regarding the removal of microplastics (MP) from textile wastewater, with particular attention to surface filtration technologies. Despite the growing interest in the topic of microplastics, the scientific literature is still limited with regard to experimental studies conducted on real textile wastewater and, above all, with respect to comparisons between results obtained at laboratory, pilot, and demonstration scales. This thesis is carried out within the European project LIFE-CASCADE (Closed-loop water systems in textile industrial districts: multimodal orchestrated removal of emerging pollutants from textile wastewater), funded by the LIFE Program of the European Union. The project aims to evaluate, at laboratory and demonstration scales, different treatment technologies for the removal of emerging contaminants—including PFAS and microplastics, both at the level of individual textile companies and centralized wastewater treatment plants, in order to identify the most effective and replicable solutions in European textile districts. The preparation of this thesis is therefore the result of a combined activity of experimental research and internship, carried out in the period between September 2025 and February 2026, directly supported by the activities of the LIFE-CASCADE project.

1.2 Objectives of the Thesis

The general objective of the thesis is to analyze the role of surface filtration technologies in the removal of microplastics from wastewater treatment systems, with particular reference to textile wastewater, which represents one of the most critical matrices in terms of microplastic load and typology. In this context, the work first aims to evaluate the removal efficiency of microplastics through surface filtration processes, analyzing their behavior under controlled conditions. In parallel, the thesis analyzes the performance of two demonstration-scale surface filtration plants—a disc filter and a belt filter—installed at a centralized WWTP and operating on real wastewater. Through the comparison between results obtained at laboratory scale from previous tests conducted on Lariana wastewater (WW) and those observed at demonstration scale, the work finally aims to evaluate the transferability of microplastic removal performances between different operational scales. In particular, the laboratory activities were conducted at the Environmental Engineering Laboratory of Politecnico di Milano, while the internship was carried out at the Lariana Depur wastewater treatment plant (WWTP).

1.3 Structure of the Thesis

Chapter 1: General context of the work, outlining the issue of microplastics in aquatic systems, with particular attention to textile wastewater, and defining the motivations and objectives of the research.

Chapter 2: Overview of the state of the art, analyzing the presence of microplastics in textile wastewater, their fate in wastewater treatment systems, and the main removal technologies investigated in the literature, with a specific focus on surface filtration technologies.

Chapter 3: Materials and plants used in experimental activities, including the characteristics of the analyzed wastewater, the laboratory-scale pilot plant, and the demonstration plants installed at the wastewater treatment plant.

Chapter 4: Adopted experimental methodologies, sampling strategies, and analytical techniques used for the extraction, identification, and quantification of microplastics.

Chapter 5: Results of the tests conducted at laboratory scale at Politecnico di Milano.

Chapter 6: Results of the experiments carried out at demonstration scale at the wastewater treatment plant.

Chapter 7: Comparison between the results obtained at the demonstration scale and previous lab results conducted on Lariana WW, with the aim of evaluating the transferability of microplastic removal performances from laboratory to real scale.

Chapter 8: Conclusions highlighting the main findings of the study, discussing their implications, and outlining possible future developments.

2 Overview of Microplastics in Textile Wastewater and Treatment Technologies

In recent years, the presence of microplastics in aquatic environments has attracted increasing attention from the scientific community and the public, as these particles are widely distributed, abundant, and difficult to remove. In this context, wastewater treatment plants are now recognized both as important accumulation points and as potential secondary sources of microplastics released into the environment. Among the various sources of microplastic emissions, the textile sector plays a particularly relevant role, mainly due to production and finishing processes that promote the release of microfibers into industrial wastewater. This chapter, therefore aims to provide an overview of the current state of the art on microplastics, focusing on their occurrence in textile wastewater, their fate within wastewater treatment plant systems, and the main removal techniques reported in the literature, with particular emphasis on surface filtration technologies.

2.1 Microplastics in Textile Wastewater

Textile industries are a major source of microplastic pollution source. Microplastics originating from textiles typically are natural or synthetic fibers in the length range of 1 µm to 5 mm with a length-to-diameter ratio of at least 3:1 and are therefore often referred to as microfibers. Among synthetic textiles, the most widely used fibers are polyester (PET), polyamide (nylon), acrylic, polypropylene (PP), polyethylene (PE), and elastane (spandex). Throughout their life cycle—during manufacturing, use, washing, and disposal—these materials can release synthetic microfibers as a result of mechanical, thermal, and chemical stresses. Unlike natural fibers, synthetic microfibers are made of non-biodegradable polymers, which persist in the environment and can accumulate in different aquatic compartments.

A recent review reports that synthetic microfibers are now found from coastal areas to the open ocean and may account for 40–90% of total microplastic pollution (Chouchene et al., 2025).

Textile-derived microfibers are considered one of the largest contributors to microplastic pollution in freshwater systems, accounting for up to 90% of detected microplastic fibers, particularly as a result of laundry and washing activities (Gambino et al., 2025) . This high release is mainly linked to textile wet processing, where fabrics are exposed to abrasion, bending, compression, and tensile stress under turbulent conditions. The combined effects of mechanical action, elevated temperatures, chemical agents, and water turbulence can weaken the fabric structure and promote fiber detachment, leading to significant microfiber emissions into wastewater.

The general textile supply chain consists of five main processes that transform raw materials into a finished garment: (i) fiber production; (ii) yarn production; (iii) fabric production; (iv) fabric processing (pre-treatments and finishing, including dyeing/printing and final treatments); and (v) textile fabrication, as shown in Figure 1.

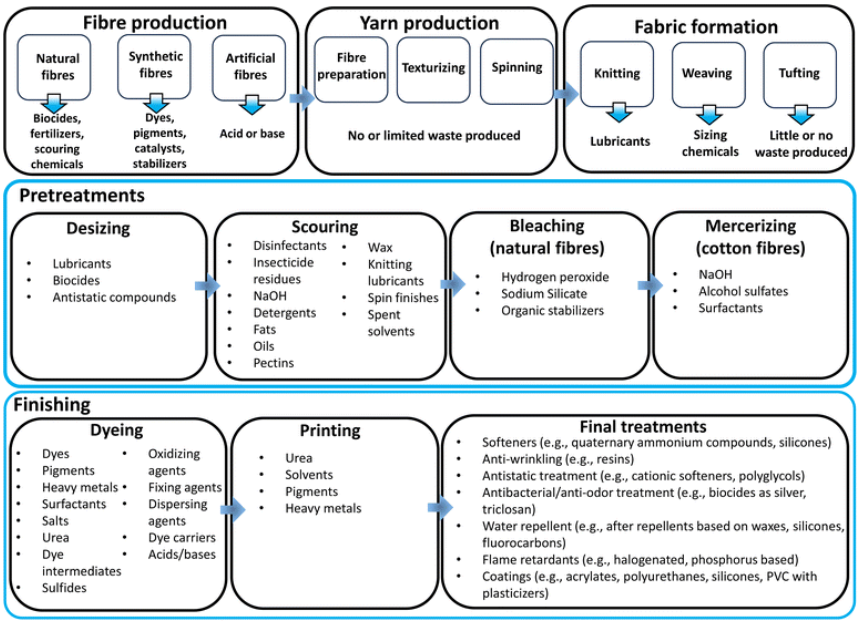

Figure 1: Main processes involved in the textile supply chain and chemical category that can be released and discharged into wastewaters during each process (Gambino et al., 2025).

The textile supply chain includes all the steps needed to turn raw materials into finished products. These steps generally follow a clear order: fiber production, yarn making, fabric construction, pretreatments (to prepare the fabric), and finishing processes (like dyeing, printing, and applying final treatments). Each of these phases uses specific chemical substances and can release pollutants into the environment.

In particular, dyeing, printing, and finishing—often called "wet processes"—are among the most polluting stages, accounting for around 17–20% of global water pollution (Gambino et al., 2025). The process starts with the production of fibers, which can be natural (like cotton or wool), artificial (like viscose), or synthetic (like polyester or nylon). Once the fibers are ready, they're spun into yarn using mechanical techniques. To help protect the fibers during this process, substances like polyvinyl alcohol (PVA) or carboxymethyl cellulose (CMC) are applied. These create a thin coating around the fibers to strengthen them during handling, but they're later washed away in the desizing phase—adding to the amount of chemicals in wastewater. When yarns are turned into fabric—through weaving, knitting, or tufting—it's common to apply another light layer of sizing to prevent the threads from breaking. Lubricants and other protective agents are also used to make the process smoother. These, too, are eventually rinsed out, contributing further to chemical waste.

The fabric processing stage represents the most critical phase in terms of environmental impact. Prior to dyeing or printing, textiles undergo a series of pre-treatment processes designed to remove impurities, improve fiber wettability, and ensure uniform coloration and finishing. Conventional pre-treatments typically include desizing, scouring, bleaching, and mercerization. These steps help remove dirt and unwanted residues from the fabric and make it more receptive to dyes. To do this, various chemicals are used depending on the process:

- Desizing: removes the coating applied earlier using enzymes or surfactants that break down the film.
- Scouring: uses hot alkaline solutions (like sodium hydroxide) to get rid of waxes, oils, fats, proteins, and other natural or added substances—especially in cotton.
- Bleaching: lightens the fabric by breaking down natural color pigments.
- Mercerization: treats the fabric (usually cotton) with a strong soda solution to improve shine, strength, and dye absorption.

These treatments are usually done in hot water baths, producing large volumes of wastewater characterized by high alkalinity and elevated values of biochemical oxygen demand (BOD), chemical oxygen demand (COD), and total organic carbon (TOC). Moreover, the harsh chemical and thermal conditions applied during pre-treatment can weaken fibers structure, increasing the susceptibility of especially synthetic fibers to microfiber release. Dyeing and printing are responsible for imparting colour and patterns to textiles. Dyeing generally involves immersion of the entire fabric in dye baths at elevated temperatures and under strong mechanical agitation, conditions that can promote fiber abrasion and the release of microfibers into process water.

Despite the different application methods, both processes rely largely on synthetic dyes and generate similar types of wastewaters. In addition, a significant fraction of dyes remains unfixed and is removed during post-dyeing washing, leading to effluents that may contain up to 50% of the initially applied dyes (Catarino et al., 2025). In printing processes, additives such as urea are used to improve dye solubility and moisture retention, but their decomposition contributes to high nitrogen loads in wastewater.

The final stage of wet processing is finishing, where textiles acquire their desired aesthetic, functional, and performance properties. Finishing treatments can be mechanical or chemical, with chemical finishing being particularly water- and chemical-intensive. These treatments may include softeners, flame retardants, antimicrobial agents, and water- or oil-repellent finishes, some of which involve persistent and potentially toxic substances. High-temperature curing and padding techniques are often required, increasing energy and water consumption. These treatments can also lead to the release of microplastics, as they may alter the fiber surfaces and make them more prone to shedding during use or washing.

2.1.1 Microplastic Concentrations in Textile Wastewater

As mentioned in the introduction, research on microplastics (MPs) in textile wastewater is still limited, particularly with regard to industrial textile wet processing.

While numerous studies have focused on quantifying microfiber release during domestic laundering, only a small number of investigations have addressed industrial processes such as dyeing, printing, and finishing, despite these stages being recognized as major sources of microfiber emissions into wastewater. For this reason, the most relevant peer-reviewed and open-access studies published over the last five years were compiled into Table 1 to summarize the key available data on microplastic and microfiber release from textile wet processing.

Table 1: Overview of the main studies addressing microplastic removal from textile wastewater (Rathinamoorthy & Raja Balasaraswathi, 2023)

Reference	*Process*	*Sampling collection site*	*Microfiber quantification (MPs/L)*	*Microfiber release estimation*	*Microfiber size range*
Zhou et al., 2020	Textile printing and dyeing (Rayon printing wastewater)	Influent point of the wastewater treatment facility	54,100 MPs/L	430 billion microfibers per day after 85% removal	100–300 µm
Chan et al., 2021	Dyeing and finishing of polyester fleece fabrics	Factory effluent discharge point	361.6 ± 24.5 MPs/L	1.1 billion microfibers per day	30–499 µm
Akyildiz et al., 2022	Wet processing (dyeing, rinsing, softening, finishing)	Influent point of the wastewater treatment facility	893–4452 MPs/L	—	10–100 µm
Rathinamoorthy & Raja Balasaraswathi, 2023	Textile screen printing process	Wastewater origin point: printing table (undiluted effluent)	1,394,205.22 ± 426,262 MPs/L	41.8 million microfibers per day	100–500 µm

In the first study (Zhou et al., 2020), microplastics in the influent streams were investigated at three textile mills in the Keqiao industrial park, in southeast coastal area of China , where each plant had different dyeing and printing processes. Textile mill A mainly performed fabric washing, chemical finishing, and dyeing; textile mill B was focused on printing processes followed by intensive washing-off steps; while textile mill C combined alkali reduction, dyeing, and printing of synthetic fibers. For each textile mill, influent wastewater samples were collected at the inlet of the associated wastewater treatment facility, representing the combined raw industrial effluent generated by the entire wet-processing train prior to wastewater treatment. The highest microfiber concentration was observed at Mill B, which processes rayon fabrics through printing operations, reaching values up to 54,100 microfibers per liter.

This extremely high concentration was attributed to intensive wet processing steps involving high temperatures, mechanical stress, and the use of surfactants during soaping and rinsing stages. Lower but still significant concentrations were measured in the influents of Mill A and Mill C, with values respectively on the order of 10^3–10^4 microfibers per liter, associated respectively with fabric dyeing and alkali reduction combined with dyeing and printing of synthetic fibers.

The second paper (Chan et al 2020 accepted, s.d.) analyzed a textile wet processing facility located in Changzhou, Jiangsu Province, China, producing approximately 3,000 tonnes of polyester (PET) per month. The sampling point was at the factory discharge. Industrial wastewater samples were collected to assess the presence of microfibers, using an optimized sampling strategy based on both temporal and volumetric replication. Temporal replication consisted of hourly sampling over a 6-hour period, with individual samples combined into a composite sample representative of 2–3 production cycles. Volumetric replication was performed using triplicate samples for volumes of 1, 3, 5, and 10 L, and duplicate samples for 0.5 L. Microfibers were quantified by stereomicroscopic analysis. The results showed an average concentration of 361.6 ± 24.5 MP/L in the treated industrial effluent. Ninety-two percent of the detected fibers were shorter than 1,000 µm, with a mean fiber length of 451.0 ± 509.1 µm. The minimum concentration was observed in the 10 L samples (~260 MPs/L), while the maximum concentration occurred in the 0.5–1 L samples (~366 MPs/L), reflecting the higher variance associated with smaller sampling volumes. Considering an average daily effluent production of approximately 3,000 m^3, the total release of microplastic fibers from the facility was estimated at 1.1×10^9 MPFs per day, highlighting industrial textile wet processing as a significant upstream source of microfiber pollution.

In the third reference (Akyildiz et al., 2022) the authors analyzed 10 wastewater samples (1 L each) collected over a five-month period in 2022 from a textile facility located in Istanbul, Turkey, producing a mixture of natural and synthetic fibers, mainly polyester (PET) and polyamide (PA). Five samples were collected from the influent of the plant's on-site wastewater treatment system, which operates through a physico-chemical process based on multi-stage coagulation–flocculation and sedimentation. The wastewater originates from multiple wet textile processing operations, including dyeing, rinsing, softening, chemical finishing, and mechanical finishing. Each 1-L wastewater sample was pre-treated with hydrogen peroxide (H_2O_2) to remove organic matter and subsequently filtered by membrane filtration. Microfibers were visually identified and counted using optical microscopy, while their polymeric composition was determined by µ-FTIR spectroscopy. The microfiber concentrations in the influent ranged from 893 to 4,452 MFs/L. Both natural fibers (cotton and wool) and synthetic or regenerated fibers (acrylic, polyester, polypropylene, polyamide, and viscose) were detected.

More than 65% of the microfibers were shorter than 1 mm, indicating a predominance of small-sized fibers in the textile wastewater. In general, the highest MP concentrations were observed in slurry wastewater from a textile printing process, reaching $1.39 \times 10^6 \pm 4.26 \times 10^5$ MPs/L, almost exclusively composed of fibers. This value derives from a study conducted in a flat screen-printing facility in Tirupur (India), where 30 L of wastewater slurry was collected directly from printing table cleaning operations and 500 mL filtered through a 600 µm sieve to remove macro-particles, diluted 1:3 with distilled water, and subsequently analyzed for fiber content (Rathinamoorthy & Raja Balasaraswathi, 2023).

Overall, available studies indicate that microplastic concentrations in textile wastewater vary strongly depending on the type of textile processing performed. Differences in raw materials, processing intensity, and chemical treatments result in a wide range of microfiber levels in the generated effluents. As presented in the table, the highest concentrations are associated with dyeing and printing operations, where textiles undergo strong mechanical stress, high temperatures, and repeated exposure to chemicals. These conditions favor fiber weakening and breakage, leading to enhanced microfiber release into the wastewater. Consequently, effluents originating from dyeing and printing processes often contain substantially higher microplastic loads compared to other textile operations, with reported concentrations in extreme cases reaching up to about 10^6 microfibers per liter (Gambino et al., 2025).

2.2 Fate of Microplastics in Municipal WWTPs

The wastewater treatment plants are designed to remove organic pollutants (biochemical oxygen demand), nutrients (nitrogen and phosphorus), suspended solids, fats and oils, as well as pathogens (bacteria and viruses) before discharge to the receiving body. The most diffused WWTP consists of two parts, a mechanical treatment plant (preliminary and primary treatment) and a biological one (secondary treatment). Tertiary treatment is introduced whereas there are more stringent requirements regarding the outflow from WWTP and when the treated wastewater is reused. Although sewage treatment plants are not designed to remove microplastics, a review of 21 studies (Iyare et al., 2020) shown an average removal value of 88% applying preliminary/primary plus secondary treatment, and 94% for WWTPs applying preliminary/primary plus secondary plus tertiary treatment. Many studies confirm that the majority of MP, on average, 50–85% , is removed by combination of preliminary and primary treatment, further 8–35% via secondary treatment and only 2–8% via tertiary treatment (Figure 2).

However, despite the high MP removal efficiency, significant amounts—ranging from 5.0×10^5 to 1.4×10^{10} MP particles per day—can still reach the receiving environment due to the high volume of incoming wastewater (Komorowska-Kaufman & Marciniak, 2024).

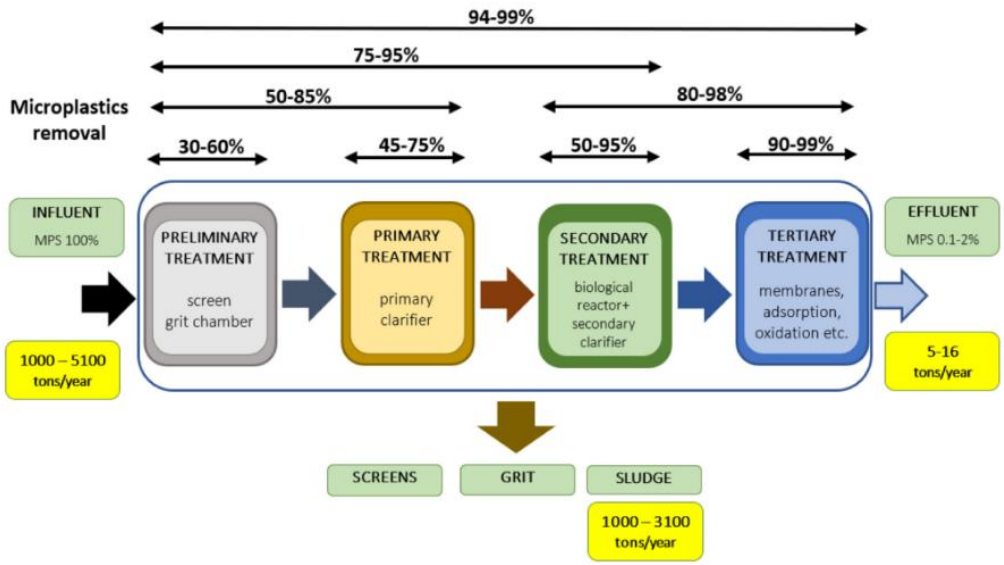

Figure 2: Average MPs removal in different stages of WWTP (Komorowska-Kaufman & Marciniak, 2024).

By the time wastewater reaches the primary treatment stage, MPs have already passed through physical processes such as screening and grit removal and are about to undergo primary sedimentation. These preliminary steps are particularly effective in removing larger particles, typically in the 100–5000 µm size range. In fact, studies show that up to 60% of MPs present in the influent can be removed after these treatments. Preliminary treatments combined with the primary clarifier can increase removal efficiency up to 85% primarily because fibers, fragments, and flakes larger than 330 µm are efficiently retained, whereas smaller particles, such as cosmetic microbeads, tend to pass through these treatment stages.

The secondary stage, usually based on activated sludge systems or membrane bioreactors (MBRs), further reduces the MP load. Biological and physical mechanisms, including biofilm formation, microbial activity, and mixing—contribute to MP retention and partial degradation. Some bacteria, such as Rhodococcus and Ideonella sakaiensis, are known to degrade plastic polymers. Furthermore, extracellular polymeric substances produced by microbial communities can trap MPs, and some small particles may be ingested by protozoa and metazoans. Removal efficiency in the secondary treatment stage range between 50% and 95% depending on factors such as sludge retention time and nutrient concentrations, which influence the extent of MP capture and biofilm development.

Tertiary treatment technologies, if present, significantly enhance MP removal. Membrane filtration and membrane bioreactors systems have shown microplastic removal performance up to 99.9% of MPs. Other technologies are also effective, as rapid sand filters achieving removal rates of approximately 97%. Dissolved air flotation systems demonstrate similarly strong performance, with average removal efficiencies around 95%. Disc filters , on the other hand, exhibit a much wider range of efficiencies, varying from 40% to 98.5%, depending on operational conditions and system configuration (Iyare et al., 2020). In general, the literature shows significant variations in MP concentrations, influenced by several factors such as the size of the population served, the type of wastewater sources (municipal or industrial), the presence of combined sewer systems, economic conditions, and lifestyle. Additional variability arises from the use of different sampling techniques, pretreatment procedures, and methods for MPs characterization.

2.3 Surface Filtration: Belt and Disk Filters

The scientific literature retrieved using the keywords *"surface filtration"*, *"microplastics removal"*, and *"wastewater treatment plants"* is relatively limited. Compared to more established separation technologies, such as dissolved air flotation or membrane filtration, surface filtration has received considerably less attention in the context of microplastic (MP) removal from wastewater. This limitation is even more evident when focusing on specific surface filtration technologies of interest, belt filters and disc filters. To date, only a small number of studies explicitly investigate the application of these systems for MP removal, and even fewer assess their performance as standalone treatment processes rather than as part of integrated or tertiary treatment schemes. As a result, available data on removal efficiencies, operational conditions, and long-term performance of belt and disc filtration systems for microplastic mitigation remain scarce, highlighting a significant knowledge gap in the current literature.

2.3.1 Surface Filtration in Wastewater Treatment: Current Principles

According to Metcalf & Eddy Inc., surface filtration consists of removing particulate material suspended in a liquid by mechanical sieving by passing the liquid through the filter material.

In contrast to depth filtration, surface filtration primarily retains particles on the external surface of the filter medium rather than within its internal structure. Surface filtration has been used in several applications, and its popularity is increasing because the filters can produce high-quality effluent, require less footprint, have low backwash rates, and show reduced maintenance requirements. These characteristics make surface filtration particularly attractive for retrofitting existing WWTPs or for applications where space constraints are critical.

In surface filtration systems, suspended solids are primarily retained on the outer layer of the filter medium. The wastewater flows through the fabric from the outside in, progressively depositing solids and forming a cake layer on the surface. This cake layer acts as a secondary filtration barrier, enhancing overall removal efficiency by capturing particles smaller than the nominal pore size of the filter medium. The formation and properties of the cake layer are influenced by several factors:

- Particle size: Smaller particles form denser, less permeable cakes, while larger ones result in more porous layers.
- Solids concentration: High levels of suspended solids promote faster cake formation and increased resistance.
- Filtration pressure: Higher hydraulic pressure compresses the cake, reducing porosity and slowing down the flow.
- Fluid composition and viscosity: Wastewater containing polymers, organic matter, or clays tends to drain more slowly and forms thicker cakes over time.

Once the cake starts to develop, it significantly contributes to filtration by increasing hydraulic resistance and capturing progressively finer solids. A stable, uniform cake layer enhances consistent filtration, minimizes bypassing or channeling, and maintains high removal rates. However, excessive thickness or compressibility can reduce overall performance. Among the surface filtration technologies reported in the literature are microscreens (drum microsieving), membrane-based systems such as microfiltration (MF) and ultrafiltration (UF), as well as disc filters and rotating belt filters. Of these, disc filters and rotating belt filters are generally considered the most promising options.

2.3.2 Current Evidence on Microplastic Removal by Belt Filters

A review of the scientific literature using the keywords *"rotating belt filters"*, *"microplastics removal"*, and *"WWTP"* returned only a limited number of studies suggesting that the application of belt filters for microplastic removal is still an emerging research topic. Most of the existing studies investigate belt filter systems as part of combined treatment configurations, where surface filtration is preceded by agglomeration step.

Sturm et al., (2024) investigated, at laboratory scale, a combined treatment system for microplastic removal consisting of two sequential units: an initial agglomeration–fixation step, based on the addition of a specific agglomerating reagent, followed by a mechanical separation unit represented by a belt filter equipped with a filter fleece. The fluid tested was a simplified laboratory test water (model water), rather than real industrial or municipal wastewater, intentionally selected to ensure controlled and reproducible experimental conditions. In this configuration, the belt filter mainly acts as a physical separation unit for previously formed microplastic agglomerates, rather than serving as the primary removal mechanism for individual particles. Fragmented microplastics of a single, known polymer type were artificially added to the test water, allowing the authors to isolate the treatment performance from the variability typically associated with heterogeneous wastewater matrices. Microplastic quantification was performed by membrane filtration followed by optical microscopy. The combined system demonstrated a high removal efficiency, achieving an average microplastic reduction of 97.92 ± 2.31%.

A similar approach was adopted in the study conducted by Korzin et al., (2025) who examined a pilot-scale treatment system consisting of a 200 L stirred reactor with dosing of an organosilane-based agglomerating reagent, followed by an inclined belt filter equipped with a nonwoven polyester belt with a pore size of 70–80 µm. Experimental tests were carried out on industrial wastewater over a period of 25 days, treating daily batches ranging from 400 to 1200 L (average ~680 L/day). High and stable removal efficiencies were observed throughout the entire experimental period, reaching 97.4% by mass and 99.1% by particle count. Microplastic identification was performed using fluorescent staining and fluorescence microscopy. These studies indicate that rotating belt filters can achieve very high microplastic removal when applied within integrated treatment schemes. In both cases, the use of organosilane-based agglomerating reagents plays a key role, as these compounds promote microplastic attachment, aggregation into larger flocs, and chemical stabilization through a sol–gel process, making the particles easier to retain on the filter surface.

However, current evidence also suggests that such performance is strongly dependent on the presence of pretreatment steps, and that further research is needed to better assess the effectiveness of belt filters when operated as standalone surface filtration units.

2.3.3 Current Evidence on Microplastic Removal by Disk Filters

Several peer-reviewed studies have investigated the use of disc filters for microplastic removal as tertiary treatment units downstream of secondary clarification, highlighting their role as polishing technologies rather than as primary separation processes, which remain understudied.

According to Simon et al., (2019), the secondary effluent underwent a polishing treatment using a Hydrotech HF2220 disc filter composed of 13 discs. Each disc was equipped with a polyester cloth medium with a pore size of 18 µm, providing a total treatment capacity of 1200 $m^3\ h^{-1}$. The extracted particles were analyzed using µFT-IR imaging, achieved by coupling an FT-IR microscope with an FT-IR spectrometer. Infrared maps of the entire sample area were analyzed pixel by pixel using the MPhunter software, which applies spectral correlation against a reference database to identify polymer types. The results showed a clear reduction in microplastic concentrations after disc filtration, with number-based concentration decreasing from 29 to 3 MPs L^{-1}, corresponding to a removal efficiency of 89.7%, while the mass-based concentration decreased from 1.27 to 0.31 µg L^{-1}, resulting in a removal efficiency of 75.6%.

A further full scale investigation was carried out by Kwon et al., (2022) at three full-scale WWTPs in Gyeongsangbuk-do Province, Republic of Korea. All three WWTPs have a similar treatment line consisting of bar screening, grit removal, primary clarifier and a conventional activated sludge process. The effluent flows into the coagulation process before the last surface filtration treatment, a disc filter. The removal efficiency achieved by the disc filters alone ranged from 43.13% to 72.50% and total microplastic removal for WWTP-A, WWTP-B, and WWTP-C was between 98.10%-98.92%. In all WWTP, fibers were the most efficiently removed microplastic type during disc filtration, with removal rates between 52.38% and 81.25%, followed by microbeads (43.67–62.89%) and fragments (35.71–42.35%). Operational conditions such as flow rate and pressure were found to significantly influence microplastic removal, with higher flow rates leading to reduced filtration performance. In this case, the pressure in all WWTPs is the same, but WWTP-B uses a larger flow rate than WWTP-A and C.

The results showed that the microplastic removal rate in WWTP-B was lower due to the larger flow rate and pressure that can damage the filter quicker than normal. The larger flow rate can reduce microplastic removal efficiency because microplastic sizes, which are relatively larger than the fiber's pores, will be forced out.

Finally, Talvitie et al., (2017) at the Viikinmäki WWTP in Helsinki, Finland, tested two disc filter cloths with different pore sizes: 10 µm and 20 µm. The removal efficiency for microplastics using the disc filter was respectively 40% and 98.5%. In that setup, the wastewater underwent primary clarification, a conventional activated sludge (CAS) process, and a tertiary denitrifying biological filter. The pilot-scale disc filter unit (Hydrotech HSF 1702-1F) included two rotating discs; each composed of 24 filter panels. The system operated at a flow rate of approximately 20 m^3/h, corresponding to a hydraulic retention time of about 4 minutes within the filter.

Overall, disc filters are typically applied as polishing units operating with fine mesh sizes (generally 10–40 µm), and their microplastic removal performance is strongly influenced by filter characteristics such as pore size, hydraulic loading rate, and operational conditions, as well as by the properties of the incoming wastewater. According to the reviewed studies, microplastic removal efficiencies achieved by disc filters alone generally range from approximately 40% to 90%, confirming their effectiveness as tertiary treatment technologies while also highlighting their sensitivity to operating parameters.

3 MATERIALS

This chapter presents the materials considered in the study. In this context, "materials" refers to the wastewaters used during the experimental activities, including those tested at laboratory scale (lab-scale) and the influent wastewater from the Lariana WWTP, which was analyzed through demonstration-scale (demo-scale) experiments.

3.1 EFFLUENTS TESTED

Pilot-scale experiments on textile effluents were conducted at the Environmental Engineering Laboratory of the Politecnico di Milano, while demonstration-scale plants were installed and operated at the Lariana Depur S.p.A. WWTP in Fino Mornasco (CO). Consequently, the wastewater streams analyzed in this chapter differ depending on whether the pilot plant or the demo plants are considered. At laboratory scale, the pilot plant was fed with three different types of textile wastewater, each originating from a different textile company. An overview of the main production processes of these companies, together with the corresponding sampling points, is presented in Figure 3.

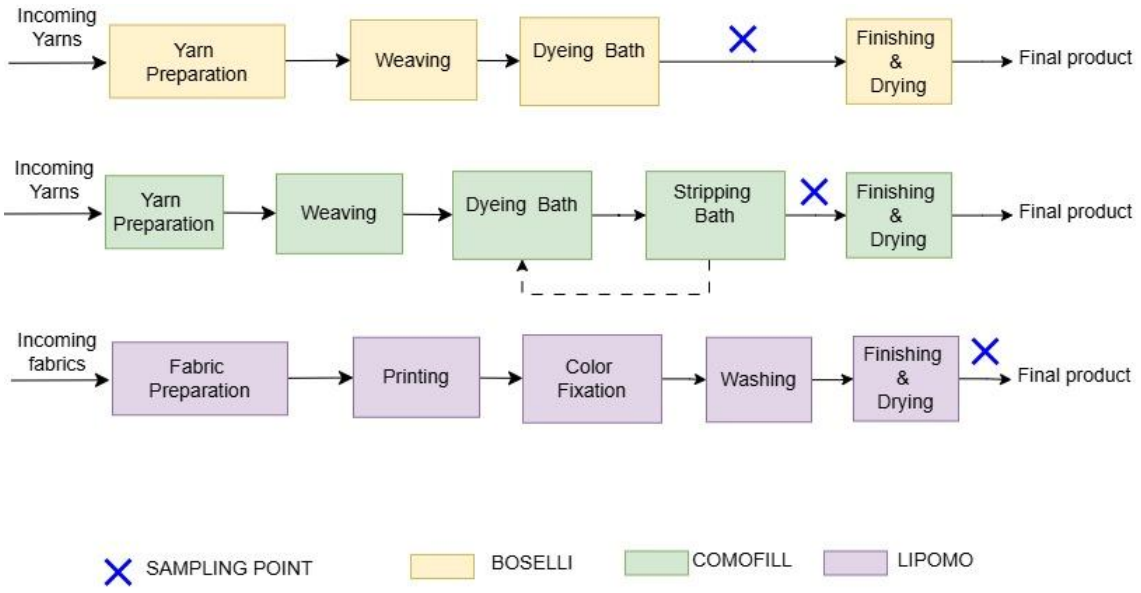

Figure 3: Main production processes of the three textile companies Boselli, Comofil, and Lipomo, with sampling points indicated by blue X symbol.

3.1.1 BOSELLI WASTEWATER

Boselli (E. Boselli & C. S.r.l.) is a Italian textile manufacturer based in Olgiate Comasco, in the province of Como. The company operates an integrated production system, controlling the entire production process from yarn to finished fabric and finishing.

The wastewater investigated in this study was generated during PES dyeing operations on a jet machines and was collected from the discharge of a dyeing bath following the processing of a fabric composed of 92% polyester and 8% elastane, with a surface mass of 128 g m^{-2} and a total processed length of 206 m corresponding to 52.4 kg of fabric material. During the dyeing process, prepared fabrics are treated in large vessels containing aqueous dye solutions composed of dyestuffs and auxiliary chemicals. Process parameters such as temperature and treatment time are carefully controlled to achieve the desired color shade and ensure adequate dye fixation. At the end of the dyeing cycle, the residual dye bath is discharged and represents the wastewater stream analyzed, visually represented in Figure 4.

Figure 4: Residual dye bath effluent collected at the end of the dyeing cycle at the Boselli textile facility.

The Boselli wastewater sample was collected on 06/10/2025 (V=110 L). After sampling, the wastewater was stored in high-density PE containers and subsequently stored at 4 °C.

The Boselli dye bath WW was previously analyzed by CTSS on 22 October 2024 (Table 2), in terms of physico-chemical parameters and microplastic content. The results of this preliminary characterization provided a useful reference for the interpretation of the experimental results obtained in the present study, offering a general indication of the wastewater composition.

Table 2: Preliminary characterization of Boselli wastewater.

Parameter	*Value*
pH (–)	4.56
Electrical conductivity (µS·cm^{-1})	1785
COD (mg·L^{-1})	7740
TSS (mg·L^{-1})	89
Total Microplastics (n°/L)	145771

This effluent is representative of dyeing wastewater from synthetic fabrics, characterized by moderate COD, acidic pH, and a high load of microplastic fibers, making it suitable for investigating removal mechanisms under controlled conditions.

3.1.2 Comofil wastewater

Comofil S.r.l. is a yarn dyeing mill located in Como (CO), northern Italy. The company specializes in the dyeing of synthetic (e.g., polyester, nylon), artificial (e.g., viscose) and natural (e.g., cotton, linen, silk) fibers. The wastewater investigated in this study (Figure 5) was generated from the discharge of a stripping bath treating 150 kg of 100% polyester fabric.

Figure 5: Wastewater generated during the stripping process at the Comofil textile company.

As a consequence of the stripping process, the wastewater contains the dyes removed from the yarn, together with reducing chemicals and their degradation products, often including sulfur-based compounds. In particular, the process was carried out in a dyeing bath with a total volume of 1500 L, operated for 10 minutes at a temperature of 90 °C. The bath composition included 4 g/L of caustic soda and 1 g/L of sodium hydrosulfite, which acted as the main reducing agent. This type of effluent is generally characterized by high chemical oxygen demand (COD) and intense dark coloration, as confirmed in this case. The Comofil wastewater sample was collected on 06/10/2025 (V= 110 L). After sampling, the wastewater was stored in high-density PE containers and transported to the laboratory within 24 hours and subsequently stored at 4 °C. The Comofil effluent had previously been characterized on 4/10/2024 in terms of physico-chemical parameters and microplastic content by CTSS, as reported in Table 3.

Table 3: Preliminary characterization of Comofil wastewater.

Parameter	*Value*
pH (–)	12.35
Electrical conductivity ($\mu S \cdot cm^{-1}$)	4770
COD ($mg \cdot L^{-1}$)	478
TSS ($mg \cdot L^{-1}$)	32
Total Microplastics (n°/L)	1800

This effluent was selected as representative of stripping wastewater from synthetic yarn processing, characterized by highly alkaline pH, elevated conductivity, and the presence of residual dyes and reducing agents, providing a challenging matrix for assessing treatment performance and microplastic removal under extreme chemical conditions.

3.1.3 LIPOMO WASTEWATER

Stamperia di Lipomo S.p.A. is a textile printing and finishing company located in Lipomo. The wastewater investigated is the final WW generated by multiple production processes. This composite wastewater reflects the overall impact of the different wet treatments performed on-site.

The effluent includes wastewater originating from fabric pretreatment operations such as desizing, scouring, bleaching, and mercerizing. These processes typically generate alkaline wastewater streams rich in organic matter. Additional contributions derive from textile printing operations and from post-printing washing steps, which represent the main source in terms of wastewater volume. This fraction is characterized by high color intensity as shown in Figure 6, elevated chemical oxygen demand (COD), and the presence of residual dyes, thickeners, salts, urea, and, in some cases, metals and nitrogen-containing compounds. Smaller contributions may also originate from wet finishing operations.

Figure 6: Wastewater collected at the final discharge of the Lipomo textile printing facility.

The Lipomo wastewater sample was collected on 01/12/2025, with a total collected volume of 110 L. The sampling point corresponded to the final company discharge. This sampling approach was adopted to obtain a representative picture of the overall wastewater generated by the facility. After sampling, the wastewater was stored in high-density PE containers and transported to the laboratory within 24 hours and subsequently stored at 4 °C. This preservation protocol was consistent with that applied to the other wastewater samples considered in this study. The Stamperia di Lipomo effluent had previously been characterized on 19/12/2024 in terms of physico-chemical parameters and microplastic content by CTSS, and the main results are summed up in Table 4.

Table 4: Preliminary characterization of Lipomo wastewater.

Parameter	*Value*
pH (–)	8.87
Electrical conductivity (µS·cm^{-1})	2480
COD (mg·L^{-1})	734
TSS (mg·L^{-1})	152
Total Microplastics (n°/L)	115200

This effluent was selected as representative of a composite textile effluent, generated by multiple wet processing operations, characterized by slightly alkaline pH, high COD, and a significant microplastic load, and therefore suitable for evaluating treatment effectiveness under realistic and heterogeneous industrial conditions.

3.1.4 Alto Seveso WWTP

The Alto Seveso wastewater treatment plant is a centralized industrial WWTP constructed and managed by Lariana Depur S.p.A. Within the framework of the European LIFE CASCADE project, Lariana Depur S.p.A. participates as an official project partner and is directly involved in monitoring and characterization activities of treated wastewater. In particular, the company was responsible for delivering the experimental filtration activities at the demo-scale carried out at the Lariana WWTP, which constitutes the basis of the experimental investigation presented in this thesis. The centralized treatment plants operated by Lariana Depur receive contributions from textile industries, whose effluents are characterized by high variability in composition and by the presence of emerging contaminants, including synthetic microfibers.

According to the Lariana Depur 2024 report, the wastewater entering the Alto Seveso WWTP is mainly composed of stormwater, accounting for up to 71% of the total treated volume. The remaining fraction consists of approximately 18% domestic wastewater and 11% industrial wastewater, corresponding to a total annual volume of 1,406,704 m³/year (Figure 7).

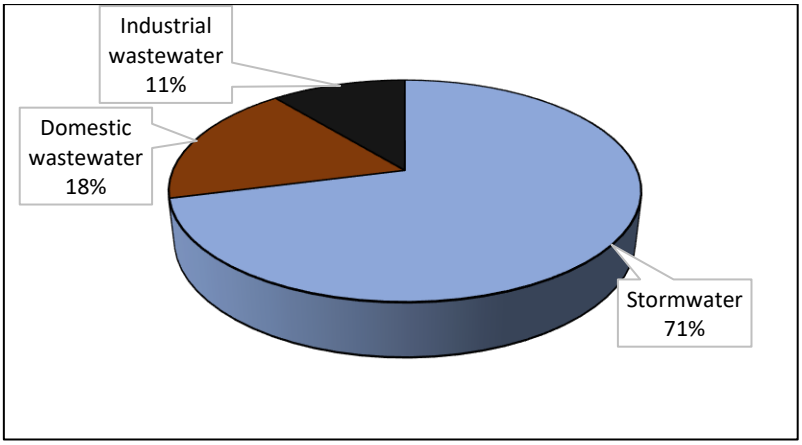

Figure 7: Percentage contribution of stormwater, domestic wastewater, and industrial wastewater to the total influent treated at the wastewater treatment plant.

The average daily inflow to the plant is 28,070 ± 11,799 $m^3 \cdot day^{-1}$, highlighting a pronounced hydraulic variability typical of combined sewer systems. Influent quality data, reported as mean ± standard deviation over the monitoring period 2023–2025, indicate average values of COD equal to 230 ± 131 $mg \cdot L^{-1}$, total suspended solids of 78 ± 62 $mg \cdot L^{-1}$, pH of 7.77 ± 0.30, and electrical conductivity of 1143 ± 349 $\mu S \cdot cm^{-1}$. Within this framework, Table 5 compares the characteristics of the laboratory-scale textile wastewater tested in this study with the average influent composition of the Alto Seveso WWTP. This comparison provides a scale-up perspective, showing that laboratory experiments were conducted under concentrated, yet representative conditions of the textile-related pollutant loads encountered in centralized wastewater treatment plants.

3.2 Laboratory-Scale Pilot Plant at Politecnico di Milano

Laboratory-scale filtration tests were carried out at the Environmental Engineering Laboratory of Politecnico di Milano. The experiments were performed using a laboratory-scale surface filtration pilot plant, hereafter referred to as the Laboratory Surface Pilot Plant (LSPP), which was designed to investigate the fundamental mechanisms governing surface filtration processes under controlled operating conditions. The primary objective of the laboratory-scale filtration tests was to evaluate the intrinsic performance of surface filtration using filters with different mesh sizes and materials, and to assess the resulting microplastic retention efficiency.

3.2.1 Detailed plant layout and main components of LSPP

The pilot plant layout and overall configuration are shown in Figure 8. The pilot system consists of a closed-loop hydraulic circuit in which the test fluid is continuously supplied to a pressurized surface filtration unit under controlled operating conditions. The main components of the pilot plant are schematized in Figure 8.

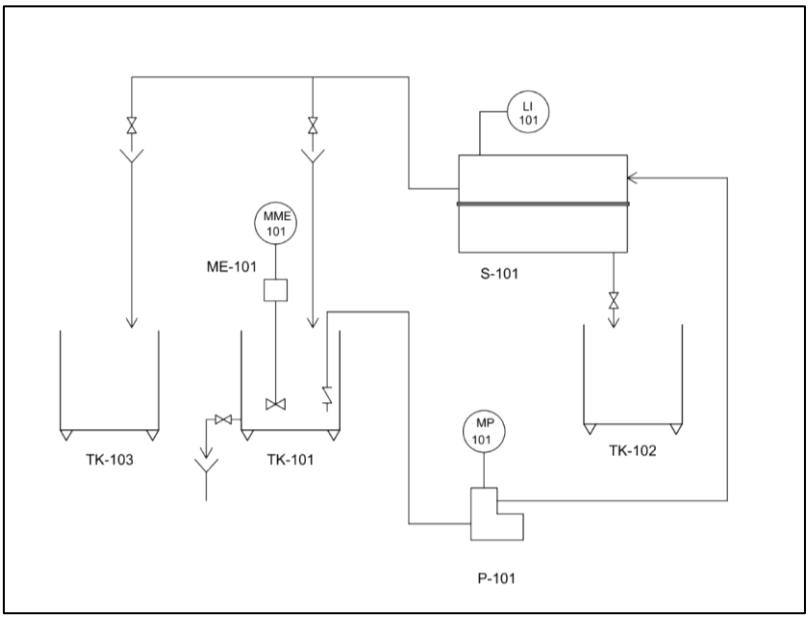

Figure 8: Simplified scheme of the surface filtration apparatus.

- **S-101**: surface filtration pilot unit;
- **P-101**: peristaltic feed pump;
- **TK-101**: feed tank;
- **LI-101**: vertical graduated rod for direct measurement of head loss (expressed as cm of water column);
- **ME-101**: propeller-type mixer installed inside the feed tank;
- **MME**-101: Motor of mechanical equipment
- **TK-102**: filtrate collection tank;
- **TK-103**: overflow tank.

The tested wastewater is initially loaded into the feed tank TK-101, which is manufactured from plastic material and has a nominal volume of 60 L. The tank is equipped with a graduated scale marked in 5 L increments, allowing direct visual control of the working volume, which is typically limited to a maximum of 50 L during operation. To ensure uniform test conditions, a propeller-type mixer (ME-101) is installed inside the feed tank to guarantee adequate homogenization of the suspension. The mixer operates at constant rotational speed and is positioned vertically, slightly above the bottom of the tank. This configuration prevents sedimentation of suspended solids while avoiding excessive shear stress on the particles. As a result, a minimum liquid volume of approximately 5 L must be maintained in the tank to guarantee effective mixing conditions.

From the feedtank, the wastewater is conveyed to the filtration unit by means of a peristaltic pump P-101 (ProMinent DULCO ® flex CONTROL DFXA). The pump operates within a flow rate range of 10–50 $L \cdot h^{-1}$, enabling precise control of the hydraulic loading applied to the filter. The suction line of the pump is equipped with a protective strainer, preventing the ingress of coarse particles that could damage the pumping system or interfere with flow regulation. The pumped wastewater then enters the surface filtration unit S-101, which is constructed of AISI 304 stainless steel and consists of two coupled elements forming a sealed filtration chamber. The unit is designed to accommodate flat filter media with nominal dimensions of 28.8 cm × 15.6 cm. The influent enters the filtration chamber through two lateral inlet slots located on the upper cover, promoting uniform distribution of the flow over the entire filter surface. After passing through the filter medium, the filtrate exits from the lower section of the unit and is conveyed to the filtrate collection tank.

As a result of the filtration process, particles with dimensions greater than or equal to the nominal mesh opening are retained on the filter surface, while smaller particles pass through the medium and are collected in the filtrate tank TK-102, a plastic made tank of 50L volume. An additional overflow tank TK-103 prevents excessive pressure buildup within the filtration chamber and ensures stable and safe operation of the pilot plant. In fact, as filtration progresses, the accumulation of retained solids leads to an increase in hydraulic head loss across the filter. When a critical head loss is reached, the influent flow is diverted directly to TK-103 without passing through the filter medium. Furthermore, the terminal section of the upper cover of the filtration unit allows the insertion of a small-diameter vertical tube acting as a piezometric column. The rise of the liquid inside this tube provides a direct measure of the hydraulic head within the filtration chamber. Head loss is visually monitored using the graduated rod LI-101, expressed in centimeters of water column, enabling real-time assessment of filter clogging during experimental runs. Finally, all pilot plant components are interconnected through plastic piping appropriately sized for the operational flow rates. An adjustable threaded rod system allows fine regulation of pipe positioning and elevation, enabling flexible adaptation of the pilot plant layout to different experimental configurations.

3.2.2 Tested filters on LSPP

The experimental tests carried out on the surface filtration pilot plant involved three different types of flat filter media, allowing the evaluation of filtration performance under varying material properties and nominal cut-off sizes. The selected filter media for testing were:

- Stainless steel (AISI 304) woven wire mesh with a nominal opening of 20 μm;
- Polyester/polyamide (MITA) free-fiber filters, including:
  - MICRO 12 with an equivalent filtration grade of 5 μm;
  - CLASSIC POLSTOFF with an equivalent filtration grade of 10 μm.

The stainless steel (AISI) filters, supplied by *Nuove Energie*, are characterized by a rigid rectangular woven mesh geometry with a nominal pore size of 20 μm. These filters are pre-shaped to fit the filtration unit and are representative of surface filtration media typically applied downstream of preliminary treatment units or as tertiary polishing steps in wastewater treatment plants.

A second category of filter media is represented by the MITA filters, composed of free-fiber materials made of polyester and/or polyamide. Prior to installation, these filters were cut to dimensions of 28.8 cm × 15.6 cm and subsequently trimmed along the perimeter to a depth of approximately 0.5 cm, ensuring proper hydraulic sealing within the filtration unit. Unlike rigid mesh filters, MITA filters show a combined surface–depth filtration behavior. In depth filtration, particles are retained within the complex pore structure of the medium rather than forming a cake only on the surface. During operation, the free fibers undergo compression, twisting, and interlacing, generating a three-dimensional porous matrix capable of efficiently retaining suspended solids. This retention mechanism is analogous to that observed in granular depth filters, such as sand filters. Due to this filtration behavior, MITA filters require a pre-wetting step prior to each filtration test to promote proper fiber arrangement and ensure repeatable performance. Owing to their fine filtration grades and combined surface–depth retention mechanisms, MITA filters are particularly suitable for tertiary treatment applications, especially upstream of final effluent discharge. The CLASSIC POLSTOFF filter consists of free polyamide fibers supported by a polyester weave, with an equivalent filtration grade of 10 μm and an areal weight of 1250 $g \cdot m^{-2}$. The MICRO 12 filter is composed entirely of polyester fibers and support weave, exhibits a finer equivalent filtration grade of 5 μm, and has an areal weight of 1400 $g \cdot m^{-2}$. Both filters have a free fiber length of 12 mm and comparable weft and warp densities. The filter tested at lab scale are represented in Figure 9.

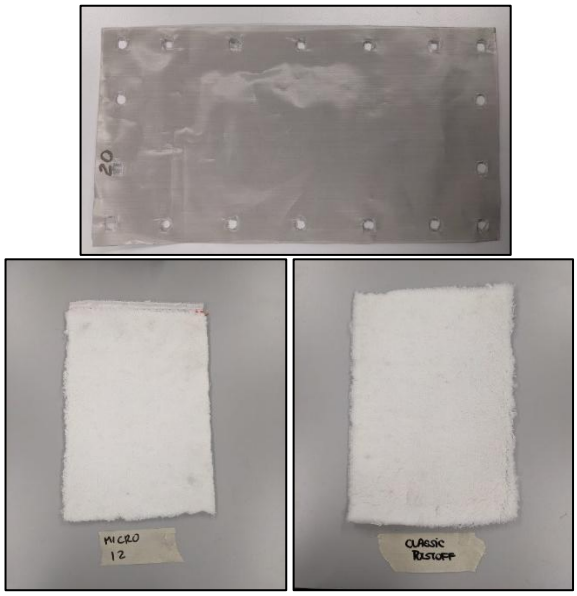

Figure 9: Filter media tested in the laboratory surface filtration pilot plant: stainless steel AISI 20 µm filter (top), MITA MICRO 12 polyester free-fiber filter (bottom left), and MITA CLASSIC POLSTOFF polyamide-based filter (bottom right).

The main physical and structural characteristics of the filter media tested in the laboratory-scale surface filtration pilot plant are summarized in Table 5.

Table 5: Main characteristics of the filter media tested.

Parameter	AISI 20	MITA POLSTOFF	MITA 12
Material	Stainless steel (AISI 304)	Polyamide fibers + polyester support	Polyester fibers + support
Filtration type	Surface filtration	Surface–depth filtration	Surface–depth filtration
Equivalent filtration grade (µm)	20	10	5
Free fiber length (mm)	—	12	12
Weft density (threads·cm^{-1})	—	11	12
Warp density (threads·cm^{-1})	—	19	19
Areal weight (g·m^{-2})	—	1250	1400

3.3 Demonstration-Scale Pilot Plants at Lariana

Filtration tests on the two demonstrative filtration pilot plants were carried out at the LarianaDepur WWTP. By the end of April 2025, the two demo plants were built and installed as preliminary treatment units, located downstream of the grit removal section. Therefore, the installation of the two pilot units was specifically conceived to allow comparative evaluation of different surface filtration technologies under identical hydraulic and influent wastewater conditions. According to the overall plant configuration in Figure 10, the installation of the pilot units in the preliminary treatment section allows direct treatment of raw wastewater after grit removal and before biological and tertiary processes. This positioning ensures that the filtration systems operate under representative influent conditions while avoiding interference from downstream biological or chemical treatment stages. As shown in the plant flow diagram, the treated flow subsequently follows the conventional treatment line, including biological treatment, tertiary processes, and final discharge to the Seveso River.

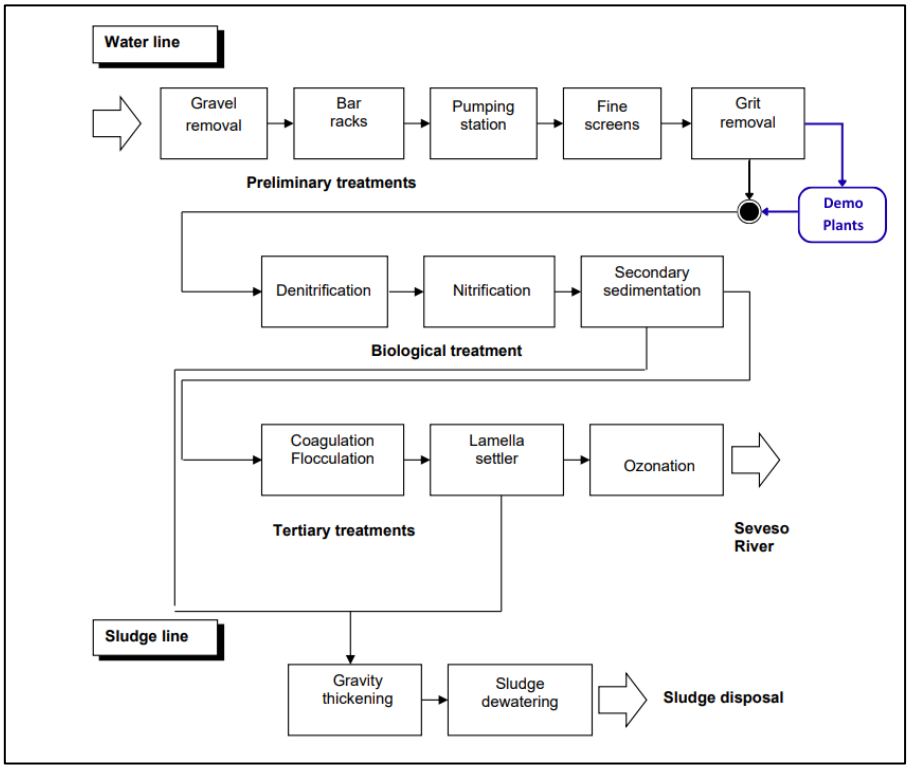

Figure 10: Alto Seveso WWTP flow diagram.

The demonstration scale pilot plants installed consist of a disc filter unit and a belt filter unit.

3.3.1 Overall P&I configuration

The entire pilot plant system is operated under automated control architecture managed by programmable logic controllers (PLCs). The PLCs supervise pump actuation, level control, flow monitoring, alarm management, and the activation of auxiliary systems, such as filter washing, according to predefined control logics. This automation mechanism ensures safe and stable operation of both demonstrative filtration units, whose piping and instrumentation diagram (P&ID) is reported below (Figure 11).

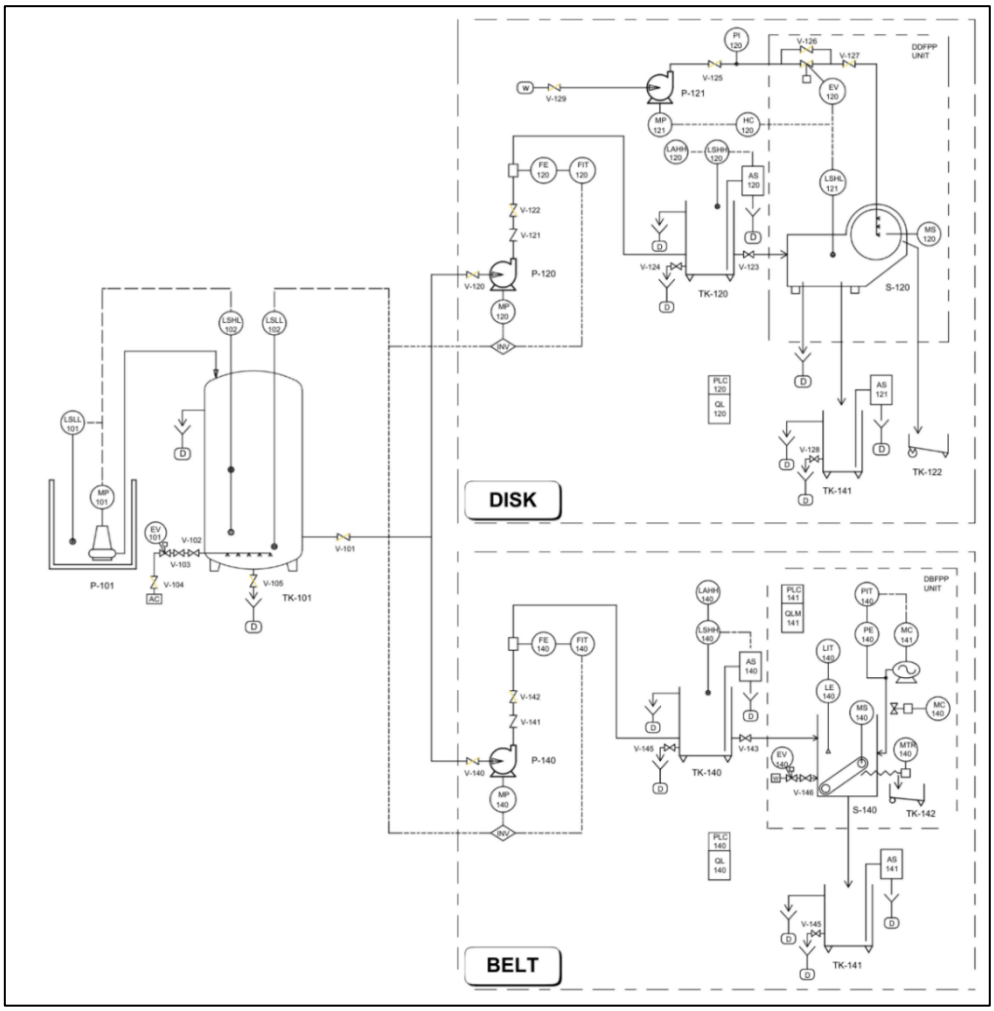

Figure 11: Piping and Instrumentation Diagram (P&ID) of the demonstration-scale filtration pilot plants installed at Lariana Depur.

The wastewater feeding both demonstrative filtration pilot plants is managed through a common feed tank (TK-101), which serves as a hydraulic buffer for the downstream disc (DDFPP) and belt (DBFPP) units.

After preliminary screening and grit removal, raw wastewater is transferred to TK-101 by the submersible centrifugal pump P-101, operating in discontinuous mode and designed for urban wastewater. At the operating point, P-101 delivers a flow rate of approximately 50 $m^3 \cdot h^{-1}$ with a head of 7.5 m, ensuring stable filling of the tank.The liquid level inside TK-101 is continuously monitored by conductivity level switches LSHL-102 and LSLL-102, which provide level-based control of pump P-101. The high-level switch prevents overfilling of the tank, while the low-level switch protects downstream equipment from cavitation conditions. From TK-101, wastewater is distributed to the two pilot units through independent feed lines, each equipped with a dedicated centrifugal pump (P-120 for the disc unit and P-140 for the belt unit) and flow measurement devices.

3.3.2 Disc filtration unit

The demonstration-scale disc filtration unit installed at the Lariana WWTP (Figure 12) corresponds to the CONOSCREEN CS 701 model and operates according to dynamic tangential filtration principle. This filtration mode is based on the tangential flow of wastewater along a moving filtration surface, generating shear forces that limit fouling and enable continuous solid–liquid separation under steady operating conditions. The unit is designed for the treatment of both urban and textile wastewater. The disc unit is equipped with automatic samplers installed on the influent and effluent process lines.

Figure 12: View of the DISC demonstration-scale filtration pilot plant installed at the Lariana Depur WWTP.

Wastewater is continuously fed to the filtration unit by pump P-120, equipped with variable frequency control and characterized by a nominal head of 4.8 m at maximum flow. The influent flow rate enters the disc filter (Figure 12) through a DN50 flanged inlet, while the filtered effluent exits through a DN125 outlet and is conveyed to the filtrate tank TK-122. The concentrated solid fraction is discharged separately by gravity into the solids collection tank TK-141, as indicated in the P&ID. The filtration unit S-120 consists of an AISI 304 stainless steel casing divided into three separate chambers: a chamber for the incoming wastewater to be filtered, a chamber dedicated to overflow discharge, and a chamber for the collection and discharge of the filtered effluent. Inside the filtration chamber, a pair of parallel rotating conical discs is installed. Each disc is fitted with metallic filter meshes made of AISI 304 stainless steel, with selectable filtration cut-off values ranging from 72 to 500 µm, depending on the installed mesh set. During operation, wastewater is pumped between the conical discs and flows tangentially across the filter meshes. The liquid fraction passes through the mesh openings, while suspended solids are retained between the disc surfaces (Figure 13).

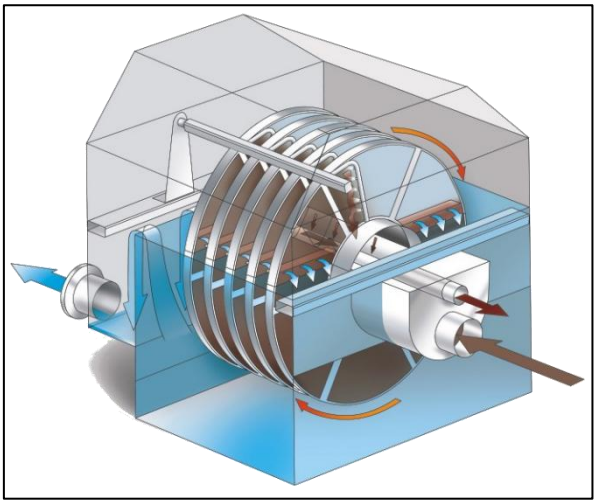

Figure 13: Schematic representation of the disc filtration unit.

When the influent level inside the unit reaches the threshold defined by the high-level switch LSHL-121, a backwashing cycle is activated. The backwashing system is supplied by the centrifugal multistage pump P-121, which delivers approximately 2 $m^3 \cdot h^{-1}$ at a pressure of 4 bar. Backwash water is drawn from the WWTP treated effluent and distributed through dedicated spray nozzles directed onto the disc surfaces. The activation of the washing system is controlled by the electro valve EV-120 and can be configured by the PLC control strategy. As solids continue to accumulate and thicken, once a predefined threshold is reached, the excess material is automatically discharged through the frontal opening between the conical discs, without interrupting filtration.

The discharged solid fraction exhibits a dry solids content in the range of 7–12% (Figure 14) which can be adjusted by modifying the rotational speed of the discs. This feature allows partial control over the degree of solid dewatering directly within the filtration unit.

Figure 14: Solid fraction discharged from the disc filtration unit.

3.3.3 Belt filtration unit

The demonstration-scale belt filtration unit installed at the Lariana WWTP is a surface filtration system that operates according to a gravity-driven filtration principle and is based on a continuously rotating polyethylene filter belt housed within a stainless-steel casing.

Figure 15: View of the Belt demonstration-scale filtration pilot plant installed at the Lariana Depur WWTP.

The system is suitable for the treatment of both urban and textile wastewater under continuous operating conditions. Wastewater feeding the belt filtration line is conveyed from the upstream feed tank to the belt filtration unit S-140 (Figure 15) by means of the horizontal centrifugal pump P-140. The pump operates in continuous mode allowing flow regulation in the range of 10–40 $m^3 \cdot h^{-1}$, with a nominal head of 6.3 m at maximum flow rate. Pump operation and regulation are directly managed by PLC-140. Wastewater enters the belt filtration unit (Figure 16), where the liquid level is detected by the level electrode LE-140 and converted into a continuous signal by LIT-140 for PLC-140 control. When the level remains below the operating threshold, the belt is stationary, allowing wastewater to accumulate on the filter cloth. Once the level exceeds the set threshold, the PLC activates the belt drive motor (MTR-140), and the belt speed is modulated to maintain stable operating conditions. The belt filtration unit is installed on a compact skid, with 1550 mm in width, 1350 mm in length, and 1500 mm in height, making it suitable for pilot-scale applications where space constraints are relevant.

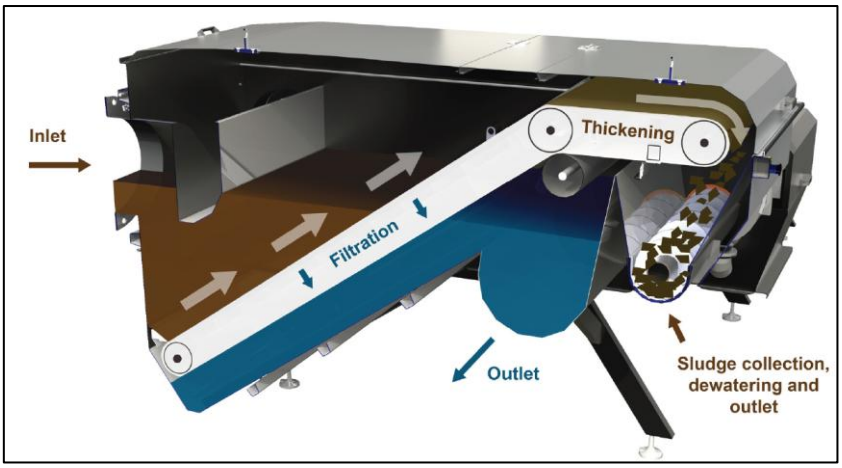

Figure 16: Main components of the belt filter and their role in the filtration process.

The influent wastewater is evenly distributed onto the polyethylene filter mesh through a dedicated inlet and distribution zone, preventing localized overloading and minimizing particle damage.

The filter mesh is mounted on a cogwheel system that ensures continuous and stable belt movement. As filtration proceeds, retained solids are conveyed along the belt towards the discharge section. An integrated screw conveyor (TR-140) transports the solids and provides partial mechanical dewatering prior to discharge. In addition, an automatic air-cleaning system (air knife) continuously cleans the filter surface during belt rotation. As a precautionary measure, an auxiliary hot-water flushing step is implemented, consisting of a 2-minute cleaning cycle activated at 6-hour intervals.

The filtered effluent is discharged to the downstream collection tank TK-141 and subsequently conveyed along the WWTP treatment line. Separate solids are collected in a dedicated solids collection unit, where further dewatering occurs, resulting in a dry solids content typically ranging between 30% and 45% (Figure 17).

Figure 17: Solid fraction discharged from the belt filtration unit.

3.3.4 Technical specifications

The Demonstration Disc Filtration Pilot Plant (DDFPP) and the Demonstration Belt Filtration Pilot Plant (DBFPP) were designed to operate under continuous filtration conditions, allowing a direct comparison of two surface filtration technologies within the same pilot-scale framework.

The table below (Table 6) aims to sum up the main technical and operational parameters of the two-demonstration unit.

Table 6: Comparative technical and operational parameters of the Demonstration Belt Filtration Pilot Plant and the Demonstration Disc Filtration Pilot Plant.

Parameter	BELT filter	DISC filter
Operation	Continuous filtration	Continuous filtration
Filter media material	Polyethylene	AISI 304 stainless steel
Filtration capacity (µm)	33–840	75–250
Indicative flow rate ($m^3 \cdot h^{-1}$)	20–36	2.5–10
Filtration principle	Gravity-driven surface filtration	Dynamic tangential filtration
Filter configuration	Continuous moving belt	Rotating conical discs
Number of filtering elements	1 belt	2 discs
Characteristic dimension of filter element (mm)	Belt width: 465 / 400 mm (total/effective)	Disc diameter: 700 mm
Submerged filtration area (m^2)	0.192	0.79
Supply tank volume (m^3)	2	2
Machine and tank material	AISI 316 L ; AISI 304 stainless steel	AISI 304 stainless steel

The DBFPP is based on gravity-driven surface filtration and operates with a filtration angle of 25°, which promotes solids transport and partial dewatering on the filter surface. The unit is designed to work within a filtration range of approximately 50–300 µm and can treat flow rates of up to 30 $m^3 \cdot h^{-1}$, making it suitable for pilot-scale applications in both industrial and municipal wastewater treatment. In contrast, the DDFPP unit operates continuously within an indicative flow rate range of 2.5–10 $m^3 \cdot h^{-1}$, with typical operating conditions between 5 and 10 $m^3 \cdot h^{-1}$. Both filtration units are equipped with a 1.5 kW feed pump and operate under a three-phase power supply (400 V, 50 Hz). The installed filtration power differs between the two technologies, amounting to 3.4 kW for the belt filter and 0.37 kW for the disc filter.

4 METHODS

This chapter presents the experimental methods applied in this work and outlines the methodological framework used to conduct the filtration tests on both laboratory scale and demonstration scale. The chapter also illustrates the operating conditions, sampling strategies, and analytical procedures applied; the final subsection provides a description of the microplastic extraction protocol followed, as well as the analytical and identification techniques used to determine microplastic concentrations.

4.1 LABORATORY-SCALE FILTRATION TESTS

Laboratory-scale surface filtration tests were carried out using the pilot-scale filtration unit described in Chapter 3.2, operated under controlled hydraulic conditions. Filtration tests were organized to assess the performance of three different filter media: AISI stainless steel (20 µm), MITA CLASSIC POLSTOFF (10 µm), MITA MICRO 12 (5 µm)—applied separately to each of the three textile wastewaters presented in Chapter 3.1. Before each test, filters were cleaned, dried at 80 °C, and weighed in dry conditions; the AISI stainless steel filter additionally underwent ultrasonic cleaning for 15 minutes. All experiments were conducted in batch mode with closed-loop operation to ensure constant influent characteristics throughout each filtration test. A constant filtration flow rate of 40 $L \cdot h^{-1}$ was selected as the reference operating condition (Figure 18), representing a compromise between hydraulic representativeness and stable system operation, and allowing direct comparison among the three different filter media.

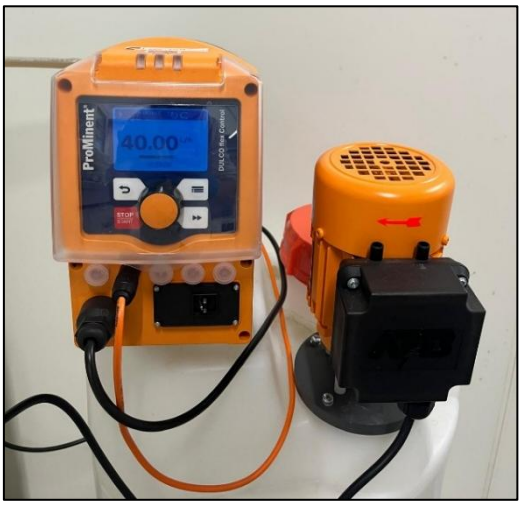

Figure 18: Peristaltic pump operated at the selected reference flow rate.

The effective filtration area was kept constant and defined by the geometry of the installed flat filter medium. For each test, a total wastewater volume of 25 L was filtered, while 35 L was initially introduced into the feed tank (TK-101) to guarantee adequate mixing during pumping. Prior to filtration, the wastewater was homogenized for 30 minutes using an internal propeller mixer, and a 5 L aliquot was collected in a plastic tank for further physicochemical characterization and microplastic extraction analyses. Hydraulic head loss across the filter was continuously monitored through a piezometric column, and a threshold value of 50 cm of water column was adopted as the operational limit. In the event of excessive head loss before completion of the target filtration volume, the peristaltic pump was temporarily stopped and the flow rate was gradually increased in steps of 5 $L \cdot h^{-1}$, up to a maximum of 50 $L \cdot h^{-1}$, to mitigate filter clogging; if stable operation could not be restored, the test was terminated.

At the end of each filtration test, the pilot filtration unit was disassembled to retrieve the filter medium. The filter was placed in a glass beaker and dried in a laboratory oven maintained at approximately 40 °C. The drying time was not fixed but continued until the filter was no longer perceived as wet when handled. Prior to weighing, the filters were conditioned in a desiccator for at least 30 minutes to allow thermal stabilization and minimize moisture interference. The filter mass was determined using a laboratory balance with a precision of ± 0.01 g, and the difference between the initial and final dry weight was used to estimate the amount of retained particulate solids, including microplastics. Furthermore, a 20 L filtrate sample was collected and stored in a plastic container at 4 °C for further analysis.

Before each test, all equipment was thoroughly rinsed several times with deionized water to prevent cross-contamination between different wastewater matrices. All experiments were performed at room temperature under constant mixing conditions to ensure homogeneous influent characteristics and reproducible operating conditions. The main experimental parameters used for the laboratory filtration tests are summarized in Table 7.

Table 7: Summary of operating conditions and experimental parameters applied during laboratory-scale filtration tests.

Parameter	Value	Notes
Reference Flow Rate ($L \cdot h^{-1}$)	40	Standard operating condition
Wastewater Volume In Feed Tank (L)	35	Ensures continuous supply
Filtered Volume Per Test (L)	25	Target treated volume
Pre-Mixing Time (min)	30	Homogenization
Filtration Area (cm^2)	200	Defined by filter geometry
Extracted Volume From Feed Tank (L)	5	Used for physicochemical analysys and MP extraction
Extracted Volume From Filtrate Tank (L)	20	

4.1.1 Sampling strategy

A structured sampling strategy was adopted to support both physicochemical analyses and microplastic extraction while minimizing contamination and sample alteration. For each filtration test, wastewater samples were collected at two main points: the influent and the filtrate (Figure 19).

Figure 19: Feed tank (left) for influent sampling before filtration and the filtrate tank (right) for sampling after passage through the filter medium.

Before starting each filtration run, 5 L of well-mixed wastewater were collected from the feed tank and used for influent characterization and microplastic analysis. After filtration, 20 L of the total filtered volume were collected from the filtrate tank and used for the same analytical purposes. The remaining filtered volume was discarded. All samples were collected in clean containers, sealed immediately after sampling, and stored at 4 °C until analysis. Sample handling and storage conditions were kept consistent throughout all tests to ensure comparability of results. The sampling volumes were selected to ensure sufficient material for both water quality analyses and microplastic extraction procedures.

4.1.2 Chemical and physicochemical analyses

Physicochemical analyses were performed on both influent and filtrate samples to evaluate the effect of surface filtration on conventional water quality parameters. The monitored parameters included pH, electrical conductivity, soluble chemical oxygen demand (sCOD), and total suspended solids (TSS). The first parameters (pH and electrical conductivity) were determined using a combined pH and conductivity meter, while soluble COD was determined using commercial cuvette tests supplied by Hach Lange ™ (LCK514). The sample was pre-filtered through a 0.45 µm filter in order to remove suspended solids and quantify only the dissolved organic fraction.

The selected kit has a measurement range of 100–2000 mg L^{-1} O_2 and is based on the dichromate digestion method followed by photometric determination. On the other hand, total suspended solids (TSS) were determined gravimetrically according to Standard Methods (APHA 2540 D). Glass fiber filters (GFC, 1.2 µm) were pre-conditioned, dried at 103–105 °C, cooled in a desiccator, and weighed through an analytical balance prior to filtration. After filtration using a pressurized system, filters were dried again at the same temperature until they gained constant weight, and they were re-weighed to determine suspended solids concentration.

4.2 Demonstration-scale filtration campaign

The demonstration-scale filtration campaign carried out at the Lariana WWTP extended over a prolonged experimental period, allowing evaluation of process performance under representative operating conditions. The campaign goal was to assess the behavior of two different filtration technologies when applied to real wastewater streams.

By operating the filtration units over several months and under a range of controlled hydraulic loading conditions, the experimental activity enabled the investigation of both short-term filtration efficiency and longer-term operational dynamics. This approach provided a good basis for comparing the Demonstration Disc Filtration Pilot Plant (DDFPP) and the Demonstration Belt Filtration Pilot Plant (DBFPP), as well as for evaluating the influence of key operational parameters such as flow rate, filtration duration, filter mesh size.

4.2.1 Test campaign organization

The first filtration test started on 14 May 2025 at 08:30, while the experimental campaign concluded on 30 January 2026 at 8:00, for a total of approximately nine months of operation. Overall, the testing program included 45 experimental runs, performed on both the Demonstration Disc Filtration Pilot Plant (DDFPP) and the Demonstration Belt Filtration Pilot Plant (DBFPP). The test campaign was organized in a way schematically shown in Figure 20.

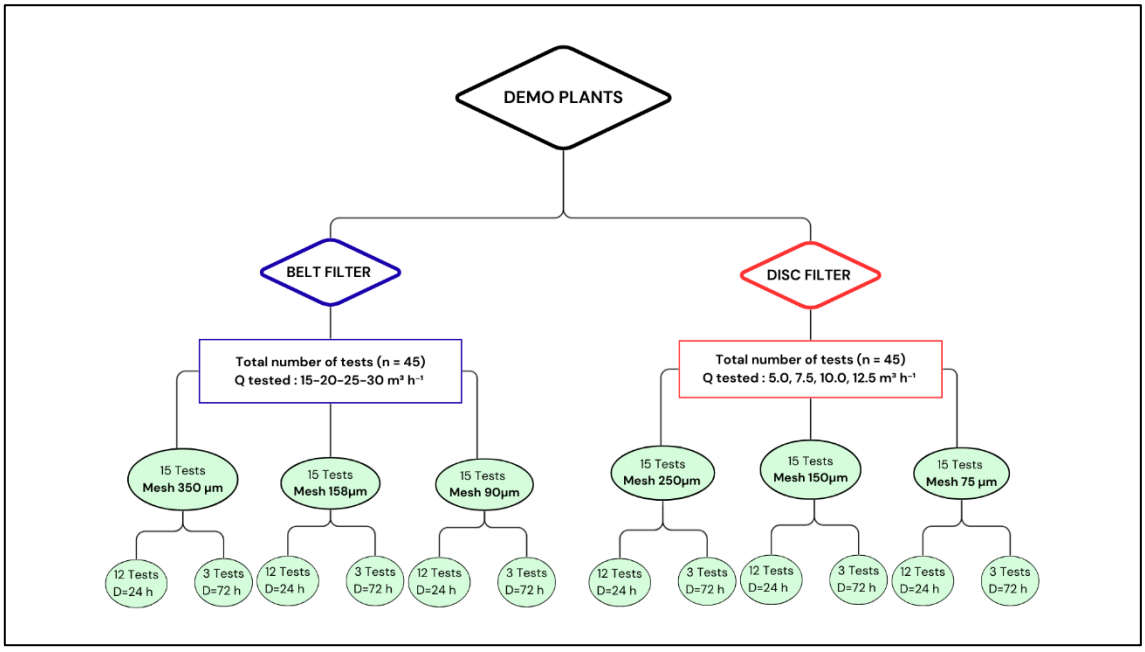

Figure 20: Schematic representation of the organization of the demonstration-scale filtration tests

As shown above, the tests carried out for each demonstration plant were organized into four macro-blocks. The first three macro-blocks each consisted of 12 filtration tests; all performed under the reference operational condition with a test duration of 24 h.

The fourth macro-block included the remaining 9 tests, which were intentionally extended to 72 h in order to investigate long-term filtration behavior and clogging dynamics under continuous operation; this block comprised three tests for each mesh size tested.

For each demonstration plant, different filtered flow rates were applied according to the respective design and operational principles. The belt filtration unit was operated at 15, 20, 25, and 30 $m^3 \cdot h^{-1}$, while the disc filtration unit was tested at 5.0, 7.5, 10.0, and 12.5 $m^3 \cdot h^{-1}$. Considering the effective filtration areas of 0.192 m^2 for the belt filter and 0.091 m^2 for the disc filter, these operating conditions corresponded to hydraulic loading rates of 78–104–130–156 $m^3 \cdot m^{-2} \cdot h^{-1}$ for the belt unit and 55–83–110–137 $m^3 \cdot m^{-2} \cdot h^{-1}$ for the disc unit. Most filtration cycles were conducted with a standard duration of 24 h, representing the reference operational condition. Only the final series of tests (Series 37–45) were extended to 72 h to evaluate long-term filtration performance and clogging dynamics under continuous operation. These long-duration tests were conducted at a flow rate of 25 $m^3 \cdot h^{-1}$ for the belt filter and 7.5 $m^3 \cdot h^{-1}$ for the disc filter.

Furthermore, to ensure representative influent conditions, filtration tests were preferentially scheduled between Tuesday and Thursday, corresponding to periods in which the industrial wastewater contribution to the plant influent is typically more stable and representative of normal operating conditions. Within this experimental framework, three MP extraction tests were carried out for each of the first three macro-blocks, selecting representative tests among the 24-h runs, while an additional three MP extraction tests—one for each mesh size—were performed within the 72-h macro-block. All MP extraction tests were conducted under the same hydraulic conditions, at a filtered flow rate of 25 $m^3 \cdot h^{-1}$ for the belt filter and 7.5 $m^3 \cdot h^{-1}$ for the disc filter, in order to ensure consistency and comparability of MP removal performance. Overall, this resulted in a total of 12 MP extraction tests conducted during the entire experimental campaign. The main parameters are reported in Table 8.

Table 8: Operational and hydraulic parameters adopted for the microplastic (MP) extraction tests during the filtration test campaign on the Demonstration Disc Filtration Pilot Plant and the Demonstration Belt Filtration Pilot Plant.

Parameter	DISC filter	BELT filter
Mesh Tested (µm)	250 – 150 – 75	350 – 158 – 90
Test Day	Tue–Wed–Thu	Tue–Wed–Thu
Total Mp Extractions (N°)	12	12
Filtered Flow Rate (m^3/h)	7.5	25
Hydraulic Loading Rate (m/h)	83	130
Sampled Streams	In – Out – Separate solid	In – Out – Separate solid

4.2.2 SAMPLING STRATEGY

At both the demonstration filtration units, wastewater sampling was performed using two automatic samplers installed on the influent and effluent liquid streams (Figure 21).

Figure 21: Samplying system (Endress+Hauser Liquistation CSF28)

The sampling systems (Endress+Hauser Liquistation CSF28) operate according to a vacuum suction principle.

The units are refrigerated samplers capable of maintaining the collected samples at controlled temperature conditions (approximately +4 °C ± 0.5 °C). Each of them is equipped with multiple collection bottles, up to four bottles of 13 L capacity, allowing composite sampling throughout the filtration cycle. The maximum suction head is approximately 6 m, ensuring reliable sample withdrawal from the process lines. The automatic samplers were used exclusively for the collection of liquid streams. At the end of each sampling cycle, the collected composite samples stored in the sampler bottles were transferred into 2 L laboratory bottles for subsequent physicochemical and microplastic analyses. Separated solids generated during the filtration process were not collected automatically; instead, they were manually retrieved from the accumulation tank of each filtration unit using a small scoop. Immediately after collection, an aliquot of each sample was analyzed for physicochemical characterization, while the remaining sample volume was stored in a refrigerated chamber at 4 °C to allow potential repetition of analyses.

4.2.3 Chemical and physicochemical analyses

Physicochemical analyses were carried out on influent and filtrate samples to evaluate filtration performance. The monitored parameters included pH, electrical conductivity, chemical oxygen demand (COD), total suspended solids (TSS), and solids fractions (TS, VS). The parameters pH and electrical conductivity were determined using a combined pH and conductivity meter equipped with a glass electrode and conductivity cell. Total Suspended Solids (TSS) were determined gravimetrically according to *Standard Methods for the Examination of Water and Wastewater* (APHA 2540 D). Differently from the procedure described in Section 4.1.2, a 0.45 µm cellulose acetate filter was used for sample filtration. Regarding the total solids (TS), they were determined gravimetrically by drying well-mixed samples at 103–105 °C until constant weight. The dried residue was subsequently ignited at 550 °C in a muffle furnace to distinguish fixed and volatile fractions; the mass loss upon ignition corresponds to volatile solids (VS), representing the organic fraction of the solids. Total COD was determined according to Standard Methods (APHA 5220 C) using the open reflux dichromate method. Twenty milliliters of each sample were digested under reflux for 2 h with 10 mL of 0.25 M potassium dichromate in strongly acidic conditions (H_2SO_4), in the presence of silver sulfate as a catalyst. After digestion, the excess dichromate was titrated with 10 mL of 0.125 N ferrous ammonium sulfate (FAS) using ferroin as indicator, with the endpoint identified by a color change from blue-green to reddish brown. Under these conditions, the method covers a chemical oxygen demand range of 0–1000 $mg \cdot L^{-1}$.

4.3 MICROPLASTIC ANALYTICAL METHODS

Microplastic analyses performed at both laboratory and demonstration scale were carried out following an extraction step, and then analysis and identification. The extraction phase that I performed at LIA lab and at Lariana Depur lab was intended to prepare the samples for subsequent quantitative MP analysis by isolating and concentrating microplastics from the original matrix. Following extraction, MP identification and quantification were performed by two different laboratories, namely Centro Tessile serico sostenibile (CTSS) and University of Brescia (UNIBS), which analyzed the demonstration-scale samples from the Lariana WWTP and the laboratory-scale filtered wastewater samples, respectively. The methods they use are reported in 4.3.2 for completeness.

Although the same extraction procedure was applied in all cases, minor adaptations were introduced to account for the different nature and complexity of the wastewater matrices, with the aim of ensuring effective removal of interfering materials and improving the recovery of MP.

4.3.1 COMPLETE MICROPLASTIC EXTRACTION PROTOCOL

The extraction of microplastics (MPs) was performed following a complete extraction protocol, adopted to ensure effective removal of organic and inorganic interfering materials prior to MPs identification and quantification. The full procedure was applied as originally defined (Zoccali, 2024) and is graphically summarized in Figure 22, where all the sequential steps of the extraction workflow are illustrated.

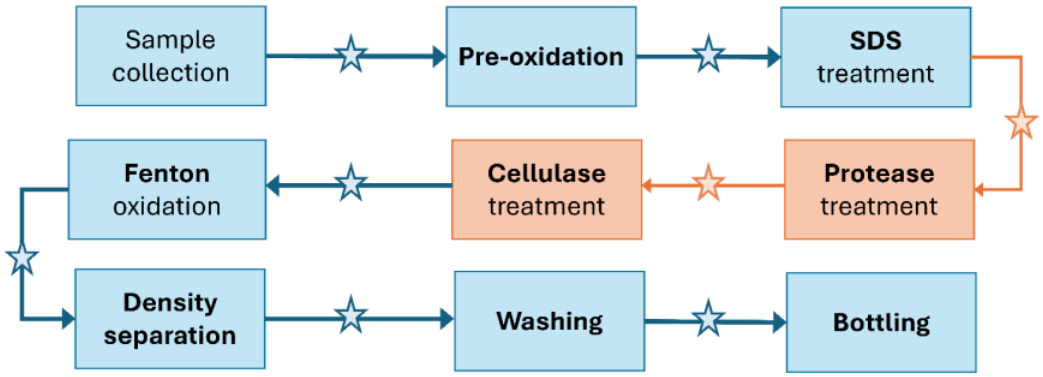

Figure 22: MPs extraction protocols. The steps of the simplified procedure are shown in blue, while additional steps for the complete protocol are indicated in orange.

.

Pre-oxidation step

"50 mL of H_2O_2 (35% w/w) were gradually added to the sample in a glass beaker, carefully monitoring the oxidation reaction, particularly the formation of foam and bubbles. This process was repeated twice daily for six days or until no bubbles or foam were observed after H_2O_2 addition."

SDS treatment

"The solution was filtered using the 10 µm mesh stainless steel filter. 250 mL of SDS solution (5% w/w) were measured and a portion was used to recover MPs from the previous step (MPs recovery). The beaker was placed in a water bath at 50 °C and agitated at 115 rpm for at least 24 hours."

Enzymatic digestion with Protease

"The sample was filtered using the 10 µm mesh stainless steel filter. 250 mL of TRIS buffer solution (pH = 8.2) were measured, with a portion used for MPs recovery from the previous step. Subsequently, 0.5 mL of Protease enzyme (Protease from Bacillus sp.®, ≥ 16 U/g, Sigma-Aldrich) was added to the sample, which was then placed in a water bath at 50 °C and agitated at 115 rpm for at least 40 hours."

Enzymatic digestion with Cellulase and Viscozyme

"The sample was filtered using the 10 µm mesh stainless steel filter. 250 mL of acetate buffer solution (pH = 4.8) were measured, with a portion used for MPs recovery from treatment with Protease. Subsequently, 1 mL of a Cellulase enzyme blend and 0.5 mL of Viscozyme® L, were added to the sample. The Cellulase enzyme blend (≥ 1,000 U/g) was prepared by mixing 9.5 mL of cellulase from Aspergillus sp. (≥ 1,000 U/g, Sigma-Aldrich) with 1 g of Xylanase enzyme powder (BakeZyme® HS 10.000 BG). Following incubation at 50 °C and 100 rpm for at least 40 hours, the samples were filtered and recovered in 138 mL of deionized water (MPs recovery) using the 10 µm mesh stainless steel filter. The sample was stored at 15–20 °C until the next step."

Fenton's oxidation

"207 mL of H_2O_2 (35% w/w), 65 mL of 0.1 M NaOH and 62 mL of 0.1 M $FeSO_4$ were measured separately… The temperature during this exothermic reaction was kept between 25–30 °. After 4–5 hours from the start of the reaction, the reaction rate stabilized, and the samples were left under the hood, at room temperature, to react overnight."

Density separation

"MPs were transferred to approximately 150 mL of zinc chloride ($ZnCl_2$) solution (density: 1.50–1.70 g/cm³). The mixture was mixed by insufflating compressed air in a separatory funnel for 15 min, then left to settle for 24 hours. Sediment was discharged every 2 hours and replaced with more $ZnCl_2$ until no sediment remained."

Final washing and concentration

"Approximately half the volume was discharged, while the rest, containing floating MPs, was rinsed with 1 L of deionized water to remove $ZnCl_2$ residues. MPs were collected, transferred to 600 mL of deionized water, incubated at 50 °C and 100 rpm overnight. Finally, the sample was filtered and rinsed with 100 mL of EtOH (30% w/w), before transferred into a small glass bottle (volume = 100 mL)."

4.3.2 Microplastic identification and quantification by µFTIR spectroscopy

Prior to MPs' identification and quantification, an additional filtration step was performed to obtain filters with a clearly identifiable number of particles. A representative sub-sampling of the liquid suspensions was conducted according to Standard Methods for the Examination of Water and Wastewater. The sample container was gently agitated to create a stable vortex ensuring homogeneous particle distribution. An aliquot of 1–2 mL was withdrawn using a glass pipette from mid-depth and at an intermediate radial position between the vortex core and the container wall. The collected sub-sample was filtered onto the prepared silicon filter (silicon area = 1 cm²; pore size = 5 µm) using a laboratory vacuum filtration unit. After filtration, the filter was rinsed at least three times with Milli-Q water and ethanol to remove residual matrix components while retaining MPs. The filter was then placed in a covered glass Petri dish and left to dry at room temperature prior to analysis (UNIBS) while samples analyzed at CTSS were dried in an oven at 40 °C for at least 8 hours. After these steps, microplastic identification and quantification were performed using micro-Fourier Transform Infrared spectroscopy (µFTIR). Although the analyses were carried out in two different laboratories and using distinct instrumental configurations, both approaches rely on the same analytical technique of spectroscopy: the acquisition of infrared absorption spectra from individual particles and their comparison with reference spectral libraries for polymer identification.

The differences between the two analytical setups presented below mainly concern the measurement mode, transmission versus reflectance, the type of supporting filter, and the operational strategy adopted for particle detection and analysis. These methodological choices were driven by the different characteristics of the analyzed samples, including particle concentration, matrix complexity, and particle size distribution, as well as by the specific instrumentation available at each laboratory.

4.3.2.1 µFTIR ANALYSIS OF LABORATORY-SCALE SAMPLES (UNIBS)

The laboratory samples were shipped to the University of Brescia. There, the sample container was gently agitated to create a stable vortex, ensuring homogeneous particle distribution. An aliquot of 1–2 mL was withdrawn using a glass pipette from mid-depth and at an intermediate radial position between the vortex core and the container wall. The collected sub-sample was filtered onto the prepared silicon filter (silicon area = 1 cm^2; pore size = 5 µm) using a laboratory vacuum filtration unit.

After filtration, the filter was rinsed at least three times with Milli-Q water and ethanol to remove residual matrix components while retaining MPs. The filter was then placed in a covered glass Petri dish and left to dry at room temperature before analysis. The dried filters were analyzed using a Nicolet iN10 MX microscope (Thermo Scientific, USA) equipped with a cooled mercury cadmium telluride (MCT) detector. MPs identification and quantification were performed manually by directly analyzing the filters and acquiring spectra from individual microparticles. Each µFTIR spectrum was collected in transmission mode over the 4,000–675 cm^{-1} range, with a spectral resolution of 8 cm^{-1} and an acquisition time of 12 s per measurement (64 scans). Spectral processing was carried out using OMNIC™ Specta™ software, and particle identification was achieved through comparison with both commercial and internally developed spectral libraries. Based on spectral matching, particles were classified as MPs or organic material and subsequently counted. When a high number of particles was present, only a portion of the filter area was analyzed, and total MP abundance was estimated by proportional scaling relative to the total filter area.

4.3.2.2 µFTIR ANALYSIS (CTSS)

The extracted and bottled samples from the Lariana WWTP were shipped to CTSS for subsequent analysis. Once there, the extracted sample was rinsed three times with Milli-Q water and Triton X solution (0.1% w/w) to ensure complete recovery of MPs.

After filtration, the filter was washed at least three times with Milli-Q water and ethanol to remove residual matrix components while retaining all particles. The filter was then placed in a glass Petri dish, covered with a glass lid or aluminum foil, and dried under controlled conditions depending on the laboratory; specifically, samples analyzed at CTSS were dried in an oven at 40 °C for at least 8 hours. Once dried, each silver membrane filter (diameter = 25 mm; pore size = 0.2 µm) was placed in the sample slide holder and analyzed using a Spotlight 400 FTIR microscope (PerkinElmer). To assess sample homogeneity and verify particle distribution, the entire filter surface was initially mapped through a Visible Image Survey. When required, additional verification was performed using a Leica MZ12 stereomicroscope to reduce uncertainty in particle identification. Following image acquisition, µFTIR analysis was conducted in point mode by manually collecting spectra from individual particles. Spectra were acquired in reflectance mode over the 4,000–650 cm^{-1} range using 8 or 16 scans per particle. Depending on the concentration and spatial distribution of microplastics, individual particles and fibers larger than 20 µm were analyzed separately. In cases of high particle density, only a representative portion of the filter area (typically 1/4, 1/8, or 1/16) was examined, and the total number of MPs was subsequently estimated by proportional scaling. The acquired spectra were processed and compared with reference databases, including the commercial Polymers Library and internally developed spectral libraries, to determine polymer identity.

4.3.3 Methodological adaptations between laboratory-scale and demonstration-scale analyses

As mentioned, this complete extraction protocol was applied to both laboratory-scale and demonstration-scale activities. However, due to the different nature and complexity of the wastewater matrices, particularly the textile wastewater treated at laboratory scale compared to the municipal wastewater from the Lariana WWTP, minor adjustments to specific extraction parameters were required. Consequently, differences were introduced while preserving the overall structure and sequence of the extraction protocol. These adjustments were implemented to ensure effective degradation of organic matter, complete recovery of microplastics, and comparability of the analytical results across different matrices and experimental scales. The main changes for laboratory-scale and demonstration-scale samples are summarized in Table 9.

Table 9: Main extraction parameters adopted for laboratory-scale and demonstration-scale microplastic analyses.

	Type of sample	*Samples analyzed (n°)*	*Sampled volume (L) or mass ($g_{DRYMATTER}$)*	*Pre-oxidation cycles (n°)*	*Cellulase enzyme blend - to-Viscozyme ratio (ml: ml)*	*Duration density separation (days)*
LAB TESTS	Influent	3	4	12	1: 0.5	3-4
	Effluent	9	8	6	1: 0.5	3-4
DEMO TESTS	Liquid	30	0.25-0,50	12-14	1: 0.5	7-10
	Solid	7	1 – 0,5	30-36	1: 1	10-15

5 LABORATORY-SCALE RESULTS

This section presents the results of the laboratory-scale filtration tests performed on the three textile wastewaters described in Chapter 3. Results are first introduced by summarizing the operating conditions of the laboratory-scale tests for each wastewater type. Subsequently, the outcomes of physicochemical analyses are presented, focusing on influent characteristics and corresponding filtrate quality. Finally, filtration performance is evaluated in terms of TSS and COD removal efficiencies, as well as microplastic retention.

5.1 BOSELLI – LABORATORY FILTRATION TESTS

5.1.1 OPERATING CONDITIONS AND HYDRAULIC BEHAVIOR

The laboratory-scale filtration tests performed on the Boselli wastewater are summarized below. The main operating conditions and key measured or calculated parameters, including test duration, hydraulic loading rate, head loss development, clogging occurrence, and retained solids mass, are reported in Table 10.

Table 10: Operating conditions of the laboratory-scale filtration tests conducted on the Boselli textile wastewater.

Filter tested	Test duration (min)	HLR (m/h)	Final head loss (cm)	Overflow (Yes/No)	Retained solids (g)
AISI20	60	2	-	No	0
MITA12	57	2.1	-	No	0.03
MITA POLSTOFF	60	2	-	No	0.39

The results reported show that all filter configurations were operated under comparable hydraulic loading conditions and test durations.

No head loss development was observed during any of the filtration runs, and no clogging or overflow events occurred, indicating stable hydraulic behavior for all tested filters over the experimental period. The mass of retained solids varied among the filter media, with negligible retention observed for the AISI20 filter and the MITA12 filter, and a more pronounced solids retention for the MITA POLSTOF filter. These differences suggest an increasing solid capture capacity associated with the finer and more structured filter media under the applied operating conditions. The very low amount of retained solids observed for all filter configurations suggests that the Boselli wastewater is likely characterized by a predominance of very fine suspended particles. This indicates that a significant fraction of the particulate matter may consist of particles smaller than the effective filter mesh or may be present in a colloidal form. In addition, possible inaccuracies during wastewater sampling, such as insufficient mixing of the storage tank prior to sample collection, may have contributed to the unusually low retained solids values.

5.1.2 Physicochemical characteristics and filtration performance

The main physicochemical characteristics of the Boselli wastewater influent and corresponding filtrates are summarized in Table 11. The reported parameters refer to single measurements and describe the quality of the raw wastewater generated from a polyester–elastane fabric dyeing process prior to filtration (influent) and after filtration through the different filter media (filtrates).

Table 11: Physicochemical characteristics of the Boselli wastewater influent and corresponding filtrates.

Parameters	Influent	Filtrate-AISI20	Filtrate-MITA12	Filtrate-MITA POLSTOFF
pH	4.67	5.25	5.33	5.94
Electrical Conductivity ($\mu S \cdot cm^{-1}$)	420	295	473	300
TSS ($mg \cdot L^{-1}$)	17	12	14.9	11
Filtered COD ($mg \cdot L^{-1}$)	903	800	785	747
COD / TSS	53	68	52	68

The analyses conducted on the influent are consistent with previous characterizations of the same wastewater type, confirming an acidic pH, moderate COD concentration, and a low suspended solids content, typical of dyeing effluents dominated by soluble organic matter.

Filtration resulted in a slight increase in pH for all tested filter media, with values remaining within the acidic range. Electrical conductivity exhibited no clear variation after filtration and remained of the same order of magnitude as the influent, suggesting that the process had a negligible effect on the dissolved ionic fraction. Furthermore, Boselli wastewater is characterized by a very high COD/TSS ratio and the overall nature of the wastewater was not significantly modified by filtration. Regarding filtration performance, limited removal of suspended solids and chemical oxygen demand was observed overall (Figure 23).

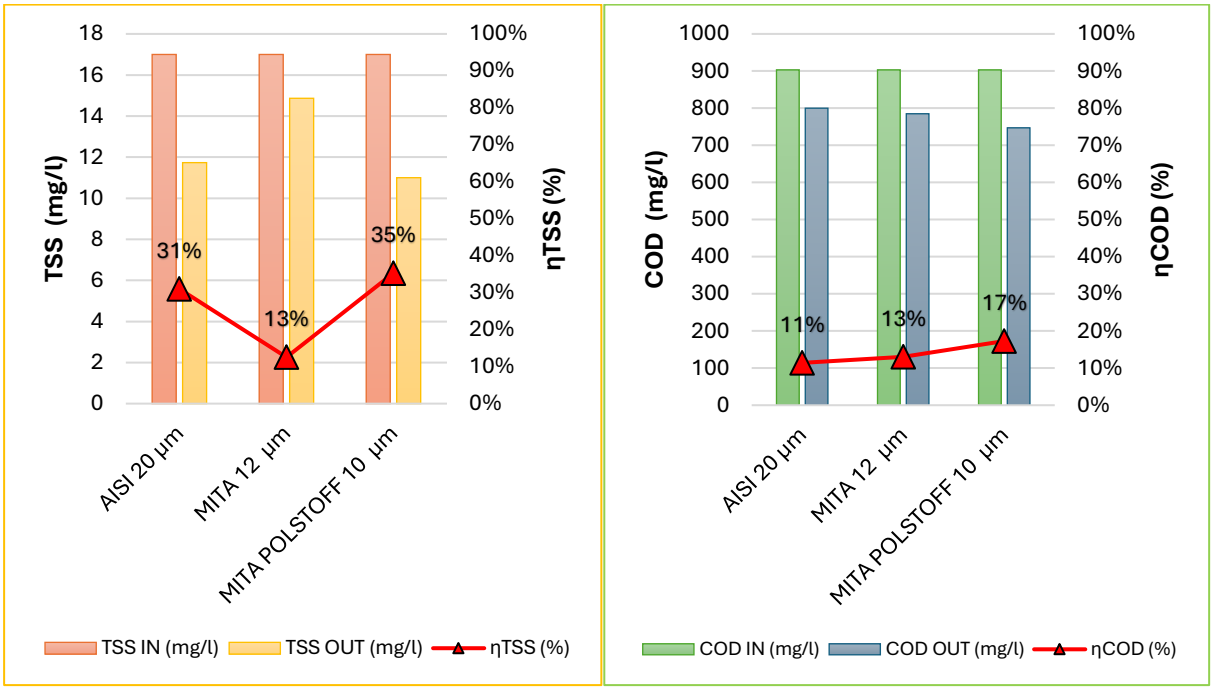

Figure 23: Bar plots showing TSS and COD removal, together with the corresponding influent and outlet concentrations.

The analysis results show that TSS removal efficiencies remain overall low for all the tested filters, with values ranging approximately between 10% and 35%. Among the three filtration media, the MITA 12 filter, characterized by the smallest equivalent filtration grade, exhibits the lowest TSS removal performance according to the analyses conducted. This behavior can be primarily attributed to the intrinsic characteristics of the treated wastewater, which is of textile origin and therefore characterized by relatively low concentrations of suspended solids and by a predominance of fine and fibrous particles.

Under these conditions, differences in nominal mesh size are less influential, and the overall removal performance becomes strongly affected by analytical uncertainty associated with TSS measurements. Filtered COD concentrations showed a moderate decrease after filtration, with removal efficiencies ranging between 11% and 17%, and the highest COD removal observed for the MITA POLSTOFF filter. Nevertheless, COD levels remained relatively high in all filtrates, confirming that the organic load was largely present in soluble form as supported by the high COD/TSS ratio equal to approximately 60.

5.1.3 Microplastic Removal performance

The data related to the extraction analyses on MPs are not currently available and, therefore, will not be presented. This decision is due to the problems encountered during the analysis and quantification phase of MPs, which did not allow results to be obtained within the time frame for the presentation of the present thesis work. Consequently, in order to ensure the correctness and quality of the information reported, these data were excluded from the present work.

5.2 Comofil – laboratory filtration tests

5.2.1 Operating conditions and hydraulic behavior

The laboratory-scale filtration tests performed on the Comofil wastewater are summarized in Table 12.

Table 12: Operating conditions of the laboratory-scale filtration tests conducted on the Comofil textile wastewater.

Filter tested	Test duration (min)	HLR (m/h)	Final head loss (cm)	Overflow (Yes/No)	Retained solids (g)
AISI20	60	2	-	No	0.06
MITA12	57	2.1	-	No	0.27
MITA POLSTOFF	60	2.2	-	No	1.05

Under the tested operating conditions, no significant head loss development was observed for any of the filter media, and no clogging or overflow events occurred during the filtration runs. As reported, the retained solids mass was evaluated for each filter configuration. In one case, the gravimetric determination of retained material in the MITA12 test resulted in a negative value (-0.41g). This outcome was attributed to measurement uncertainty associated with low suspended solids concentrations and weighing sensitivity. For this reason, the retained solids mass was instead estimated by calculating the product of the difference between influent and filtrate TSS concentrations and the treated volume (ΔTSS × V), providing a more reliable representation of the actual solids retained by the filter. In general, the test results indicate stable hydraulic performance and suggest that, under the applied hydraulic loading rates and test durations, all filter configurations operated without hydraulic limitations.

5.2.2 Physicochemical characteristics and filtration performance

The main physicochemical characteristics refer to single measurements of the Comofil wastewater influent and corresponding filtrates are summarized in Table 13. The influent originates from a polyester yarn stripping process and, in agreement with previous characterizations of similar effluents, showed strong alkaline pH, high electrical conductivity, and very high COD concentrations, associated with the presence of residual dyes and reducing agents

Table 13: Physicochemical characteristics of the Comofil wastewater influent and corresponding filtrates.

Parameters	Influent	FILTRATE-AISI20	FILTRATE-MITA12	FILTRATE-MITA CLASSIC
pH	11.94	12.3	12.27	12.33
Electrical Conductivity ($\mu S \cdot cm^{-1}$)	5470	4780	4830	4890
TSS ($mg \cdot L^{-1}$)	20	10	9.00	7
Filtered COD ($mg \cdot L^{-1}$)	1953	1224	1256	1166
COD/TSS	98	122	139	166

Filtration tests did not induce significant changes in pH, which remained strongly alkaline for all filter media, neither substantially affect electrical conductivity, which showed only minor variations after filtration. These results indicate that the filtration process had a limited impact on the dissolved ionic fraction of the wastewater, as expected for physical surface filtration processes. The influent COD/TSS ratio (COD_IN/TSS_IN ≈ 98) confirms the predominance of soluble organic matter, explaining why COD removal was significant but still limited compared to suspended solids removal. In contrast, a clear reduction in suspended solids was observed for all tested filters (Figure 24).

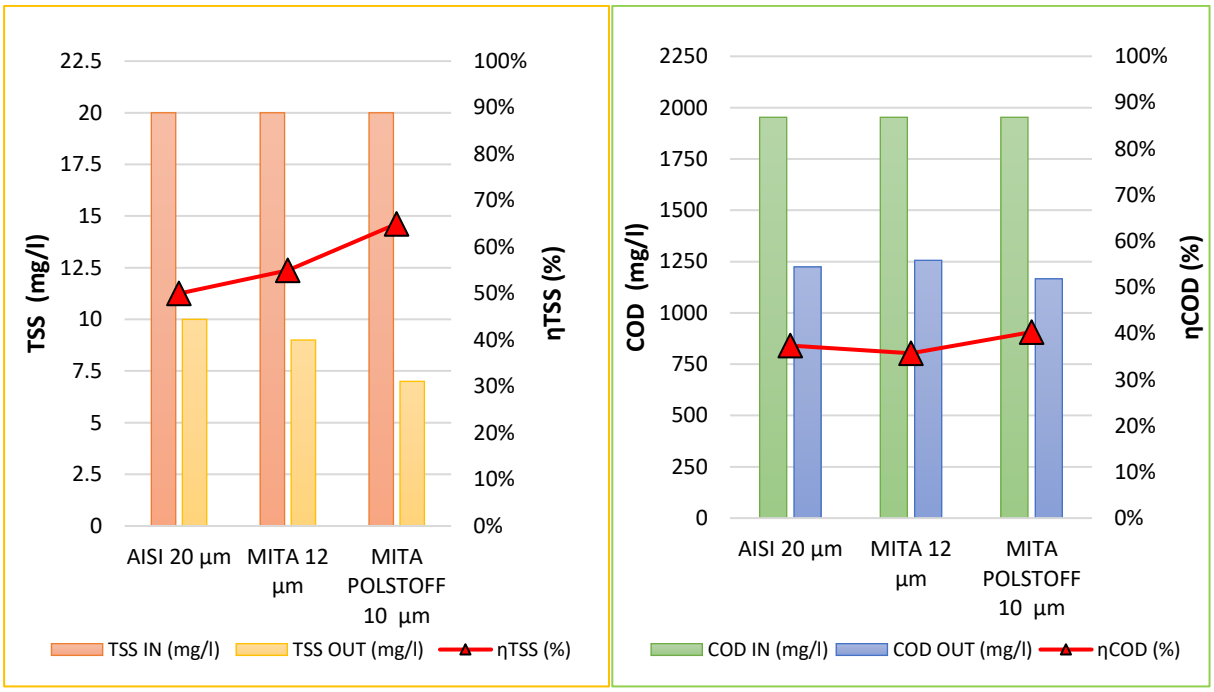

Figure 24: Bar plots showing TSS and COD removal, together with the corresponding influent and outlet concentrations.

TSS concentrations decreased from 20 mg·L^{-1} in the influent to 10, 9, and 7 mg·L^{-1} for the AISI20, MITA12, and MITA POLSTOFF filters, respectively. Contrary to expectations, TSS removal efficiency did not increase proportionally with decreasing filter cutoff; in fact, the highest removal efficiency (65%) was achieved by the MITA POLSTOFF filter, characterized by a nominal cutoff of 10 µm, which is higher than that of the MITA12 filter (equivalent cutoff of approximately 5 µm). A similar trend was observed for COD removal, with filtered COD concentrations ranging between 1166 and 1256 mg·L^{-1}, corresponding to removal efficiencies between 36% and 40%.

5.2.3 Microplastic Removal performance

The data related to the extraction analyses on MPs are not currently available and, therefore, will not be presented. This decision is due to the problems encountered during the analysis and quantification phase of MPs, which did not allow results to be obtained within the time frame for the presentation of the present thesis work. Consequently, in order to ensure the correctness and quality of the information reported, these data were excluded from the present work.

5.3 Lipomo – laboratory filtration tests

5.3.1 Operating conditions and hydraulic behavior

As shown in Table 14, different hydraulic behaviors were observed among the tested filter media. While the MITA12 and MITA POLSTOF filters operated without head loss development, clogging, or overflow events, the AISI20 filter exhibited unstable hydraulic performance under the applied operating conditions.

Table 14: Operating conditions of the laboratory-scale filtration tests conducted on the Lipomo textile wastewater.

Filter tested	Test duration (min)	HLR (m/h)	Final head loss (cm)	Overflow (Yes/No)	Retained solids (g)
AISI20	52	2.3	<50cm	Yes	0.88
MITA12	57	2.1	-	No	22.14
MITA POLSTOFF	62	1.9	-	No	1.06

In the case of the AISI20 filter, overflow conditions were first observed approximately 16 minutes after the start of the test, accompanied by an initial increase in head loss, which reached values of 5–7 cm after about 26 minutes.

As the filtration proceeded, head loss continued to increase, reaching peak values up to approximately 48 cm, and showing a markedly intermittent and oscillating behavior. This behavior seems to suggest the occurrence of formation and sudden release of accumulated solids within the filter structure. Furthermore, the relatively high value of retained solids reported for the MITA12 filter should be interpreted with caution, as it is likely affected by experimental uncertainty and handling inaccuracies. This interpretation is supported by an independent estimation of retained solids based on TSS measurements, which yield a substantially lower value of approximately 1.75 g. This discrepancy suggests that the measured value may be overestimated and does not fully reflect the actual solids retention under the tested conditions.

5.3.2 Physicochemical characteristics and filtration performance

The Lipomo wastewater represents the final discharge of the LIPOMO textile printing and finishing facility and based on prior characterizations, is expected to show slightly alkaline pH, high COD, elevated suspended solids, and a substantial microplastic load, reflecting the combined contribution of multiple wet processing operations. The data in Table 15 refer to single measurements.

Table 15: Physicochemical characteristics of the Comofil wastewater influent and corresponding filtrates.

Parameters	Influent	FILTRATE-AISI20	FILTRATE-MITA12	FILTRATE MITA POLSTOFF
pH	12.54	9.7	9.2	9.74
Electrical Conductivity ($\mu S \cdot cm^{-1}$)	6100	2970	2940	2870
TSS ($mg \cdot L^{-1}$)	113	96	44	86
Filtered COD ($mg \cdot L^{-1}$)	1144	495	506	486
COD/TSS	10	5	12	6

As reported in table above, the influent exhibited a strongly alkaline pH (12.54), high electrical conductivity, elevated suspended solids, and a high COD concentration, in agreement with previous characterizations of composite textile printing and finishing effluents. Filtration resulted in a marked decrease in pH for all filter media, with values ranging between 9.2 and 9.74, although the wastewater remained alkaline after treatment. Electrical conductivity showed a consistent reduction of approximately 50% for all filtrates, indicating a partial removal of ionic species associated with the particulate fraction and highlighting the contribution of suspended solids to the overall conductivity of the influent. The influent exhibited a COD/TSS ratio of approximately 10, indicating that a large fraction of the organic load was present in dissolved form. The bar plots showing TSS and COD removal (Figure 25), together with the corresponding influent and outlet concentrations, are presented below.

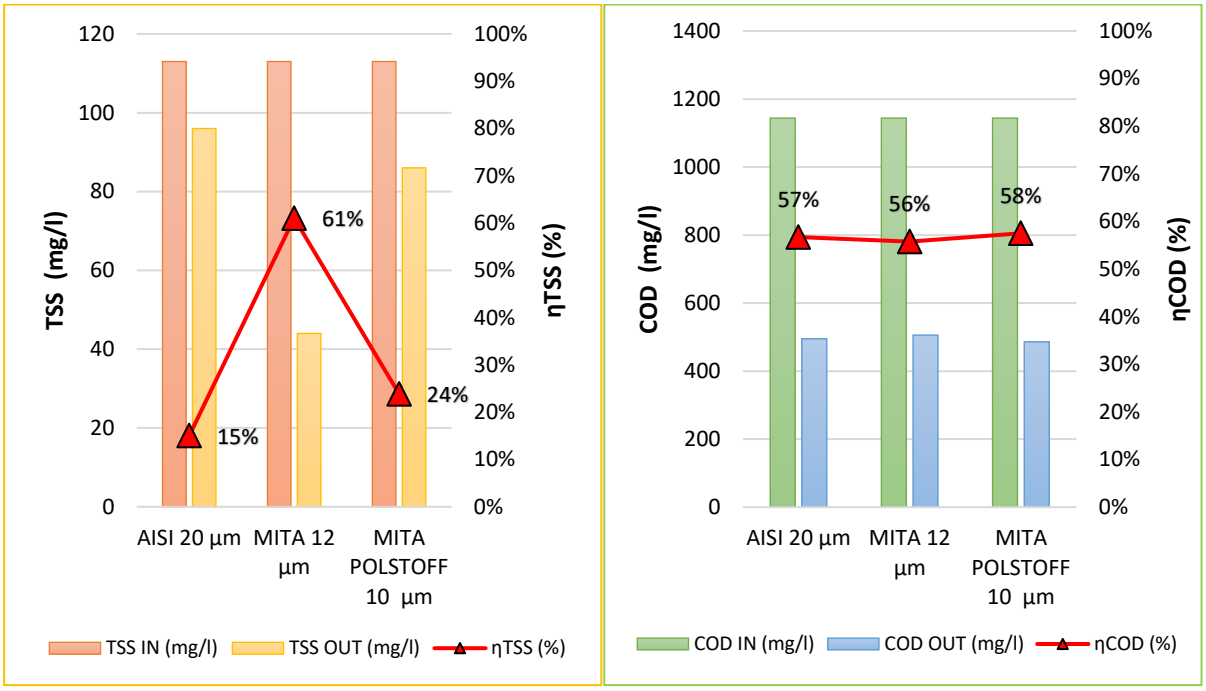

Figure 25: Bar plots showing TSS and COD removal, together with the corresponding influent and outlet concentrations.

A substantial reduction in TSS concentration was observed after filtration, with removal efficiency strongly dependent on the filter medium. The MITA12 filter, characterized by an effective cutoff equivalent to 5 µm, achieved the highest TSS removal efficiency (61%), reducing TSS from 113 $mg \cdot L^{-1}$ to 44 $mg \cdot L^{-1}$. In contrast, the AISI20 and MITA CLASSIC filters exhibited more limited TSS removal (15% and 24%, respectively). Filtered COD concentrations decreased from 1144 $mg \cdot L^{-1}$ in the influent to values between 486 and 506 $mg \cdot L^{-1}$ in the filtrates, corresponding to COD removal efficiencies of approximately 56–58% for all filter media.

This relatively constant COD removal indicates that only a minor fraction of the organic load is associated with suspended solids, while the dominant contribution is attributable to dissolved or colloidal organic matter. As a result, variations in TSS removal do not translate into proportional changes in COD abatement, which remains weakly dependent on filter cutoff and primarily controlled by wastewater composition. Despite the observed reduction, COD concentrations remain relatively high, reflecting the intrinsically elevated organic load typical of printing and finishing wastewater.

5.3.3 Microplastic Removal performance

In the case of Lipomo WW, the results related to MPs were obtained; however, also in this case, the UNIBS laboratory is carrying out further replicates in order to understand whether it is possible to refine the analysis, since the filters appear to be very loaded, albeit with recognizable particles. The results obtained in terms of microplastic concentration are reported below (Figure 26).

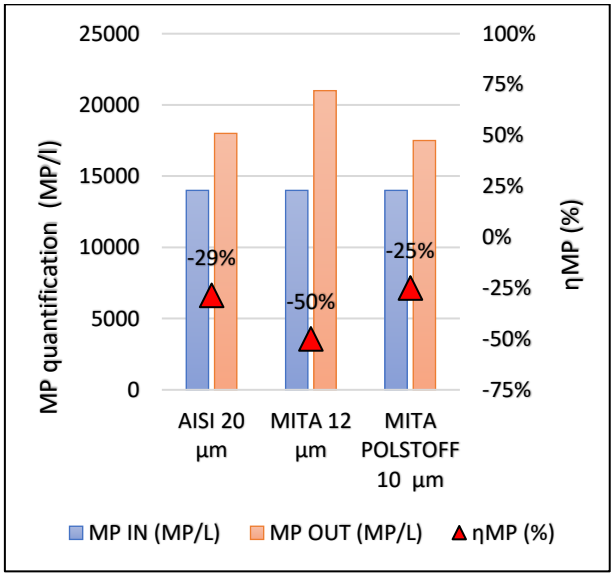

Figure 26: Laboratory-scale microplastics quantification in influent (MP_IN) and effluent (MP_OUT) and corresponding removal efficiency (η_MP) for the Lipomo wastewater, obtained using different filter meshes (AISI 20 µm, MITA 12 µm, and MITA Polstoff 10 µm).

The MP values expressed in MP/L are, however, inconsistent, as they lead to negative removal efficiencies, indicating an apparent increase of MPs at the plant outlet. This result has little physical meaning and suggests that, also in this case, the data presented cannot be considered reliable.

In all three WW analyzed, the laboratories encountered problems of filter clogging; the most probable causes can be attributed to the textile nature of the wastewater, combined with an extraction procedure that proved to be insufficiently effective in ensuring samples composed exclusively of MPs.

5.4 Overall laboratory-scale filtration performance by filter type

To provide an overall comparison of laboratory-scale filtration performance, the removal efficiencies of TSS and COD obtained with the different filter media were analyzed across the investigated textile wastewater (Figure 27).

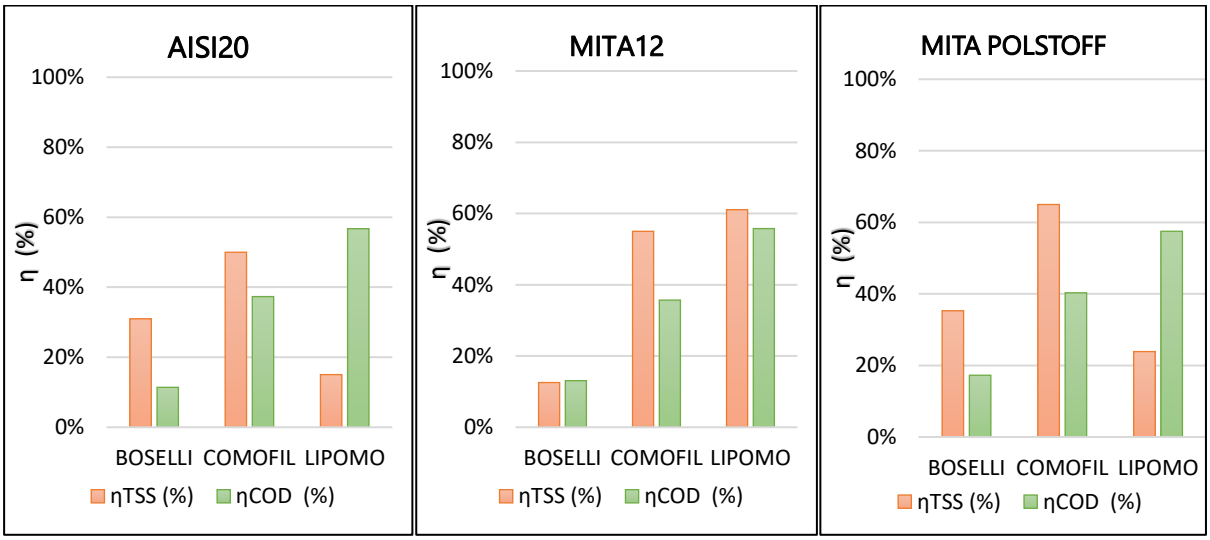

Figure 27: Laboratory-scale TSS and COD removal efficiencies obtained for the three investigated filter media across the different textiles wastewater.

Although filtration performance is strongly influenced by wastewater characteristics, some qualitative differences among the filter media can be identified from the laboratory-scale results. Overall, the AISI 20 filter achieved TSS removal efficiencies ranging approximately from 15% to 50%, while COD removal varied more widely, between about 10% and 55%, depending on the treated wastewater. The MITA 12 filter showed a broader variability in TSS removal, with very low efficiency for Boselli wastewater and values up to about 60% for Comofil and Lipomo, while COD removal generally ranged between 10% and 55%.

The MITA POLSTOFF filter exhibited TSS removal efficiencies between approximately 25% and 65%, with the highest values observed for Comofil wastewater, whereas COD removal remained between about 20% and 60%. Overall, no single filter consistently outperforms the others across all wastewaters and parameters. TSS removal appears to be more sensitive to the interaction between filter structure and wastewater characteristics than to the nominal cutoff alone, as highlighted by the variable performance observed for the same filter when treating different effluents. In contrast, COD removal shows a more homogeneous behavior across filter types, suggesting that a significant fraction of the organic matter is present in dissolved or colloidal form and is therefore weakly affected by surface filtration. Nevertheless, the lack of a clear relationship between nominal filter cutoff and removal efficiency confirms that laboratory-scale filtration performance cannot be reliably predicted only on the basis of nominal filter characteristics but must be interpreted considering wastewater composition and particulate properties. A direct comparison of microplastics removal efficiencies among the laboratory-scale tests was not possible due to the lack of complete and consistent microplastics data.

6 DEMONSTRATION-SCALE FILTRATION RESULTS

This chapter presents the results obtained from the demonstration-scale filtration tests carried out at the Lariana WWTP. Results are organized to first describe the influent characteristics during the campaign period, followed by an assessment of physicochemical removal performance and, finally, microplastic removal efficiency for both filtration technologies and mesh sizes.

6.1 INFLUENT CHARACTERIZATION

The influent wastewater treated by the two demonstration-scale filtration units originated from the same inlet stream of the Lariana WWTP. Therefore, influent characterization is the same for both units and represents the baseline conditions under which the filtration performance was evaluated. Table 16 summarizes the main physicochemical characteristics of the influent wastewater, reported as mean values, standard deviation, and minimum–maximum ranges during the experimental period, from 14 May 2025 to 30 January 2026.

Table 16: Physicochemical parameters of the influent wastewater.

Parameter	Mean	SD	Min–Max
pH	7.8	0.31	7.3-8.4
Temperature (°C)	18.0	2.98	11.0-22.9
Electrical conductivity (µS/cm)	1205	202	816.0 - 1,651
TSS IN (mg/l)	141	70	34-384
Total COD IN (mg/l)	302	89	137-542
Total COD IN / TSS IN	2.39	0.57	1.41-4.03

The influent pH remained relatively stable throughout the monitoring period, with an average value of 7.8 ± 0.31, falling within a slightly alkaline range typical of treated industrial wastewater. Temperature varied between 11.0 and 22.9 °C, reflecting seasonal conditions during the experimental campaign. Electrical conductivity showed moderate variability (1205 ± 202 $\mu S \cdot cm^{-1}$), consistent with the presence of dissolved salts associated with textile processing activities. Overall, the combined graphical and statistical characterization confirms that the influent wastewater was characterized by variable but representative concentrations of suspended solids and organic matter, while the COD/TSS ratio confirms the predominance of particulate-associated organic matter. These data are in line with the characterization of the Lariana influent presented in Chapter 3.

To further explore the variability of influent characteristics, boxplots of TSS and total COD concentrations are presented in Figure 28.

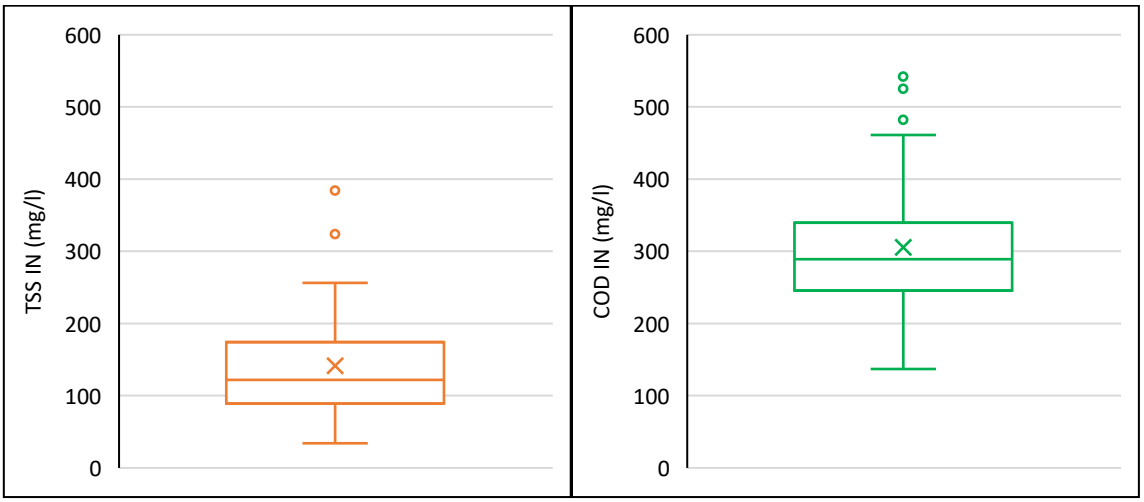

Figure 28: Boxplots showing the distribution of influent TSS (left; n=45) and total COD (right; n=45) concentrations measured during the demonstration-scale campaign.

The boxplot of influent TSS concentrations shows moderate variability, with a median of 122 $mg \cdot L^{-1}$ and an interquartile range between 89 $mg \cdot L^{-1}$ (Q1) and 166 $mg \cdot L^{-1}$ (Q3). The mean value (140.9 $mg \cdot L^{-1}$) is higher than the median, indicating slight right-skewness due to a limited number of higher values identified as outliers. The influent total COD boxplot exhibits higher variability compared to TSS, with a median concentration of 289 $mg \cdot L^{-1}$, first and third quartiles equal to 246 $mg \cdot L^{-1}$ and 335 $mg \cdot L^{-1}$, respectively. The mean total COD value (302.4 $mg \cdot L^{-1}$) exceeds the median, suggesting a right-skewed distribution influenced by episodic increases in organic load. These higher concentrations are probably associated with transient variations in upstream industrial discharges or hydraulic conditions at the WWTP inlet.

Compared to TSS, influent COD concentrations showed a broader distribution, indicating higher temporal variability in organic load compared to suspended solids. The relationship between total COD and TSS concentrations was further investigated through a scatterplot (Figure 29).

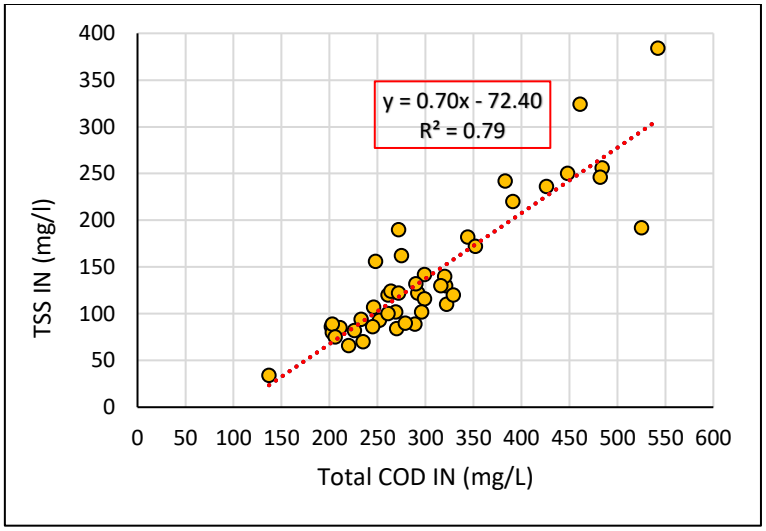

Figure 29: Correlation between influent TSS and total COD concentrations during the demonstration-scale filtration campaign (n=45).

Total COD shows a general increasing trend with TSS. A clear correlation was observed between influent COD and TSS concentrations ($R^2 \approx 0.80$), indicating a close relationship between total COD and suspended solids. Based on the regression line (TSS IN = *0.70·COD IN – 72.40*), the slope (0.70 mgTSS/mg COD) represents the incremental increase of suspended solids per unit increase of COD. This TSS/COD ratio equal to 0.70 is consistent with similar values found in municipal and industrial WW, where TSS/COD can range between 0.4 and 0.7, containing mostly volatile suspended solids (VSS).

6.2 MACROPARAMETERS REMOVAL PERFORMANCE

Removal of TSS and total COD were monitored during the experimental period. Prior to data analysis, outliers were identified and removed using the interquartile range (IQR) method. Given the strong correlation observed between influent TSS and total COD IN, it was investigated whether a similar relationship exists between total COD and TSS removal efficiencies (Figure 30).

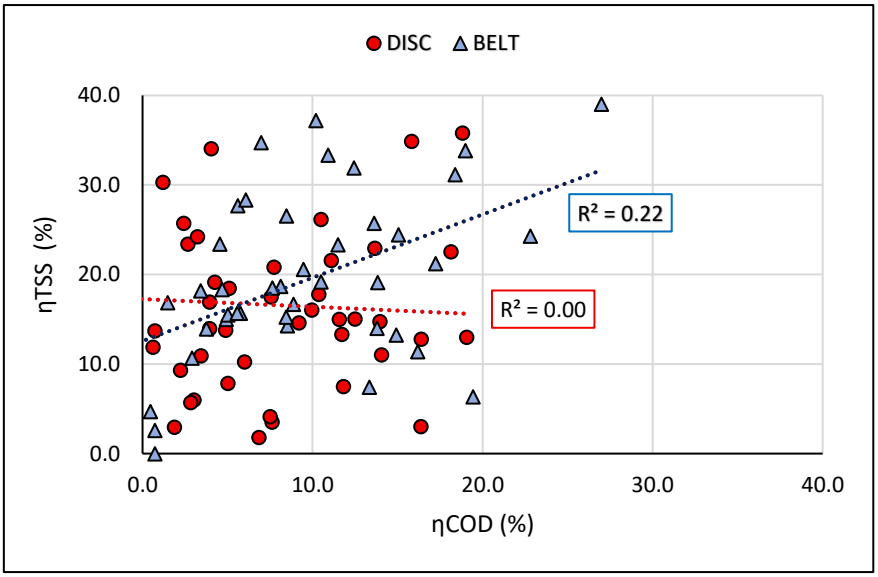

Figure 30: Relationship between COD removal efficiency (ηCOD) and TSS removal efficiency (ηTSS) for the demonstration-scale belt and disc filtration systems.

No clear correlation was observed in both disc and belt filters, as confirmed by the very low coefficient of determination. This indicates that COD removal does not scale directly with TSS removal and suggests that a fraction of COD remains in the dissolved phase, which is not efficiently removed by surface filtration alone. The relationship between TSS and COD removal efficiencies was analyzed as a function of mesh size to investigate the presence of possible correlations (Figure 31).

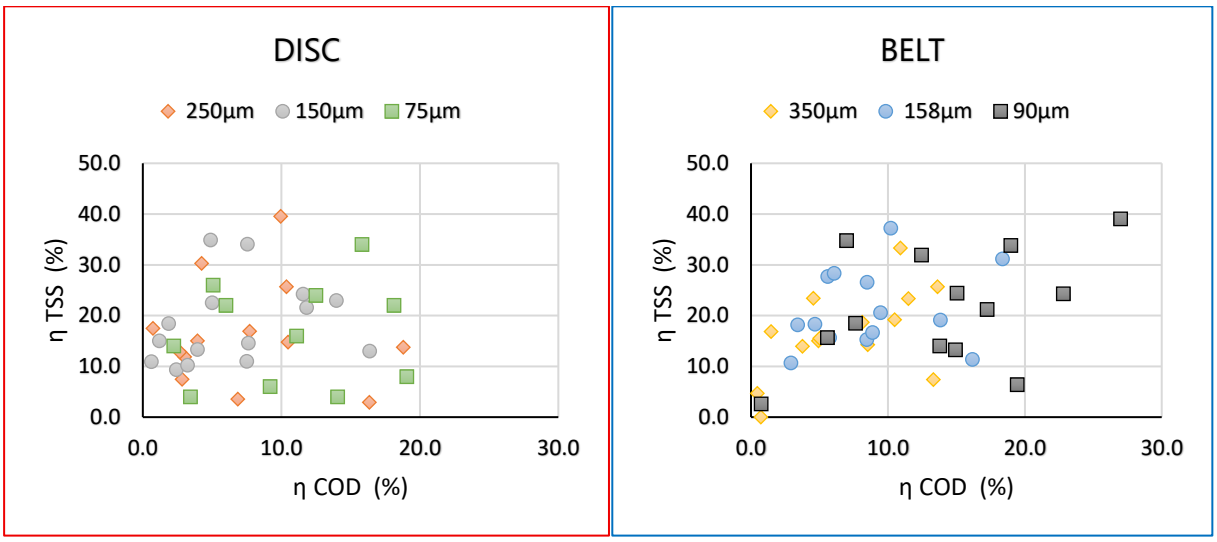

Figure 31: Total COD and TSS removal efficiencies as a function of mesh size for DISC and BELT configurations (n = 44 and n = 42, respectively).

For both filter configurations, data points corresponding to the different mesh sizes are widely scattered, indicating the absence of a clear relationship between ηTSS and ηCOD. In particular, for the BELT configuration, coefficients of determination are lower than 0.30 for all three mesh sizes, while for the disc configuration even lower values are observed, with $R^2 < 0.06$. These results confirm that, within the investigated range, mesh size does not lead to a significant relation between COD and TSS removal efficiencies.

In the following, data referring to total COD and TSS removal efficiencies are analyzed as a function of mesh size and hydraulic loading rate (HLR), in order to assess their influence on the system removal performance. Table 17 is organized into two distinct sections, corresponding to the BELT (left blue table) and DISC (right red table) configurations, in order to clearly separate the datasets.

Table 17: Average TSS and COD removal efficiencies as a function of the hydraulic loading rate (HLR) for the different mesh sizes tested comparing the performance of the BELT filter (left) and DISC filter (right).

DISC Mesh (µm)	HLR (m/h)	DATA number (n°)	ηCOD (%)	ηTSS (%)	BELT Mesh (µm)	HLR (m/h)	DATA number (n°)	ηCOD (%)	ηTSS (%)
250	55	2	14.6	25.7	350	78	1	13.3	7.4
	83	9	3.6	11.9		104	2	6.7	14.6
	110	1	3.9	17.5		130	9	6.1	16.8
	138	3	8.0	16.0		156	3	5.1	15.8
150	55	2	9.6	19.4	158	78	2	11.2	22.8
	83	7	5.8	20.7		104	2	12.3	29.7
	110	3	6.1	16.9		130	8	6.7	20.6
	138	3	7.2	13.8		156	2	11.0	13.5
75	55	1	14.1	9.2	90	78	1	19.4	19.3
	83	7	10.9	21.3		104	3	8.3	19.5
	110	3	5.9	8.4		130	7	15.6	26.8
	138	3	12.6	18.0		156	2	14.4	13.6

The number of data points associated with each operating condition shows a heterogeneous distribution. For both systems, several conditions are supported by a limited number of measurements, in some cases based on only one or two data points and therefore should be considered less statistically robust. Conversely, other operating conditions—particularly for intermediate HLR values—are supported by a larger number of observations (up to 8–9 data points), providing a more reliable estimation of average removal efficiencies.

Despite this variability in data density, the table allows a qualitative comparison of COD and TSS average removal trends as a function of mesh size and HLR for the two filtration systems. The removal efficiencies are further explored in the following section, where the same datasets are analyzed graphically to better visualize trends, dispersion, and potential relationships between operating parameters and removal performance (Figure 32).

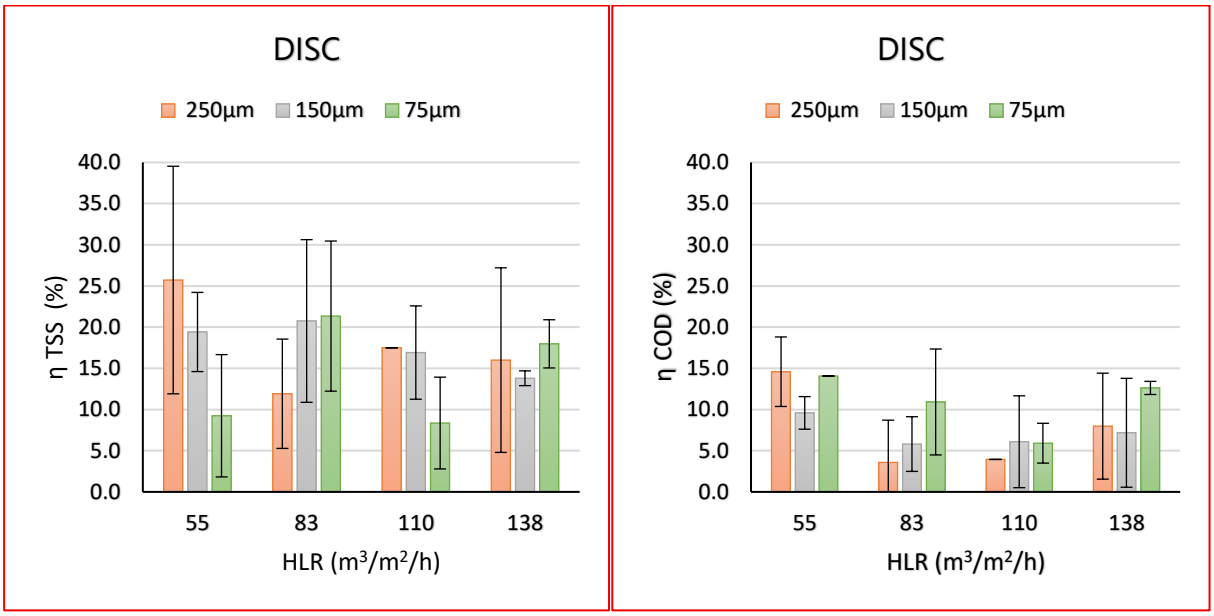

Figure 32: Average TSS and COD removal efficiencies as a function of the hydraulic loading rate (HLR) for the different mesh sizes tested for the DISC filter.

The disc filter exhibited relatively stable COD and TSS removal efficiencies across the investigated range of hydraulic loading rates (HLR), indicating a limited sensitivity to the tested hydraulic loading conditions. This behavior is consistent with the tangential filtration principle, as the shear forces generated by crossflow along the filter surface limit the formation of a stable filter cake. Accordingly, at constant mesh size, both total COD and TSS removal efficiencies do not show a clear trend with increasing HLR and it seems to confirm the fact that filtration performance is mainly governed by intrinsic filter properties rather than by cake-assisted mechanisms. Slightly higher removal efficiencies were observed for coarser meshes (e.g., 250 µm); however, this tendency is affected by high variability. Similarly, the higher removal efficiencies observed at lower HLR values should be interpreted with caution due to the few data available. At constant HLR, the influence of mesh size is more evident for TSS than for COD removal. TSS removal efficiencies typically increase when moving toward coarser meshes, although this behavior is accompanied by a higher variability. Overall, TSS removal values for the disc filter mainly range between approximately 10% and 25%.

In contrast, COD removal efficiency remains systematically lower, generally ranging between about 5% and 15%, with an average value of approximately 7.5%. Overall, these results confirm that the disc filter predominantly targets the particulate fraction, while its impact on dissolved organic matter is limited. The weak dependence of COD removal on both HLR and mesh size further supports the physical nature of the separation process and the minor role of cake formation in the disc filter configuration.

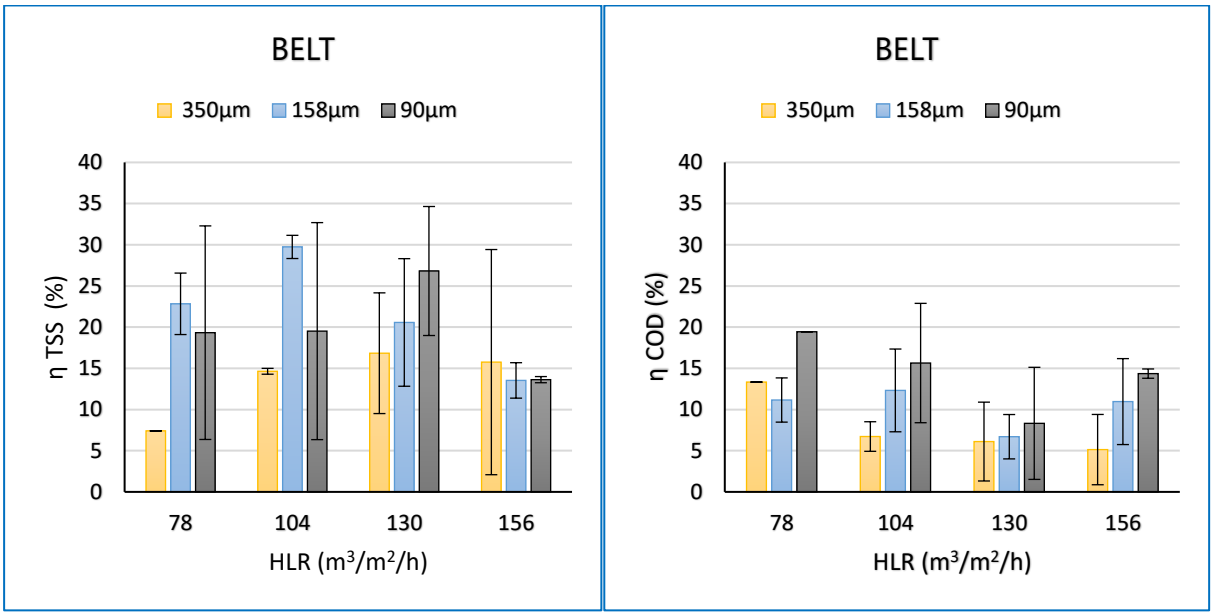

Figure 33: Average TSS and COD removal efficiencies as a function of the hydraulic loading rate (HLR) for the different mesh sizes tested for the BELT filter.

In contrast, the belt filter showed maximum removal efficiency for TSS at intermediate HLR values (Figure 33), indicating the development of a stable filter cake on the belt surface, which enhances particle retention beyond the nominal mesh size. At low HLR values, removal efficiencies were lower, likely due to insufficient cake formation, whereas at higher HLRs performance tended to level off or slightly decrease, probably as a result of reduced contact time and the more frequent belt movement required to manage the incoming solids load. At constant mesh size, this results in a bell-shaped trend for TSS with a peak at intermediate HLR values tested, while COD tends to decrease when moving toward higher HLRs, likely due to the reduced contribution of particulate organic matter retention and the increasing dominance of the soluble COD fraction. At constant HLR, the influence of mesh size is more pronounced for TSS than for COD removal. In particular, ηTSS generally increases when moving from the coarser mesh (350 µm) to intermediate and finer meshes (158 and 90 µm).

Overall, the belt filter achieved higher removal efficiencies and showed clearer trends with respect to both HLR and mesh size compared to the disc filter, particularly for TSS, with typical values ranging between approximately 7.5% and 30% and average efficiencies around 20% when using a 158 µm mesh. Conversely, total COD removal efficiencies are slightly higher and more stable than those observed for the disc filter, generally falling within the range of approximately 5% to 20%. These results confirm that filter cake formation plays a key role in enhancing the retention of solids and particulate organic matter during surface filtration under continuous, demonstration-scale operation.

To further investigate how these efficiency trends translate into actual solids separation, Figure 34 compares the average of specific number of solids physically removed ($g \cdot m^{-3}$) as a function of the hydraulic loading rate for the belt and disc filtration units with specific reference to the 75 µm mesh for the disc filter and the 158 µm mesh for the belt filter, selected as representative operating conditions.

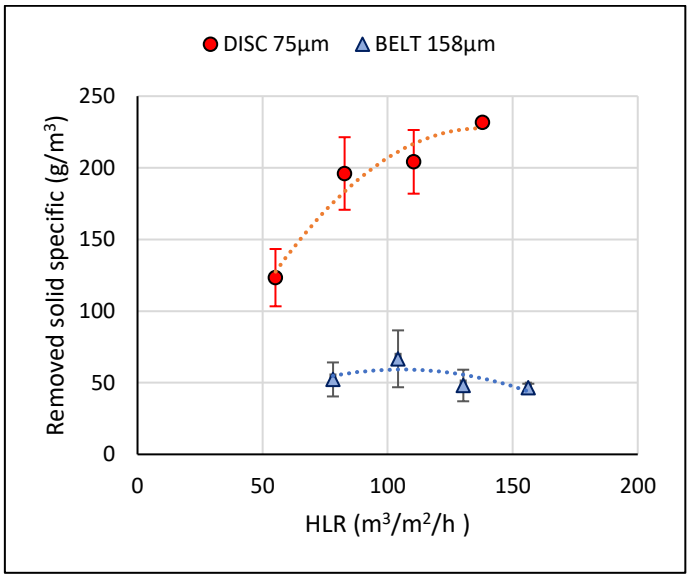

Figure 34: Specific solids removal as a function of HLR for belt and disc filters. Each symbol represents the average value of a monitoring campaign conducted per tested HLR.

The comparison highlights a clear distinction between the two filtration technologies. Since influent TSS concentrations were identical for the belt and disc filters, the observed differences in specific solids removal—defined as the mass of solids removed (kg) per treated volume (m^3)—are not driven by variations in incoming solids load, but by differences in filtration and solids-handling mechanisms. In the belt filter, progressive cake formation combined with an integrated dewatering system leads to a controlled and consistent solids removal, resulting in a markedly higher dry matter content of the discharged solids (average ≈34%).

In contrast, solids removed by the disc filter are discharged in a much more hydrated form, with a significantly lower average dry matter content (≈8.4%), making their apparent removal more sensitive to hydraulic loading conditions. Accordingly, the disc filter shows higher but more variable specific solids removal, increasing with hydraulic loading rate and reaching approximately 120–230 $g \cdot m^{-3}$, whereas the belt filter exhibits lower yet more stable values (approximately 45–65 $g \cdot m^{-3}$), largely independent of HLR once a stable filter cake is established. These differences, also reflected in the distinct operating flow rates of the two systems, which ranged from 15, 20, 25, and 30 $m^3 \cdot h^{-1}$ for the belt filter and from 5, 7.5, 10, and 12.5 $m^3 \cdot h^{-1}$ for the disc filter. This confirms that specific solids removal is primarily governed by filtration dynamics and solids-handling processes.

6.3 MICROPLASTIC REMOVAL PERFORMANCE

This chapter presents the results related to the occurrence and removal of microplastics (MP) in the demonstration pilot plant. First, the characteristics of microplastics detected in the influent are described, distinguishing between the main identified categories (fibers and fragments) and their respective contribution to the total MP count. Each point represents a single value of a monitoring campaign.

Table 18: Influent microplastics concentrations for the demonstration-scale tests conducted at the Alto Seveso WWTP. Test codes (AS2-xx) identify individual experimental runs (AS = Alto Seveso; 2 = second campaign; xx = test number).

Test codes	*Fibers IN (n°/l)*	*Fragments IN (n°/l)*	*Total MP IN (n°/l)*
AS2-08	*800*	*23,200*	*24,000*
AS2-10	*3,200*	*43,200*	*46,400*
AS2-12	*6,024*	*24,096*	*30,120*
AS2-18	*1,280*	*23,360*	*24,640*
AS2-20	*400*	*24,800*	*25,200*
AS2-24	*1,600*	*35,200*	*36,800*
AS2-29	*3,200*	*20,800*	*24,000*
AS2-32	*4,800*	*28,800*	*33,600*
AS2-35	*0*	*37,600*	*37,600*
AS2-39	*1,600*	*31,200*	*32,800*

The data reported in Table 18 show influent microplastics concentrations on the order of 10^4 particles per liter across all analyzed tests. The two 72 h tests, corresponding to influent samples associated with experiments conducted on the coarser meshes (350 µm and 158 µm for the BELT system, and 250 µm and 150 µm for the DISC system), were excluded from the analysis.

The test AS2-39 is the only case for which influent microplastics data are available for a 72 h experiment performed with the finest meshes (75 µm for the DISC filter and 90 µm for the BELT filter). Total microplastics concentrations range from approximately 2.4×10^4 to 4.6×10^4 n°·L^{-1}, indicating relatively consistent incoming loads among the different experimental runs. To facilitate interpretation, the influent data are plotted in the following section to better visualize their distribution (Figure 35).

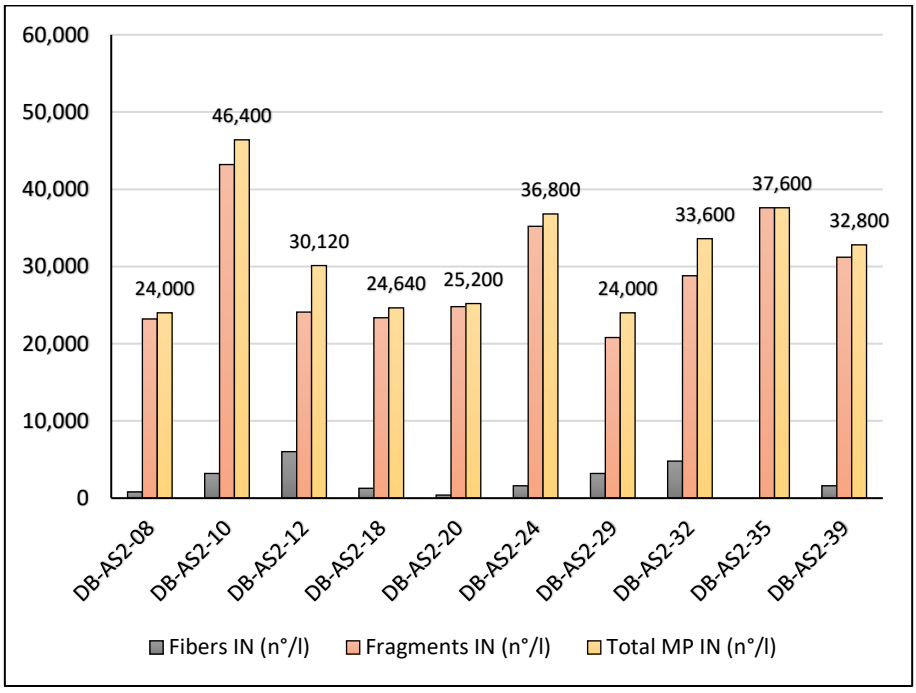

Figure 35: Bar plot of influent microplastic concentrations, subdivided into fibers, fragments, and total MP for each experimental series.

The graph reports influent microplastic (MP) concentrations (n°·L^{-1}) for all experimental tests for which analytical results provided by CTSS were available. For each test, the contributions of fibers, fragments, and total microplastics in the influent are reported. Total MP concentrations show marked variability among the different experimental campaigns, with values ranging approximately from 24,000 to 46,400 n°·L^{-1}. Fragments clearly represent the dominant microplastic fraction for all analyzed tests. In percentage terms, fragments account for the majority of total MPs, generally contributing between approximately 80% and more than 90% of the total. Although many studies report a predominance of fibers in WWTP influent, particularly in systems dominated by domestic wastewater, several investigations have documented fragment-dominated microplastic profiles in mixed urban–industrial catchments. For example, Uogintė et al. (2022) reported fragment proportions between 71% and 90% across seasons, while Bayo et al. (2023) observed fragments representing up to 60% of influent microplastics in European WWTPs.

Therefore, the predominance of fragments observed in this study is consistent with literature findings for mixed influent systems. After characterizing the influent microplastics concentration and composition (MP_IN), the analysis focused on the evaluation of single microplastics removal performance data. First, the removal efficiency as a function of mesh size was investigated for the belt filter. The test codes represent the experimental runs for which MP extractions were performed and the results were obtained (Figure 36).

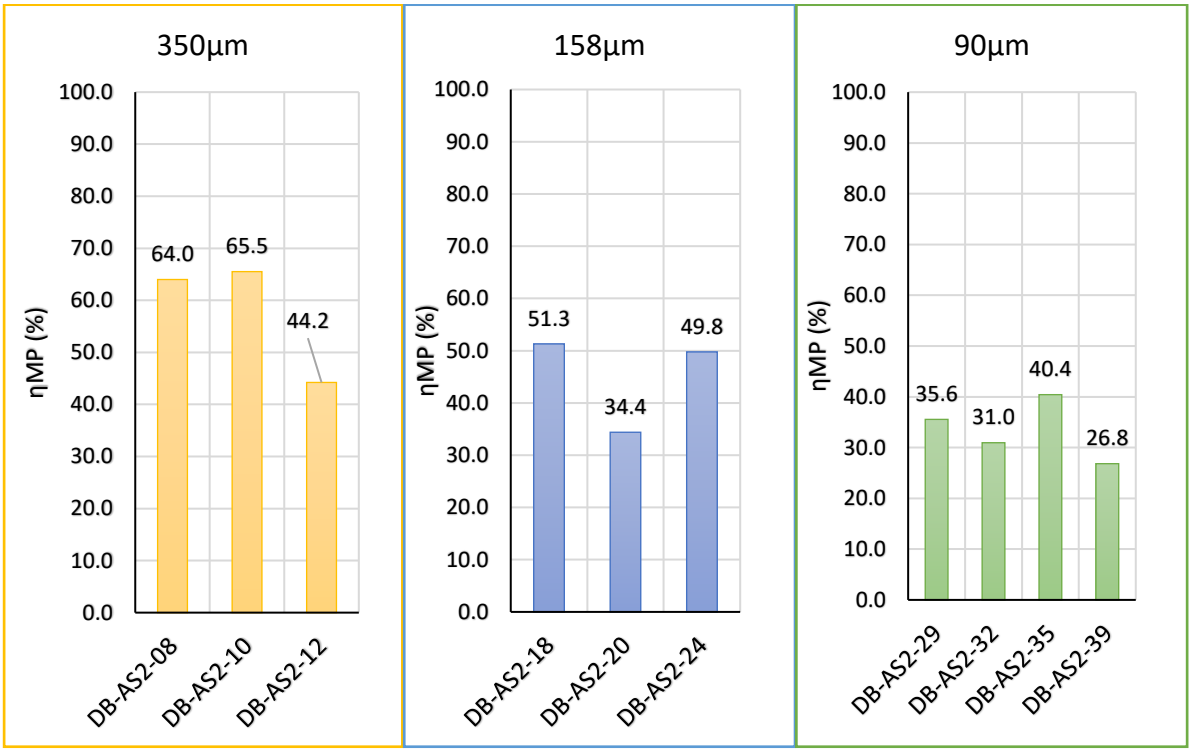

Figure 36: Removal efficiency (η_MP) for the BELT filtration systems at demonstration scale, reported as a function of mesh size and experimental run. Test codes (DB-AS2-xx) identify individual experimental runs, where "DB" refers to the "Demonstration Belt" filter.

For the belt filter, all tests refer to 24 h experimental runs, with the only exception being DB-AS2-39, which corresponds to a 72-h test. From the bar plot, it emerges that the belt filter consistently achieves positive removal values across all tests and mesh sizes, generally ranging between approximately 30% and 65%, indicating a relatively robust and stable microplastics removal performance. An apparent anomalous trend emerges, as higher removal efficiencies are observed for coarser mesh sizes, while a general decrease in MP removal is recorded as the mesh size is reduced. This behavior cannot be related to differences in hydraulic conditions, since the operating flow rate was constant across all tests and equal to 25 $m^3 \cdot h^{-1}$.

As the mesh size decreases (158 µm and 90–75 µm), removal performance does not show a systematic improvement and, under some conditions, lower removal efficiencies are observed despite comparable or lower influent MP concentrations. This behavior suggests that, for the belt system, reducing mesh size alone does not guarantee enhanced microplastic removal. This is likely due to the preferential passage of smaller or stretched particles, such as fibers and thin fragments, through the filter medium, highlighting the limitations of a purely size-based separation mechanism. However, it should be noted that the number of available data points is limited, and therefore, the robustness of these interpretations should be considered with caution. The following bar plots (Figure 37) illustrate single data of microplastics removal efficiencies (η_MP) obtained for the disc filter under the different mesh sizes tested, allowing a comparison of removal performance across the investigated experimental conditions.

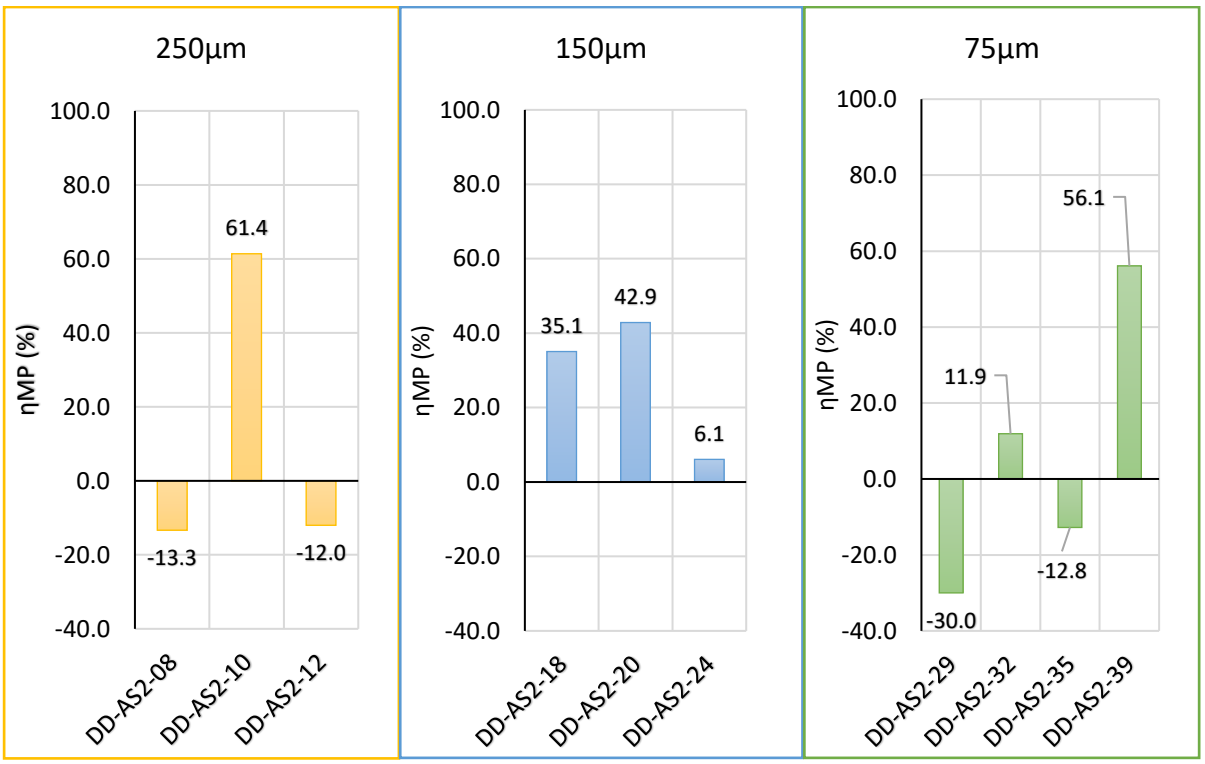

Figure 37: Removal efficiency (η_MP) for the DISC filtration systems at demonstration scale, reported as a function of mesh size and experimental run. Test codes (DD-AS2-xx) identify individual experimental runs, where "DD" refers to the "Demonstration Disc" filter.

The barplot highlights that the DISC filter shows highly variable performance across mesh sizes and tests, with values ranging from negative (-30%) to positive (+61.4%), indicating inconsistent removal behavior and a strong sensitivity to influent heterogeneity and analytical variability.

For the coarser mesh size (250 µm), relatively high removal efficiency is observed in DD-AS2-10 test, exceeding 60%. However, as observed for the belt system, a systematic improvement in removal performance with decreasing mesh size is not evident for the disc system as well. For finer meshes (150 µm and 75 µm), removal trends become highly irregular, with microplastic removal efficiencies decreasing substantially in some tests. The negative removal efficiencies observed for specific configurations (e.g., 250 µm and 75 µm) can be attributed to analytical variability in concentration measurements and to the episodic release of microplastics previously accumulated on the filter surface. The following analysis investigates the relationship between MP removal and influent microplastics concentrations (MP_IN), one single value each. Six graphs were developed: three for the belt system (Figure 38) and three for the disc system (Figure 38), each representative of a different tested mesh size.

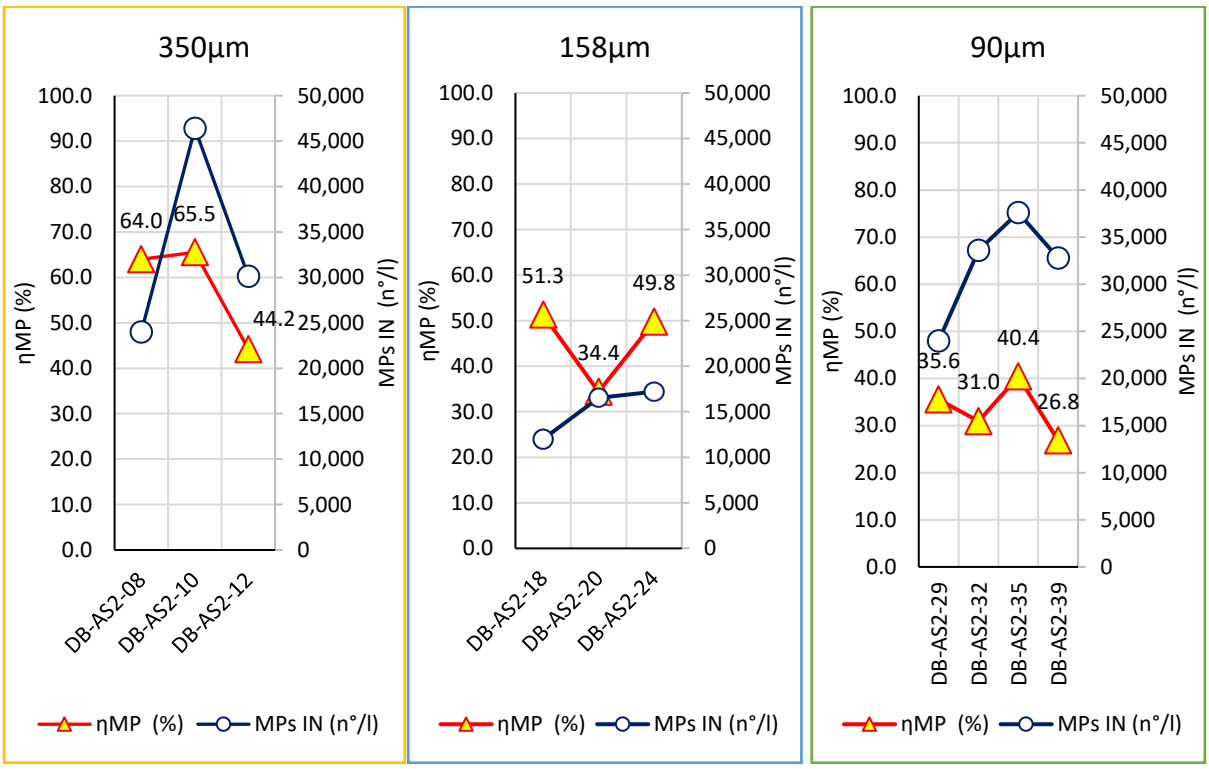

Figure 38: Microplastic removal efficiency (ηMP) as a function of influent microplastic concentration for the BELT filter at the three investigated mesh sizes (from left to right: 350 µm, 158 µm, and 90 µm).

Figure 38 shows no clear or systematic relationship between influent microplastics concentration (MP_IN) and removal efficiency (η_MP) for the belt filter. Across the three investigated mesh sizes, higher influent concentrations do not consistently correspond to higher removal efficiencies, nor does a monotonic increase in MP removal emerge with decreasing mesh size. These results seem to indicate that microplastics removal is not governed by influent concentration or mesh size alone, but rather by a

combination of particle characteristics and filtration dynamics. Overall, given the limited number of available data points, any interpretation of trends should be considered with caution.

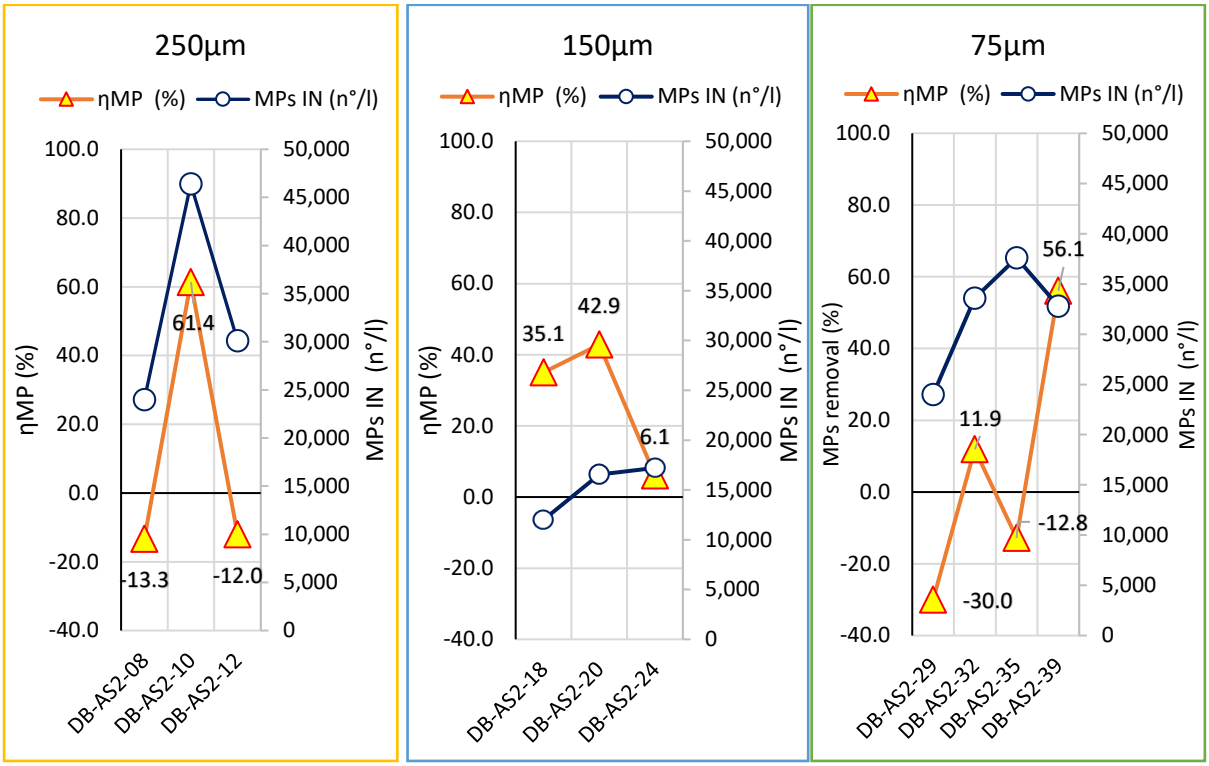

Figure 39: Microplastic removal efficiency (ηMP) as a function of influent microplastic concentration for the DISC filter at the three investigated mesh sizes (from left to right: 250 µm, 150 µm, and 75 µm).

Figure 39 shows that, also for the disc filter, no clear or systematic relationship can be identified between influent microplastics concentration (MP_IN) and removal efficiency (η_MP) across the investigated mesh sizes. Removal efficiencies remain highly scattered, with both positive and negative values observed at comparable influent concentrations. The highest microplastics removal observed for the 75 µm mesh during the 72 h test (+56.1%), as well as the high removal efficiency recorded for DB-AS2-10 (+61%), represent isolated results that are not consistently reproduced in the 24 h tests. Overall, the results highlight a pronounced variability in microplastic removal, which does not follow a monotonic trend with either mesh size or influent concentration.

Both filtration systems exhibit significant fluctuations in MP removal efficiencies even under identical mesh configurations, indicating that microplastic behavior is not governed exclusively by a simple size-exclusion mechanism. Instead, it is strongly influenced by the filtration process and by secondary effects such as cake formation and particle aggregation. To better highlight the previously described trends,

the direct relationship between microplastics removal efficiency (η_MP) and influent microplastics concentration (MP_IN) was analyzed, firstly exploring the belt filter unit (Figure 40).

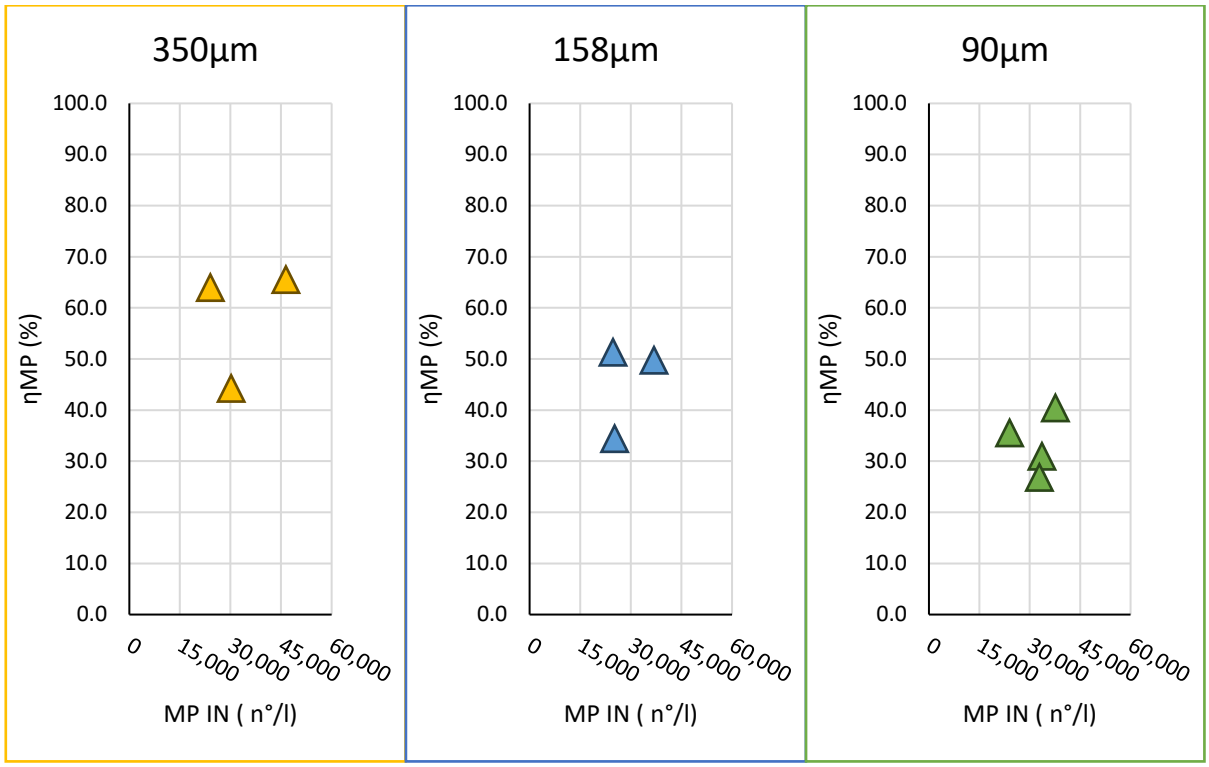

Figure 40: Correlation between influent microplastics concentration (MP_IN, n°/L) and microplastics removal efficiency (η_MP, %) for the three belt filter mesh sizes: 350 µm, 158 µm, and 90 µm.

Following the same approach adopted for the belt filter, the direct relationship between microplastics removal efficiency (η_MP) and influent microplastics concentration (MP_IN) was analyzed for the disc filter configuration (Figure 41).

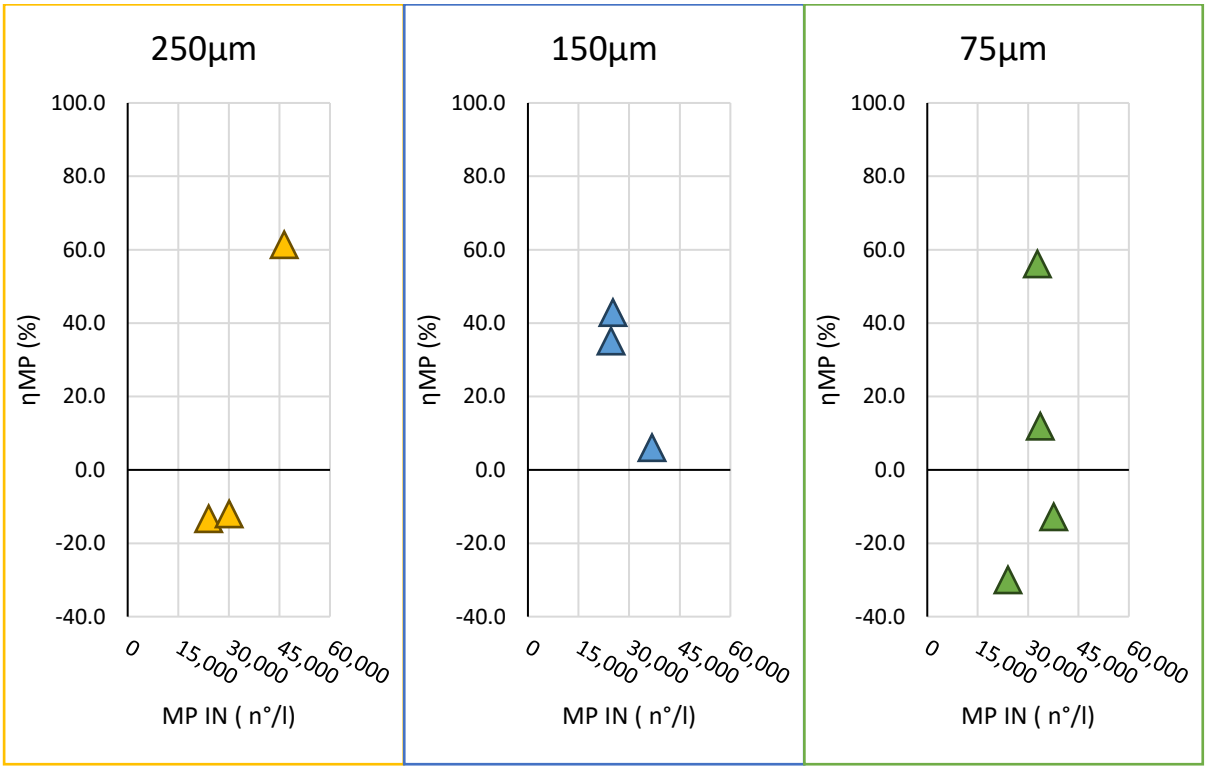

Figure 41: Correlation between influent microplastics concentration (MP_IN, n°/L) and microplastics removal efficiency (η_MP, %) for the three disc filter mesh sizes: 250 µm, 150 µm, and 75 µm.

In this context, the belt filter generally shows more consistent microplastic removal due to the development of a surface cake, whereas the disc filter is characterized by more variable and occasionally negative removal efficiencies. Overall, no clear dependence on influent MP concentration (MP_IN) is observed in both filtration units.

To further investigate whether total suspended solids removal (ηTSS) can be considered a proxy for microplastic removal (ηMP), a scatterplot was plotted (Figure 42) and a linear regression analysis was performed separately for the belt and disc units. Each symbol represents a single data point of MP removal efficiency associated with the corresponding TSS removal value.

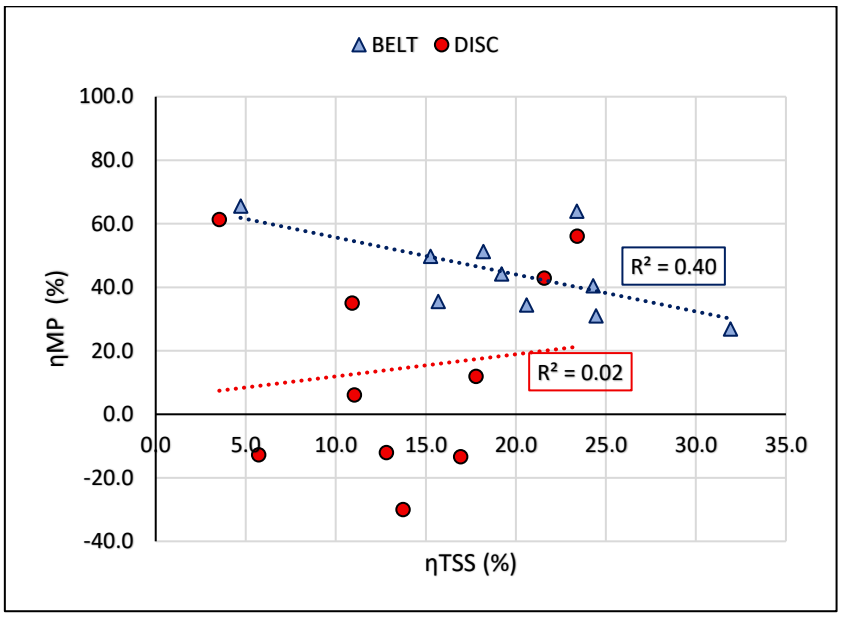

Figure 42: Relationship between ηMP and ηTSS for the BELT and DISC filters, with linear regression fits.

For the BELT filtration system, a linear regression analysis was performed to investigate the relationship between microplastic removal efficiency (ηMP) and total suspended solids removal efficiency (ηTSS). The regression yielded a coefficient of determination (R^2) of 0.40, indicating that approximately 40% of the variability in microplastic removal can be explained by variations in TSS removal. The model was statistically significant at the 95% confidence level ($p \approx 0.049$); however, given the limited number of observations ($n = 10$), the results should be interpreted with caution. As also confirmed graphically, the regression slope was negative (−1.17), suggesting that higher TSS removal efficiencies do not correspond to higher microplastic removal in the BELT system.

For the disc filter (DISC), the relationship between ηMP and ηTSS appears even weaker. The coefficient of determination ($R^2 = 0.02$) and the associated p-value ($p = 0.70$), largely exceeding the significance threshold ($p = 0.05$), confirm the absence of a statistically significant relationship between the two variables. Moreover, the presence of a negative, although non-significant, regression coefficient reflects the high data dispersion and the non-stationary behavior of the DISC system under the investigated operating conditions. Overall, although total suspended solids are often used as a general indicator of filtration efficiency, the regression results demonstrate that, under the investigated conditions, ηTSS is not statistically correlated with ηMP. Therefore, TSS removal cannot be considered a reliable proxy for microplastic removal performance. To further investigate the fate of microplastics within the filtration systems, the concentration of microplastics in the separated solid fractions was also analyzed.

It should be noted that not all the solid extractions performed during the experimental campaign were analysed for microplastics, and therefore, the available data refer to a subset of the total number of tests. Figures 43 reports the concentration of microplastics (MPs) in the solids separated by the belt and disc filters, expressed as the number of particles per gram of dry matter ($n°\cdot gDM^{-1}$). The results are presented as single data by distinguishing between fibers, fragments, and total microplastics, allowing a qualitative comparison of microplastic accumulation in the separated solid fractions for the two filtration systems.

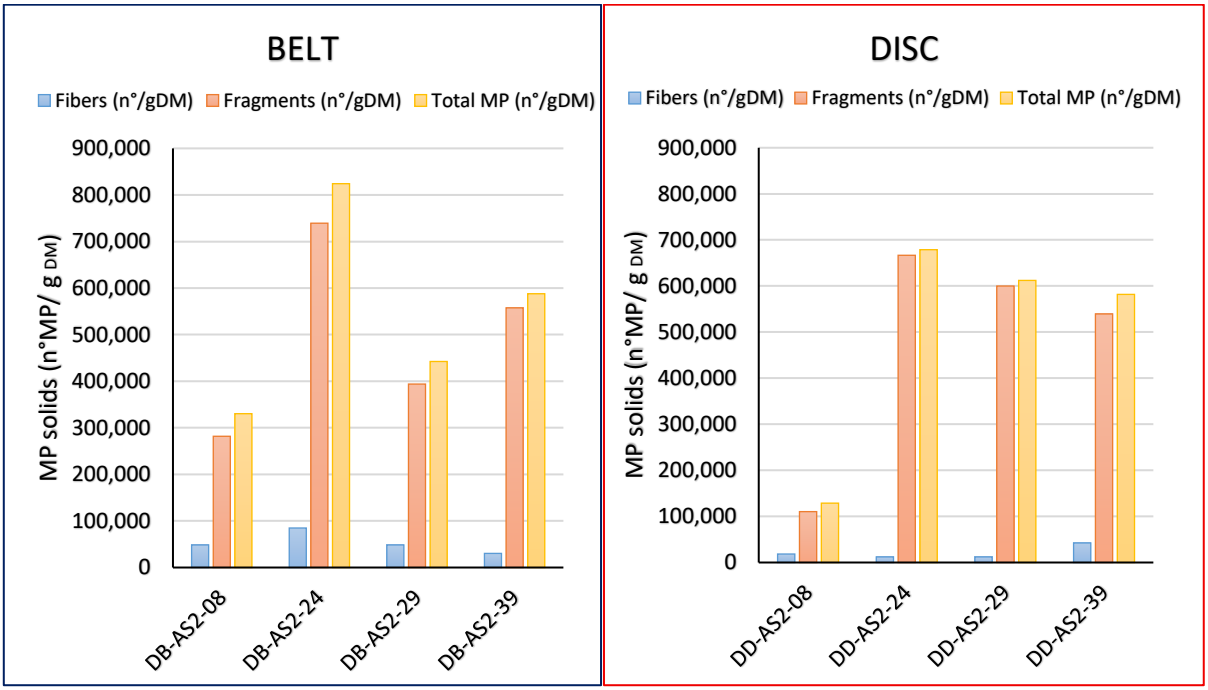

Figure 43: Microplastic concentrations in the solid fractions separated by the BELT (left) and DISC (right) filtration systems.

The dry matter content of the solids separated by the disc filter was consistently low, ranging between approximately 7.7% and 9.7%. In contrast, the BELT filter achieved substantially higher dry matter contents, ranging between 31.3% and 35.2%. In both filtration systems, the total MP concentration closely follows the trend observed for fragments, indicating that fragmentation-derived particles constitute the main microplastic form retained within the separated solids. A clear difference emerges between the two technologies. In general, the belt filter shows higher concentrations of microplastics in the separated solids compared to the disc filter. This behavior can be attributed to the operating principle of the belt filtration system, which combines gravity-driven surface filtration and mechanical dewatering, leading probably to a fragmentation of the particles passing through the screw, resulting in higher MP numbers per unit of dry mass.

Conversely, the disc filter produces a less dewatered solid fraction, due to the dynamic tangential filtration mechanism and the continuous removal of retained material without dewatering process. To further investigate the fate of microplastics during the filtration process, an additional analysis was carried out to evaluate the extent to which microplastics are transferred from the influent liquid phase to the separated solid fraction. In this context, an enrichment factor (EF) was defined as the ratio between the number of microplastics associated with the separated solids and the number of microplastics present in the influent wastewater, for each campaign for which MP data in solids were available.

$$EF = \frac{MP_{solids}\left[\frac{n°}{g_{DM}}\right] * TS\left[\frac{g_{DM}}{kg}\right] * Removed\ Solids[kg]}{Q_{feed}\left[\frac{m^3}{h}\right] * D_{test}\,(h) * 10^6} * \frac{1}{MP_{IN}\left[\frac{n°}{l}\right]} = [-]$$

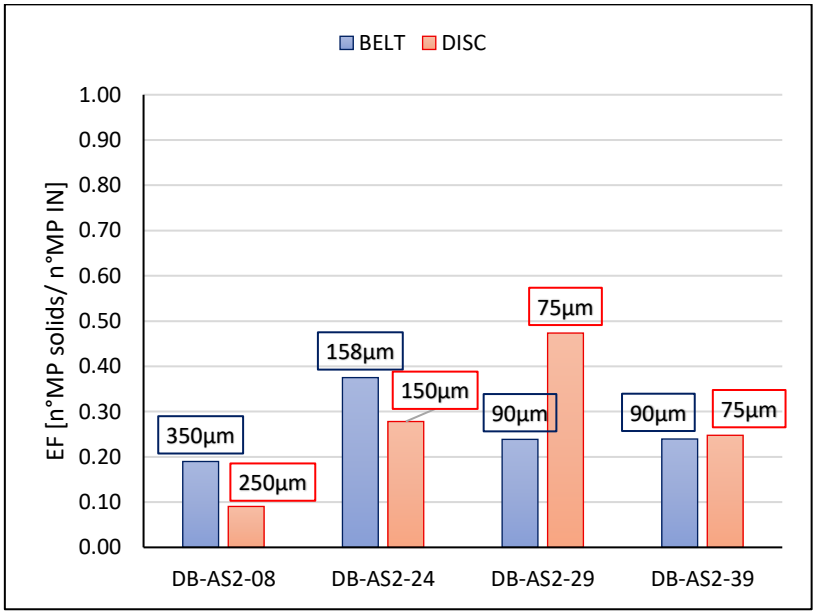

Figure 44: Enrichment factor (EF) of microplastics in the separated solid fractions for the BELT and DISC filtration systems.

As shown in Figure 44, the enrichment factor is consistently lower than one for both filtration technologies and for all the analyzed experimental runs. This indicates that only a limited fraction of the incoming microplastics is retained in the separated solids, while the majority remains in the liquid phase after filtration. The fact that EF values remain below unity highlights an important aspect of microplastic behavior: their retention is not solely governed by the overall removal of suspended solids.

A significant portion of microplastics likely occurs as small, flexible, or low-density particles that are weakly associated with the particulate matrix and can pass through the filtration systems, especially in the absence of a fully developed and stable cake layer. The belt filter generally exhibited higher and more stable EF values compared to the disc filter, suggesting a stronger coupling between microplastic removal and suspended solids separation, likely driven by surface filtration and cake formation mechanisms. Conversely, the disc filter showed a more variable behavior, reflecting the influence of tangential flow and limited cake development on microplastic capture.

7 Laboratory and Demonstration Scale Filtration Performance

This chapter aims to provide a comparative discussion of the filtration tests carried out at laboratory scale on Lariana wastewater and at demonstration scale at the Lariana WWTP. The main objective of this comparison is to evaluate whether laboratory-scale tests can provide meaningful indications of the performance of surface filtration technologies under real operating conditions. The comparison was possible because the laboratory-scale data used in this analysis originates from previous experimental tests conducted on Lariana WW, following the methodology described in Chapter 4.1. In particular, three laboratory test campaigns were performed. The results of these campaigns, expressed in terms of single data points of MP concentrations and removal efficiency, are presented below (Table 19).

Table 19: Results of laboratory-scale filtration tests conducted on Lariana wastewater using three stainless steel (AISI) filters with different mesh sizes (250 µm, 150 µm, and 75 µm).

Sampling date	Filter-Mesh tested (µm)	MP Influent (MP/L)	MP Filtrate (MP/L)	ηMP (%)
26/09/2024	AISI-250	3307	2877	12.7
12/11/2024		6015	5215	13.3
8/05/2025		3700	2188	40.9
26/09/2024	AISI-150	12381	8481	31.5
12/11/2024		4599	298	93.5
8/05/2025		2150	425	80.2
26/09/2024	AISI-75	4405	3405	22.7
12/11/2024		1600	875	45.3
8/05/2025		1800	588	67.4

As shown above, the filters tested at laboratory scale had the same mesh sizes and material as those used during the demonstration-scale testing of the disc filter at the Lariana WWTP. Therefore, a direct comparison between laboratory-scale and demonstration-scale results is possible for the disc filter configuration. Conversely, no laboratory-scale data are available for the belt filter, preventing a direct comparison between the two scales for this technology. Laboratory results indicate that microplastic (MP) concentrations in both influent and filtrate ranged between 10^3 and 10^4 MPs/L, corresponding to removal efficiencies spanning a wide range, from approximately 10% up to 95%. The highest removal efficiencies were generally achieved with the AISI 150 µm working mesh, while slightly lower performances were observed for the AISI 75 µm mesh. Contrary to initial expectations, the finest mesh did not systematically result in higher removal efficiencies. Although the AISI 75 µm filter exhibited moderate average removal efficiencies (ranging from approximately 22% to 67%), it should be noted that relatively low influent MP concentrations were measured in the last two tests. Together with the limited amount of available data, these results appear to confirm the findings reported in Chapter 6.3, that no clear relationship exists between influent MP concentrations and removal efficiency. Therefore, based on the available laboratory-scale and demonstration-scale data, average influent and effluent microplastics concentrations were calculated, together with the corresponding removal efficiencies. In this way, the results can be directly compared, as reported in Table 20.

Table 20: Comparison between laboratory-scale (LAB) and demonstration-scale (DEMO) filtration results expressed in terms of mean microplastic (MP) influent and outlet concentrations and corresponding average removal efficiencies (ηMP± SD).

Tipo	Filter-Mesh tested (µm)	Average MP IN (MP/L)	Average MP OUT (MP/L)	$\bar{\eta}$MP (%)
LAB	AISI-250	4341	3427	12.7 ± 16.1
DEMO (DISC)		33,507	26,285	21.6 ± 42.8
LAB	AISI-150	6377	3068	52 ± 32.6
DEMO (DISC)		28,880	21,653	25.0 ± 19.4
LAB	AISI-75	2602	1623	38 ± 22.4
DEMO (DISC)		32,000	29,400	8.1 ± 37.4

Despite the wastewater source being the same, differences in measured microplastic concentrations are observed between laboratory-scale and demonstration-scale tests. At laboratory scale, average MP concentrations remain within the order of 10^3–10^4 MPs/L, whereas at demonstration scale the observed range increases, reaching values between 10^4 and approximately 4×10^4 MPs/L. This discrepancy can probably be attributed to scale-dependent operational and hydraulic conditions. Laboratory-scale tests are performed on limited volumes under controlled and constant operating conditions, with prior homogenization of the influent, which results in an averaged representation of the microplastic load. In contrast, the demonstration-scale disc filter operates continuously on large and highly variable wastewater flows, capturing short-term fluctuations and peak microplastic loads. In order to better visualize the MP removal efficiency, a bar plot is presented (Figure 45).

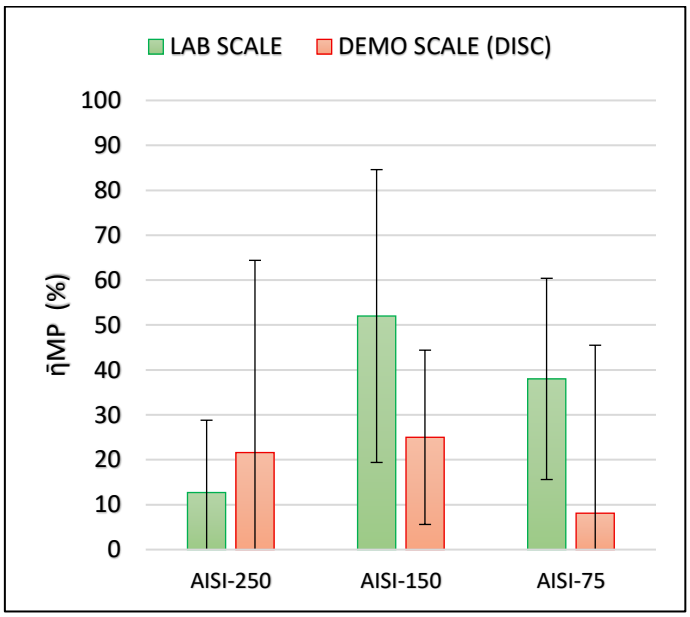

Figure 45: Comparison between laboratory-scale and demonstration-scale filtration results in terms of average microplastic removal efficiency (ηMP). Error bars represent the standard deviation.

From the comparison between filter meshes, AISI 150 µm emerges as the most effective configuration across both scales, achieving the highest microplastic removal efficiencies, with values ranging approximately between 25% and 50%, confirming the results gained at lab scale. This suggests that an intermediate mesh size represents a favorable compromise between separation efficiency and operational robustness. For the finer meshes (AISI 150 µm and AISI 75 µm), removal efficiencies obtained at laboratory scale are consistently higher than those observed at demonstration scale, likely due to the controlled hydraulic conditions.

Conversely, for the coarser AISI 250 µm mesh, this trend appears to be partially reversed, with higher removal efficiency observed at demonstration scale compared to laboratory conditions. However, this result should be interpreted with caution, as it is based on a limited number of data points and is characterized by high variability (SD = 42.8 %). Therefore, despite the intrinsic analytical uncertainty also affecting laboratory-scale measurements, the observed discrepancy may reflect statistical variability rather than a systematic difference in performance between scales. Overall, these results indicate that laboratory-scale filtration tests can provide useful qualitative information into filtration behavior and relative filter performance. Nevertheless, the limited dataset and the high variability observed at both scales introduce significant uncertainty, preventing a direct extrapolation of absolute removal efficiencies from laboratory to demonstration-scale conditions.

8 Conclusions and Future Perspectives

This work aimed to analyze the role of surface filtration technologies in the removal of microplastics from wastewater treatment systems and to assess the transferability of filtration performance between laboratory and demonstration scales. Laboratory-scale experiments demonstrated that surface filtration is effective in removing suspended solids from textile wastewater, although removal efficiencies were highly and strongly dependent on wastewater characteristics. TSS removal efficiencies ranged from negligible values up to approximately 60%, while COD removal generally ranged between 10% and 40%, remaining systematically lower due to the predominance of dissolved organic matter, as confirmed by high COD/TSS ratios. Overall, high removal efficiencies (50–65%) were obtained for the Comofil WW with all three filter media. In general, no increasing trend in removal performance was observed with decreasing mesh size for the tested filters, and none of the filters systematically outperformed the others. The comparison among different filter media highlighted that filtration performance was likely influenced not only by the nominal cut-off values, but also by the particle size distribution and the colloidal content. Microplastic removal data were obtained only for the tests conducted on the Lipomo WW, and the resulting removal efficiencies included negative values, likely attributable to analytical uncertainty.

At the demonstration scale, influent characterization showed a clear relation between total COD and TSS ($R^2 \approx 0.80$). However, this relationship did not translate into a direct correspondence between removal efficiencies: no meaningful correlation was found between total COD removal and TSS removal for either technology. Regarding process performance, the disc filter showed relatively stable but modest removal performance across the investigated hydraulic loading rates and mesh sizes, with typical TSS removal efficiency values approximately in the 10–25% range and COD removal generally between 5–15%. At constant mesh size, both TSS and COD removal efficiencies remained relatively stable over the investigated HLR range, indicating a limited sensitivity to hydraulic loading conditions. This behavior is consistent with the tangential filtration principle, which limits stable cake formation and results in removal performance mainly governed by the intrinsic properties of the filter medium rather than by cake-assisted mechanisms.

At constant HLR, the influence of mesh size was more evident for TSS than for COD, with slightly higher TSS removal generally observed for coarser meshes (250 µm) ; however, this tendency was affected by high variability and did not represent a systematic trend. In contrast, the BELT filter showed a clear dependence on both HLR and mesh size, particularly for TSS removal. At constant mesh size, TSS removal followed a bell-shaped trend with increasing HLR, reaching maximum efficiencies (approximately 30%) at intermediate hydraulic loading rates tested (104–130 $m \cdot h^{-1}$). This behavior highlights the key role of surface cake formation, which enhances particle retention when sufficiently developed but becomes less effective at low HLR (insufficient cake formation) and at high HLR (reduced contact time and increased belt movement). At constant HLR, mesh size impacted more than for the other filter unit, with higher TSS removal generally achieved using intermediate mesh sizes (158 µm) indicating that mesh size primarily influences cake stability rather than acting as a simple size-exclusion threshold. COD removal was slightly higher and more stable than for the DISC filter (typically ~5–20%), in line with improved interception of the particulate-associated COD fraction. The solids-handling mechanisms further differentiated the two systems: the belt unit produced a substantially more dewatered solid stream (higher dry matter content), whereas the disc unit discharged a more hydrated solid fraction, resulting in higher apparent but more variable specific solids removal.

Regarding microplastic (MP) concentrations at demonstration scale, influent microplastic values were consistently on the order of 10^4 particles per liter, in line with the findings of Iyare et al. (2020), who reviewed 20 WWTPs and reported influent concentrations reaching up to 10^4 particles per liter. Across all analyzed tests, fragments dominated the MP profile (typically 80–90% of total MPs), while fibers represented a minor fraction. For the BELT filter, microplastic removal efficiencies were consistently positive and comparatively stable across tests and mesh sizes, generally ranging between 30% and 65%. Nonetheless, a key finding is that decreasing mesh size did not yield a systematic improvement in MP removal. In several cases, coarser meshes showed equal or higher MP removal than finer configurations. This indicates that MP capture at demonstration scale is not governed by size exclusion alone and suggests a relevant role of filtration dynamics (e.g., cake development, aggregation). Conversely, the disc filter exhibited markedly higher variability, with ηMP spanning from negative values (down to −30%) to positive peaks (up to 61%). The occurrence of negative removal efficiencies and the strong scatter across tests point to a non-stationary behavior driven by a combination of influent heterogeneity, analytical uncertainty, and possible episodic release of MPs previously retained on the filter surface. Similarly to the belt system, the disc did not show a monotonic improvement with decreasing mesh size, reinforcing the conclusion that real-scale MP removal cannot be interpreted as a simple function of nominal mesh opening.

Across both technologies, no systematic relationship was observed between influent MP concentration and their removal, indicating that incoming MP load alone is not predictive of removal efficiency within the investigated range. Moreover, total suspended solids removal could not be used as a proxy for MP removal: it was not positively correlated with TSS removal efficiency in either system (BELT showed only a weak relationship with limited statistical robustness; DISC showed no relationship), as it seems to confirm that microplastics follow partially independent transport pathways compared to suspended solids. Microplastics were also detected in the separated solid fractions, with fragment counts driving total MP concentrations in solids for both systems. The belt filter generally showed slightly higher MP concentrations per unit dry matter than the DISC filter. The enrichment factor values were consistently below 1 for both technologies and all analyzed runs. This indicates that only a limited fraction of influent microplastics is transferred from the liquid phase to the separated solids, while the majority remains in the filtrate. The persistence of EF < 1 further supports the finding that MP retention is not only governed by suspended solids capture and that a relevant fraction of MPs likely occurs as small or flexible particles that are not efficiently intercepted under continuous operation, particularly when cake development is limited or unstable.

Finally, the comparison between laboratory-scale and demonstration-scale data for the AISI 250–150–75 µm meshes showed that laboratory tests are effective in identifying qualitative trends and relative filter performance, but they are not directly predictive of absolute demonstration-scale efficiencies. Across both scales, the AISI 150 µm mesh emerged as the best-performing configuration in terms of average MP removal, suggesting that an intermediate mesh size can potentially represent a practical compromise between theoretical retention potential and operational robustness. For finer meshes, laboratory-scale efficiencies were generally higher than demonstration-scale values, plausibly due to controlled hydraulics. For the coarser mesh (AISI 250 µm), the partially reversed trend observed at demonstration scale should be interpreted cautiously due to the limited number of data points and the high variability (SD= 42.8 %), indicating that part of the discrepancy may reflect statistical scatter rather than systematic scale effects.

In conclusion, the results of this study indicate that the objectives of the thesis were achieved, providing an overview of surface filtration performance across different scales and contributing to a better understanding of the mechanism of microplastic removal. However, it should be emphasized that microplastic removal at lab scale was not systematically investigated during the tests conducted on textile wastewater streams.

As a result, the assessment of microplastic removal performance in relation to textile effluents remains limited and indirect, and the conclusions drawn in this work primarily refer to mixed urban–industrial wastewater conditions. The results obtained in this study highlight several aspects that require further investigation before surface filtration technologies can be fully assessed and implemented for microplastic mitigation in textile wastewater treatment. A key limitation of the present work is the relatively small number of available microplastic removal data, both at laboratory and demonstration scale. The scarcity of data, combined with the high variability observed in removal efficiencies, particularly at demonstration scale, does not allow for statistically robust conclusions regarding the absolute performance of the investigated filtration technologies. Another aspect concerns the analytical methodology for microplastic extraction and quantification. The high variability observed in microplastic removal efficiencies, particularly at demonstration scale, emphasizes the need to further refine extraction, identification, and quantification procedures in order to reduce analytical uncertainty and improve data robustness. In this context, additional experimental repetitions are required to discover true process-related variability from analytical noise and episodic operational effects. Within the framework of the European LIFE-CASCADE project, which will continue until October 2027, additional experimental activities are planned to further evaluate surface filtration technologies under more representative operating conditions. Future testing will involve the application of belt and disc filtration systems directly to textile wastewater streams, rather than to mixed WWTP influents. This step is considered essential to better capture the specific characteristics of textile effluents and to assess filtration performance under conditions more comparable to those investigated at laboratory scale. Testing surface filtration units at textile industrial plants will allow a more direct comparison between laboratory-scale experiments and real-scale operation, improving the understanding of scale effects and the transferability of laboratory findings. Overall, the results of this thesis indicate that, while surface filtration shows potential for microplastic mitigation, a more extensive and statistically robust experimental dataset is required before definitive conclusions can be drawn regarding its effectiveness for wastewater treatment.

REFERENCES

Akyildiz, S. H., Bellopede, R., Sezgin, H., Yalcin-Enis, I., Yalcin, B., & Fiore, S. (2022). Detection and Analysis of Microfibers and Microplastics in Wastewater from a Textile Company. *Microplastics*, *1*(4), 572–586. https://doi.org/10.3390/microplastics1040040

Bayo, J., López-Castellanos, J., Olmos, S., & Rojo, D. (2023). Characterization and removal efficiencies of microplastics discharged from sewage treatment plants in Southeast Spain. *Water Research*, *244*, 120479. https://doi.org/10.1016/j.watres.2023.120479

Catarino, M. L., Sampaio, F., & Gonçalves, A. L. (2025). Sustainable Wet Processing Technologies for the Textile Industry: A Comprehensive Review. *Sustainability*, *17*(7), 3041. https://doi.org/10.3390/su17073041

Chan et al 2020 accepted. (s.d.).

Chouchene, K., Silva, A. L. P., Costa, A., Marinho, A., Duarte, A. C., Rocha-Santos, T., & Da Costa, J. P. (2025). Textile microfibers: Emissions, quantification and analytical characterization. A household laundry perspective. *Green Analytical Chemistry*, *14*, 100293. https://doi.org/10.1016/j.greeac.2025.100293

Gambino, I., Terzaghi, E., Baldini, E., Bergna, G., Palmisano, G., & Di Guardo, A. (2025). Microcontaminants and microplastics in water from the textile sector: A review and a database of physicochemical properties, use in the textile process, and ecotoxicity data for detected chemicals. *Environmental Science: Processes & Impacts*, *27*(2), 297–319. https://doi.org/10.1039/D4EM00639A

Iyare, P. U., Ouki, S. K., & Bond, T. (2020). Microplastics removal in wastewater treatment plants: A critical review. *Environmental Science: Water Research & Technology*, *6*(10), 2664–2675. https://doi.org/10.1039/D0EW00397B

Komorowska-Kaufman, M., & Marciniak, W. (2024). Removal of microplastic particles during municipal wastewater treatment: A current review. *Desalination and Water Treatment*, *317*, 100006. https://doi.org/10.1016/j.dwt.2024.100006

Korzin, A., Sturm, M. T., Myers, E., Schober, D., Ronsse, P., & Schuhen, K. (2025). Upstream Microplastic Removal in Industrial Wastewater: A Pilot Study on Agglomeration-Fixation-Reaction Based Treatment for Water Reuse and Waste Recovery. *Clean Technologies*, *7*(3), 67. https://doi.org/10.3390/cleantechnol7030067

Kwon, H. J., Hidayaturrahman, H., Peera, S. G., & Lee, T. G. (2022). Elimination of Microplastics at Different Stages in Wastewater Treatment Plants. *Water*, *14*(15), 2404. https://doi.org/10.3390/w14152404

Rathinamoorthy, R., & Raja Balasaraswathi, S. (2023). Characterization of microfibers originated from the textile screen printing industry. *Science of The Total Environment*, *874*, 162550. https://doi.org/10.1016/j.scitotenv.2023.162550

Simon, M., Vianello, A., & Vollertsen, J. (2019). Removal of >10 µm Microplastic Particles from Treated Wastewater by a Disc Filter. *Water*, *11*(9), 1935. https://doi.org/10.3390/w11091935

Sturm, M. T., Myers, E., Schober, D., Korzin, A., & Schuhen, K. (2024). Beyond Microplastics: Implementation of a Two-Stage Removal Process for Microplastics and Chemical Oxygen Demand in Industrial Wastewater Streams. *Water*, *16*(2), 268. https://doi.org/10.3390/w16020268

Talvitie, J., Mikola, A., Koistinen, A., & Setälä, O. (2017). Solutions to microplastic pollution – Removal of microplastics from wastewater effluent with advanced wastewater treatment technologies. *Water Research*, *123*, 401–407. https://doi.org/10.1016/j.watres.2017.07.005

Uogintė, I., Pleskytė, S., Pauraitė, J., & Lujanienė, G. (2022). Seasonal variation and complex analysis of microplastic distribution in different WWTP treatment stages in Lithuania. *Environmental Monitoring and Assessment*, *194*(11), 829. https://doi.org/10.1007/s10661-022-10478-x

Zhou, H., Zhou, L., & Ma, K. (2020). Microfiber from textile dyeing and printing wastewater of a typical industrial park in China: Occurrence, removal and release. *Science of The Total Environment*, *739*, 140329. https://doi.org/10.1016/j.scitotenv.2020.140329

Zoccali, A. (2024). Holistic control of microplastics for a safe reuse of bio-based components and water from wastewater treatment plants (PhD thesis). Politecnico di Milano.

Acknowledgements

First and foremost, I would like to express my sincere gratitude to Professor Francesca Malpei, supervisor of this thesis, for her guidance, valuable advice, careful revisions, and constant support throughout the entire journey. I am especially grateful for her trust and for giving me the opportunity to carry out the internship on which this work is based.

Thanks to this opportunity, I completed my internship at Lariana, where I was welcomed into a collaborative and supportive environment. I would like to thank the entire team, and in particular Giovanni Bergna, CEO of the company, for his kindness, availability, and trust, which were essential to completing this thesis within the planned timeframe.

A special thank you goes to Annalisa Girola and Rosa Scanu, who supported me daily during my laboratory experience. Their availability, patience, and expertise allowed me to gain valuable hands-on experience while also creating a welcoming and supportive atmosphere. I will especially miss the moments we shared and the relaxed coffee breaks together with Stefano Grigioni and Daniele Pagani, which made this experience particularly enjoyable.

The Master's degree program at the Politecnico was challenging, but my integration was made easier thanks to my friend Federico, with whom I shared early morning trips to the university. I would also like to thank Eleonora and Giada for their companionship throughout this journey.

A special thank you goes to my two "musketeers," Fabio Gozzi and Flavio Carta, friends even before being university colleagues. Their constant academic and personal support was fundamental in facing challenges and celebrating achievements, making this path both meaningful and rewarding.

I am deeply grateful to my family for their unwavering support and encouragement, and for enabling me to experience important opportunities for personal and professional growth, such as the Erasmus experience in Iceland.

In this regard, I would like to dedicate a special thank you to Silvia Panizzolo, an incredible life companion during the Erasmus experience in the land of ice and fire. Sharing this adventure together deeply enriched my personal and cultural background, between university homework and evening herbal teas.

Finally, I would like to thank all those who, directly or indirectly, contributed to the achievement of this important milestone, including the colleagues, technicians, and staff of LIA.